Influenza A virus-specific multifunctional memory T cells show functional superiority

Lotus Maria Westerhof, BSc

Submitted in fulfilment of the requirements for the degree of Doctor of Philosophy in Immunology

Institute of Infection, Immunity and Inflammation

College of Medical, Veterinary and Life Sciences

University of Glasgow

February 2024

Abstract

Cytokine production by memory T cells is very important for T cell mediated protection. Particularly multifunctional memory T cells that produce multiple cytokines have been associated with protection. However, we currently have a limited understanding of how and when these multifunctional memory T cells are generated, and of their persistence during memory cell maintenance and secondary responses. We investigated Influenza A virus-specific CD4 and CD8 T cells using a mouse model. We found that, CD4 T cells detected using MHCII tetramers declined in lymphoid and non-lymphoid organs, but we found similar numbers of cytokine producing CD4 T cells at days 9 and 30 in the lymphoid organs. In comparison to primary responding T cells, an increased proportion of memory T cells tended to produce multiple cytokines simultaneously. Analysis of the timing of release of cytokine by influenza virus-specific T cells demonstrated that primary responding CD4 T cells from lymphoid organs were unable to produce a sustained cytokine response. In contrast CD8 T cells, memory CD4 T cells, and primary responding CD4 T cells from the lung produced a sustained cytokine response throughout the restimulation period. We found an enhanced survival signature in T cells capable of producing multiple cytokines. Following re-infection, multifunctional T cells expressed low levels of the proliferation marker, Ki67, while cells that only produce the anti-viral cytokine, interferon γ, were more likely to be Ki67+. Despite this, multifunctional memory T cells formed a substantial fraction of the secondary memory pool. Together, these data suggest that memory CD4 T cells display superior cytokine responses compared to primary responding cells, and indicate that survival rather than proliferation may dictate which populations persist within the memory pool.

Table of Contents

Abstract **2**
List of Tables **7**
List of Figures **8**
Preface **10**
Acknowledgements **12**
Author's Declaration **14**
Definitions/Abbreviations **15**
Chapter 1 Introduction **17**
1.1 T lymphocytes 17
1.1.1 T cell development 17
1.2 T cell activation 19
1.3 T cell functions 21
1.4 Multifunctional T cells 23
1.5 Memory T cells 25
1.6 Influenza A virus 27
1.7 Influenza vaccines 27
1.8 T cell response to IAV 28
1.9 Key questions 28
1.10 Hypothesis 29
1.11 Data obtained by others 29
Chapter 2 Material and methods **30**
2.1 Animals 30
2.1.1 Ethics statement 30
2.1.2 Mice 30
2.2 Infections 30
2.2.1 Influenza A infection of mice 30
2.2.2 Repeated IAV infection with X31 31
2.3 Preparation of the tissues 31
2.3.1 Intravenous labelling 31
2.3.2 Euthanasia 31
2.3.3 Cell isolation 31
2.3.4 Cell counting 32
2.4 bmDC-T cell co-culture 33
2.4.1 Generations of bmDCs 33
2.4.2 Co-culture 33
2.5 Staining for flowcytometry 34
2.5.1 MHC Tetramer staining 34
2.5.2 Extracellular staining 35

2.5.3 Viability staining 35
2.5.4 Intracellular staining 35
2.6 Analysis and statistics 37
2.6.1 FlowJo 37
2.6.2 GraphPad Prism 37
Chapter 3 Multifunctional cytokine production reveals functional superiority of memory CD4 T cells 38
3.1 Abstract 39
3.2 Introduction 39
3.3 Results 41
3.3.1 Cytokine producing CD4 T cells decline most dramatically in the lung 41
3.3.2 Memory T cells are more likely to be multifunctional than primary responding T cells 46
3.3.3 The dynamics of T cell cytokine release reveals functional maturation of CD4, but not CD8, T cells 49
3.3.4 PI3kinase inhibitors reveal altered cytokine responses by primary responding and memory CD4 T cells 52
3.4 Discussion 58
3.5 Materials and Methods 61
3.5.1 Animals and infections 61
3.5.2 Tissue preparation 61
3.5.3 Influenza virus and control antigen 62
3.5.4 Bone marrow DCs 62
3.5.5 Ex vivo restimulation 62
3.5.6 Flow cytometry 62
3.5.7 Statistical analysis 63
3.6 Acknowledgments 63
3.7 Funding 63
3.8 Disclosures 63
3.9 Competing Interest 64
3.10 Author Contribution 64
Chapter 4 Multifunctional cytokine production marks influenza A virus-specific CD4 T cells with high expression of survival molecules 65
4.1 Abstract 66
4.2 Introduction 67
4.3 Results 68
4.3.1 MHC tetramers and cytokine expression enable analysis of IAV-specific T cells 68

4.3.2 While the number of IAV-specific CD4 T cells detected by MHC tetramer decline from day 9 to day 30, the numbers of cytokine+ CD4 T cells in the secondary lymphoid organs are stable 71
4.3.3 Single IFNγ+ CD4 and CD8 T cells are more likely to be in cell cycle than multifunctional T cells 78
4.3.4 scRNAseq analysis reveals heterogeneity in cytokine+ and cytokine negative memory CD4 T cells 81
4.3.5 Triple cytokine+ memory CD4 T cells express a pro-survival gene signature 96
4.3.6 TCR clones are found in multiple memory T cell clusters but are not shared between different animals..... 97
4.3.7 Single IFNγ+ T cells dominate the proliferative response during re-infection..... 99
4.4 Discussion 101
4.5 Materials and Methods 103
4.5.1 Animals and Study design.....103
4.5.2 Infections 103
4.5.3 Tissue preparation.....104
4.5.4 Ex vivo reactivation for intracellular cytokine staining 104
4.5.5 Flow cytometry staining 104
4.5.6 BD Rhapsody single cell RNA-seq 105
4.5.7 Single cell RNA-seq analysis.....106
4.5.8 Statistical analysis.....107
4.6 Data availability statement 107
4.7 Conflict of interest 107
4.8 CRediT authorship contribution statement 107
4.9 Acknowledgments 107
Chapter 5 Summary 109
5.1 Advanced detection methods to identify IAV-specific CD4 and CD8 T cells 109
5.2 Commonalities and differences in IAV-specific T cells across lymphoid organs and the lung 110
5.2.1 Cytokine production in lymphoid organs compared to the site of infection.....110
5.2.2 Phenotypical comparison of memory T cells 112
5.2.3 Tmem in the bone marrow 113
5.3 Multifunctional memory T cells 113
5.3.1 Cytokine production and T cell survival.....113
5.3.2 The timing of cytokine production by multifunctional T cells 114
5.3.3 Multifunctional T cell increase proportionally in the memory pool compared to the primary T cell pool.....116

5.3.4 Multifunctional T cells are less likely to proliferate than singular IFNγ producers. 117
5.4 IAV-specific T cells after infection and re-infection. 118
5.5 Reflection on hypothesis 120
List of References 122

List of Tables

Table 1 - Contribution to manuscript "Westerhof *et al*, EJI 2019" 10
Table 2 - Contribution to manuscript "Westerhof *et al*, EJI 2023" 11
Table 3 - List of antibodies used for flow cytomery staining 36
Table 4 - Gene expression and clustering..... 84
Table 5 - List of primers.....106
Table 6 - Pros and cons of the different methods used.....110

List of Figures

Figure 1 - Dendritic cell activating a naive T cell by providing 3 signals..... 20
Figure 2 - CD4 T cells functions at different sites. 22
Figure 3 - Functions of CD8 T cells at the site of infection. 23
Figure 4 - A multifunctional T cell that has the ability to secrete IFNγ, IL-2 and TNFα..... 24
Figure 5 – The locations of Tcm, Tem and Trm. 26
Figure 6 - IAV antigen causes some upregulation of MHC II and costimulatory molecule expression on bmDCs..... 41
Figure 7 - Gating scheme for T cell cytokine analysis..... 42
Figure 8 - Identification of influenza virus-specific cytokine producing CD4 and CD8 T cells..... 44
Figure 9 - Cytokine producing IAV-specific memory CD4 and CD8 T cell numbers stabilise in lymphoid organs but continue to decline in the lung. 45
Figure 10 - Multifunctional CD4 and CD8 T cells increase in proportion from the primary to the memory pool..... 47
Figure 11 - The proportion of IAV-specific T cells that are present in lung vasculature increases from day 9 to day 30. 48
Figure 12 - Memory CD4 T cells demonstrate more sustained cytokine production than primary responding cells. 50
Figure 13 - Memory CD4 T cells demonstrate more sustained cytokine production than primary responding cells. 51
Figure 14 - Similar proportions of CD4 T cells producing IFNγ at 2-4 hours are present in the primary responding and memory T cell pools. 52
Figure 15 - PI3Kinase delta inhibitor reduces the proportion of cytokine producing T cells. 55
Figure 16 - Memory CD4 T cell cytokine production is less affected by PI3Kinase inhibitors than primary responding CD4 T cells. 56
Figure 17 - Multifunctional memory CD4 T cells are less affected by PI3Kinase inhibitors than primary responding cells. 57
Figure 18 - MHC tetramers and cytokine expression enable analysis of IAV-specific T cells. 69
Figure 19 - Example gating of IAV-specific CD4 and CD8 T cells identified by MHC tetramers. 70
Figure 20 - Influenza virus-specific cytokine+ CD4 T cells are more likely to enter the memory pool than non-cytokine+ cells. 73
Figure 21 - IL-2 and TNF+ CD4 and CD8 T cells show minimal decline between day 9 and day 30 in secondary lymphoid organs. 74
Figure 22 - TRACE mice enable identification of CD4 T cells responding to IAV infection. 75
Figure 23 - TRACE mice enable identification of cytokine+ and negative CD4 T cells. 77
Figure 24 - Detection of IFNγ Ki67+ cells by flow cytometry. 79
Figure 25 - Single IFNγ+ CD4 and CD8 T cells are more likely to be in cell cycle 9 and 30 days after IAV infection than T cells producing multiple cytokines..... 80
Figure 26 - Example data from sorted EYFP negative naïve and EYFP+ memory CD4 T cells..... 82
Figure 27 - Triple cytokine+ CD4 T cells have a pro-survival transcriptional signature..... 83
Figure 28 - scRNAseq reveals heterogeneity in the memory CD4 T cell pool. 84

Figure 29 - Triple cytokine+ CD4 T cells produce more cytokine on a per cell basis than single cytokine+ T cells. 95
Figure 30 - Single IFNγ+ CD4 memory T cells express higher levels of PD1 and ICOS than triple cytokine+ cells. 96
Figure 31 - TCR clones are found in multiple memory T cell clusters but are not shared between different animals. 98
Figure 32 - Previous infection with IAV leads to a protective response following re-challenge infection but no changes in the proportion of cytokine+ populations. 100
Figure 33 - Triple cytokine+ T cells are less likely to be in cell cycle than single IFNγ+ T cells following challenge infection.....101
Figure 34 – Memory T cells are functionally superior to primary T cells. Multifunctional CD4 T cells express more transcripts for pro-survival molecules and less markers of proliferation than cytokine negative CD4 T cells.....121

Preface

I have chosen to write this thesis in the alternative format mainly due to the impact of the Covid-19 pandemic and my ongoing health issues. The final months of my PhD were disrupted, halting all labwork. During the UK lockdowns in 2020, I was unable to progress with my PhD. I took a suspension of studies and I moved back home to the Netherlands to set up a covid mega lab. I planned to start writing my thesis again in the course of 2021, however, I experienced a covid infection in April 2021. I was severely ill and my recovery was very slow. Then in July 2022 I was re-infected with covid which caused a huge setback in my long-covid recovery and worsened my symptoms, leaving me unable to work or complete my PhD. The graduate school convenor, Ruaidhri Carmody, pointed out to Megan and I that the alternative thesis format might help me finish my PhD. The main body of my PhD work has been published in Westerhof *et al*. 2019 and Westerhof *et al*. 2023, and therefore I decided to complete an alternative format PhD thesis. The decreased writing load that this format provides has helped me to finish the thesis in the past months.

The results chapters (Chapter 3 and Chapter 4) are from my two first author papers and these are presented as a whole, as these studies are clearly linked in both research question and experimental approach. These papers are published as open access papers under CC-BY license and therefore can be reproduced here.

The following tables (Table 1 and Table 2) describe my leadership in the project and which figures are my research and which are the work of others.

Table 1 - Contribution to manuscript "Westerhof *et al*, EJI 2019"

Figure in paper	Figure in Thesis	Type of contribution
Main Figure 1	Figure 9	Led study, performed wet lab experiments, led analysis
Main Figure 2	Figure 10	Led study, performed wet lab experiments, led analysis
Main Figure 3	Figure 12	Led study, performed wet lab experiments, led analysis
Main Figure 4	Figure 16	Not involved These were preliminary data for GLAZgo studentship
Main Figure 5	Figure 17	Not involved These were preliminary data for GLAZgo studentship

SF1	Figure 6	Supervised undergraduate student who did these studies
SF2	Figure 7	From my experiments
SF3	Figure 8	From my experiments
SF4	Figure 11	From my experiments
SF5	Figure 13	From my experiments
SF6	Figure 14	From my experiments
SF7	Figure 15	Not involved These were preliminary data for my GLAZgo studentship

Table 2 - Contribution to manuscript "Westerhof *et al*, EJI 2023"

Figure in paper	**Figure in Thesis**	**Type of contribution**
Main Figure 1	Figure 18	Led study, performed wet lab experiments, led analysis
Main Figure 2A-B	Figure 20A-B	Led study, performed wet lab experiments, led analysis
Main Figure 2C-H	Figure 20C-H	My data led to the hypothesis for this experiment, not directly involved
Main Figure 3	Figure 25	Led study, performed wet lab experiments, led analysis
Main Figure 4	Figure 27	I performed a preliminary transcriptomic analysis that was not consistent enough for publication but helped with the development of protocols for this experiment
Main Figure 5	Figure 31	I performed a preliminary transcriptomic analysis that was not consistent enough for publication but helped with the development of protocols for this experiment
Main Figure 6	Figure 33	Led study, performed wet lab experiments, led analysis
SF1	Figure 19	From my experiments
SF2	Figure 21	From my experiments
SF3	Figure 22	Not directly involved
SF4	Figure 23	Not directly involved
SF5	Figure 24	From my experiments
SF6	Figure 26	Not directly involved
SF7	Figure 28	Not directly involved
SF8	Figure 29	Data analysed by a Masters student, I generated the data
SF9	Figure 30	Not directly involved
SF10	Figure 32	Led study, performed wet lab experiments, led analysis

Acknowledgements

Writing a PhD thesis is never easy, however, for me it was more difficult than I ever could have imagined beforehand, as my life was turned upside down when I became chronically ill during the pandemic. I do not think I would have been able to do this without **Megan MacLeod** as my supervisor. She has pushed me to keep going without putting too much pressure on me and she has always been understanding of my limitations. Thank you for all the help, knowledge, explanations, support and motivation you have given me these past 6 years.

I would also like to thank everyone that I have worked with in the MacLeod group for creating a great work environment full of knowledge. And of course for letting me vent my PhD struggles and help me in the lab when needed. Thank you **Josh, Tom, Julie, Kerrie, Victoria** and **George**.

I have very much enjoyed working with **the entire LIVE group** (I am sorry, these are too many names to name for my long-covid brain). For example making my very first international PhD trip with **Holly** and **Leo**, or just getting ice cream across the road when we needed a break. But also every one else in LIVE or the PhD office that has improved my PhD experience for scientific, or non-scientific reasons such as going for lunch, after work drinks and nights out. I am sad that I no longer live in the same country as any of you, and that I have not been able to visit due to my health problems.

Richard van Hardeveld has helped me make my figures by drawing pretty cells for me, but he also supported me in my years of chronic illness, and made it possible for me to write this thesis.

I would also like to thank everyone at the CVR's "**Glasgow Respiratory Virus meeting**" for improving my knowledge of viruses, the staff within the School of Infection and Immunity **Flow Cytometry Facility** and **Biological Services** at the University of Glasgow for technical assistance and **Ruaidhri Carmody** who, as graduate school convenor directed us to the alternative thesis format.

And lastly I'd like to thank **my wee mice** that have made this research possible, and all other test animals that ever lived who have now severely improved our quality of live.

Thank you everyone, I would not have been able to do this without you all.

Author's Declaration

This research is my own work, except where reference is made to the contribution of others. This thesis is the result of my own work and has not been submitted for any other degree at the University of Glasgow or any other institution.

Lotus M Westerhof

Definitions/Abbreviations

4-1BB	Tumor necrosis factor superfamily member 9; CD137
Ag	Antigen
ANOVA	Analysis of variance
APC	Antigen presenting cell
ATAC-seq	Assay for transposase-accessible chromatin sequencing
B cell	B lymphocyte
Bcl	B cell lymphoma
bmDC	Bone marrow-derived dendritic cells
BSc	Bachelor of Science
C	Celsius
CD	Cluster of differentiation
cRPMI	Complete RPMI
d	Day
DC	Dendritic cell
DMSO	Dimethylsulfoxide
DNAse	Deoxyribonuclease
Dox	Doxycycline
EYFP	Enhanced yellow fluorescent protein
EYFPfl	Floxed enhanced yellow fluorescent protein
FACS	Fluorescence-activated cell sorting
FCS	Foetal calf serum
H	Hemagglutinin
HIV	Human immunodeficiency virus
i.n.	Intranasal
i.v.	Intravenous
IAV	Influenza A virus
ICOS	Inducable T cell costimulator; CD278
IFN	Interferon
IL	Interleukin
JAK	Janus kinases
L	Ligand
LCMV	Lymphocytic choriomeningitis virus
LIGHT	Lymphotoxin-like, exhibits inducible expression, competes with HSV glycoprotein D for HVEM, a receptor expressed by T lymphocytes
MDCK	Madin-Darby Canine Kidney
medLN	Mediastinal lymph node
MFI	Mean fluorescence intensity
MHC	Major histocompatibility complex
mRNA	Messenger ribonucleic acid
mTec	Medullary thymic epithelial cells
N	Neuraminidase
NP	Nucleoprotein
OX40	Tumor necrosis factor receptor superfamily, member 4; CD134
PFU	Plaque forming units
PhD	Doctor of Philosophy
PI3K	Phosphoinositide 3 kinases
pMHC	Peptide major histocompatibility complex

RBC	Red blood cell
RNA	Ribonucleic acid
RNAseq	Ribonucleic acid sequencing
rpm	Rounds per minute
RPMI	Roswell Park Memorial Institute
RT	Room temperature
rtTA	Reverse tetracycline controlled transactivator
scRNAseq	Single cell ribonucleic acid sequencing
SD	Standard deviation
SEM	Standard error of mean
STAT	Signal transducer and activator of transcription protein
T cell	T lymphocyte
Tcm	Central memory T cell
TCR	T cell receptor
Tem	Effector memory T cell
tet	Tetramer
Tfh	T follicular helper cell
TGF	Transforming growth factor
Th	T helper cell
Tmem	T memory cell
TNF	Tumour necrosis factor
TRACE	T cell reporter of activation and cell enumeration
Trm	Resident memory T cell
UMAP	Uniform manifold approximation and projection
VDJ	Variable diverse joining
VJ	Variable joining
WHO	World health organisation
WSN	A/WSN/1933; H1N1
X31	A/X31; H3N2

Chapter 1 Introduction

1.1 T lymphocytes

1.1.1 T cell development

1.1.1.1 T cell progenitors

T lymphocytes (T cells) need to develop to ensure a diverse repertoire to respond to various pathogens, but they need to be tolerant to self-tissue to prevent autoimmunity.

T cell development starts with hematopoietic stem cells, these can be found in the bone marrow. Some lymphoid progenitor cells will migrate to the thymus to develop into T cells. Once these developing cells reach the thymus they proliferate and T cell specific genes, such as CD3, begin to be expressed. Then these cells differentiate through three stages; TCR generation, positive selection, and negative selection[1].

1.1.1.2 TCR development

The first stage is TCR generation. TCRs consist of an α-chain (TCR-α) and a ß-chain TCR-ß). Both chains are randomly generated to ensure that a wide range of pathogens can be recognised.

First, TCR-ß chains are rearranged through VDJ recombination[2]. Proliferation of cells expressing TCR-ß and pre-TCR-α occurs. This is followed by TCR-α undergoing VJ recombination. This process, combined with random nucleotide additions, leads to a highly diverse repertoire of T cells. This process is very important as it will result in many unique TCRs that each can target a unique peptide, so these should be able to fight off a wide range of pathogens.

1.1.1.3 Positive selection

The next step is positive selection to check if the generated TCR can bind to a class I or class II MHC molecule[1, 3]. This is to ensure reactivity to foreign-peptides presented on self-MHC in the periphery.

Around 90% of newly generated Double Positive (CD4+, CD8+) T cells will fail this test. TCR-α receptor editing can be attempted, if it is successful the cell can be rescued, otherwise death by apoptosis will occur. Apoptotic cells are then cleared by macrophages.

Thymocytes that recognise pMHC II will lose CD8 to become CD4 helper T cells[4]. CD4 T cells can activate B lymphocytes and assist CD8 T cell responses (see chapter 1.3).

Thymocytes that recognise pMHC I will lose CD4 and continue to the next step as CD8 cytotoxic T cells. Once primed in the periphery, these cells can directly kill infected cells and play an important role in cytokine signalling (see chapter 1.3).

The now single positive T cells that successfully recognised the body's MHC will continue on to the last step in this process; negative selection.

1.1.1.4 Negative selection

This step represents a checkpoint to remove autoreactive CD4 and CD8 T cells[1, 3]. If T cells recognise self peptides, it can lead to autoimmunity.

Dendritic cells and medullary thymic epithelial cells (mTec) in the medulla present self-antigens to the single positive T cells. The DCs present antigens that were transported by migratory DCs or the blood. mTecs can transfer Ag to the DCs by gap junctions or when DCs take up dead mTec.

If the T cell can interact with the presented self-antigen, it will receive an apoptotic signal to induce cell death. Some of these cells will become regulatory T cells instead of undergoing apoptosis. T cells with an extremely high affinity for MHC will also be eliminated.

The T cells that did not interact with self-antigen, and did not interact too strongly with MHC, migrate from the thymus via the medullary junction as mature naïve single positive T cells. Most of the T cells will not be able to pass the entire process of positive and negative selection.

1.2 T cell activation

To activate T cells, stimulation by innate immune cells is needed. The cytokines received by the T cell during activation determine T cell differentiation.

T cell activation occurs in secondary lymphoid organs such as the lymph nodes and spleen[5, 6]. This process requires three signals (Figure 1). Signal 1 is TCR engagement with the peptide-MHC II (for CD4) or MHC I (for CD8) on the surface of an APC. At the same time, the Ag non specific signal 2 should be present. There are different molecules that can provide signal 2, also known as co-stimulation. If there is no co-stimulation this will result in anergy, or non-responsiveness of the T cell.

The most studied costimulatory molecules are CD28, that can interact with CD80 or CD86, and CD40L which binds to CD40. There are however many more possibilities for signal 2. The CD28-family of molecules includes ICOS (ICOS-L), whereas the TNF-family of signal 2 molecules, important for e.g. memory formation, contains OX40 (OX40-L), and CD27 (CD70). The different co-stimulation molecules are important at different stages of the immune response and can induce different signals in the T cells.

The CD28 molecule is widely known for its role in CD4 and CD8 T cell activation, including expansion and survival of activated cells[7]. ICOS is also important in T cell responses and memory generation. It has been shown to play an essential role in CD4 Tcm cells[8] and CD8 Trm cells[9]. In the skin, ICOS appears specifically important for the survival of IL-17 producing CD8 Trm cells[10].

TNFα family molecules are involved in promoting survival of activated cells and thus promote memory formation. For example, activated T cells need OX40 and CD30 to survive as memory cells[11, 12]. OX-40 promotes survival of CD4 T cells by increased Bcl2 and Bcl-xL expression[13]. OX40 and 4-1BB signalling is important in secondary expansion of CD8 T cells[14]. 4-1BB and CD27 have also been reported to promote survival via upregulation of anti-apoptotic molecules in CD8 T cells[15, 16]. The molecule LIGHT can also promote survival of effector T cells to Tmem, it particularly promotes survival of CD8 Tmem in non-lymphoid tissues[17].

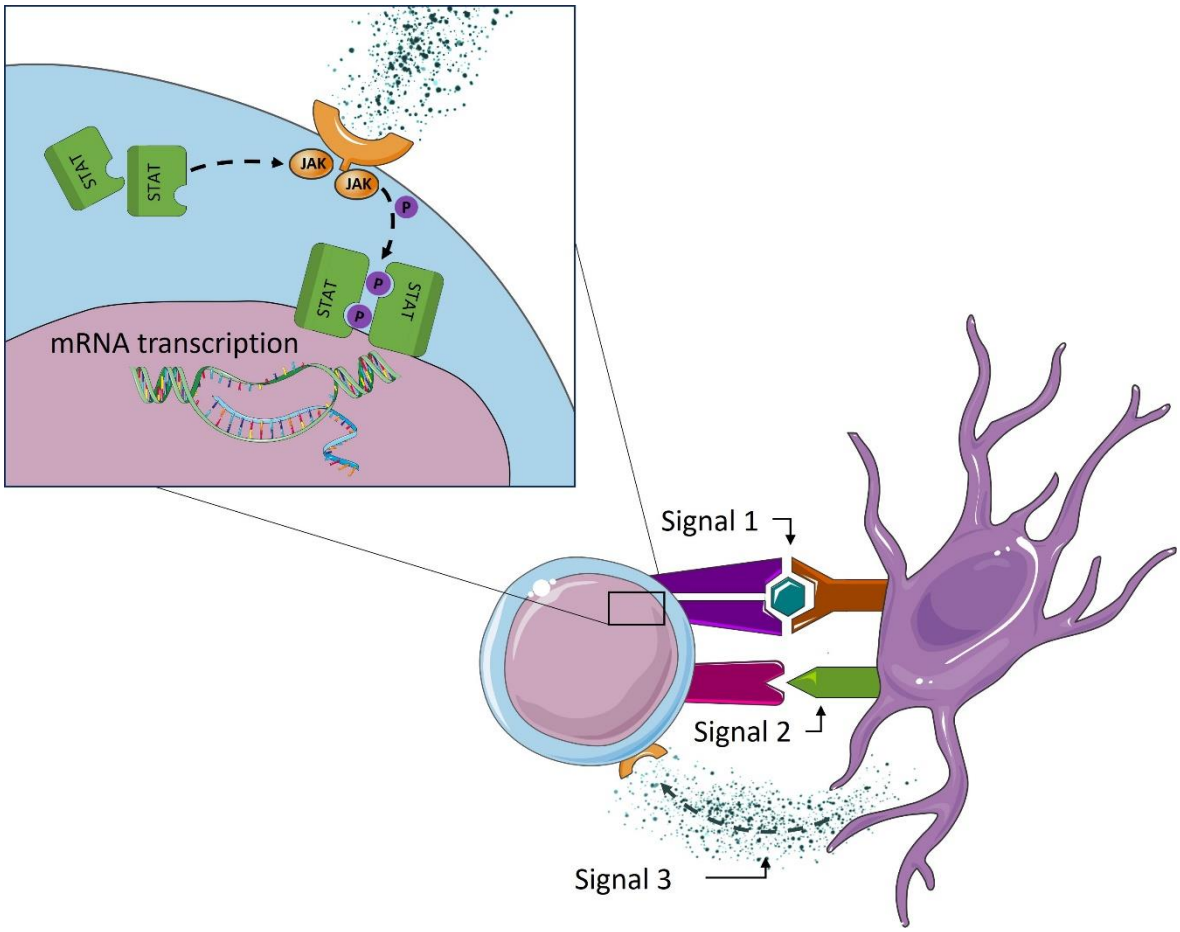

Figure 1 - Dendritic cell activating a naive T cell by providing 3 signals.

These signals are Ag specific signal 1 through the TCR, signal 2 that is provided through surface molecules such as CD28 or CD40, and signal 3 consisting of cytokines that influence cell differentiation.

Signal 3 consist of inflammatory cytokines. The different cytokines can result in different T cell differentiation[5]. For example, to differentiate into Th1, the naïve CD4 T cell needs to receive IL-12 and/or IL-18. Th1 cells are effective against most viruses and produce IFNγ. A Th2 cell needs IL-4 to differentiate, these cells protect against many parasites and produce IL-4 and IL-13. Th17 cells require TGF-β, IL-6 and IL-21 for their development, and protect against extracellular bacteria and fungi, they are known for producing IL-17 and IL-22. IL-6 and IL-21 are also important in the differentiation of Tfh which are important in protective immunity by helping B cells to produce antibodies in the secondary lymphoid organs, the Tfh can produce cytokines such as IL-10, IL-21 and IL-4 to enhance B cells responses.

PI3Kinases (PI3K) play an important role in relating T-cell activation to cytokine production[18]. Any of the three T cell activation signals have the ability to activate the PI3K signalling pathway. This pathway controls cell proliferation,

metabolism and can prevent apoptosis. Cytokines received by a T cell, from for example an infected cell activates the JAK/STAT pathway, where phosphorylated STAT moves to the nucleus where it can stimulate mRNA transcription for specific genes (Figure 1). Interferons can use this pathway to stimulate production of genes that makes cells more resistant to viral infection[19].

1.3 T cell functions

After activation, clonal expansion will occur to expand the number of Ag-specific T cells. The cells will also differentiate into various effector and memory phenotypes, depending on which signals they receive. Together this should provide an effective Ag-specific immune response, consisting of a heterogeneous pool of T cells. This means the Ag-specific CD4 and CD8 T cells can have different functions and secrete different molecules.

CD4 T cells can have important roles at two different sites[20] (Figure 2). In the lymphoid organs they can activate CD8 T cell responses either through IL-2 or by licensing DCs. Cytokines produced by CD4 T cell can also help B cells to form germinal centre responses and maturation of the B cells response through class switching and somatic hypermutation. At the site of infection, the CD4 T cells produce cytokines to attract and/or activate a variety of other immune cells. They are also capable of killing virus infected cells.

CD8 T cells at the site of infection have multiple functions[21] (Figure 3). They can directly kill infected cells. This is achieved using perforin, granzyme B and granulysin to induce apoptosis. They are also able to produce cytokines, such as IFNγ and TNFα, to attract and activate a range of immune cells.

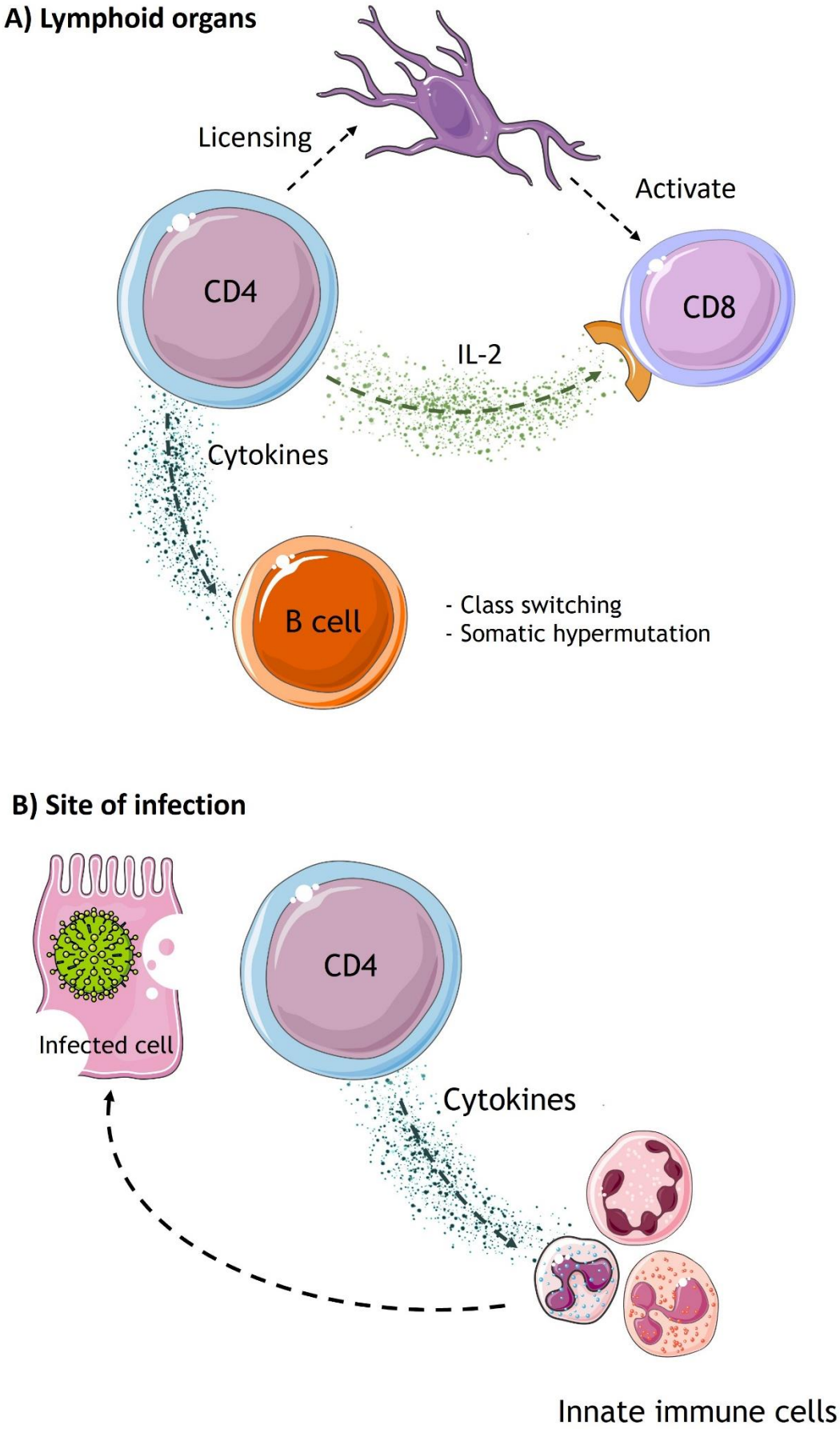

Figure 2 - CD4 T cells functions at different sites.

A) CD4 T cells can use licensing or IL-2 to activate CD8 T cells. CD4 T cells can also assist B cells in the lymphoid organs. B) The main function of the CD4 T cell at the site of infection is producing cytokines to attract and activate a variety of immune cells.

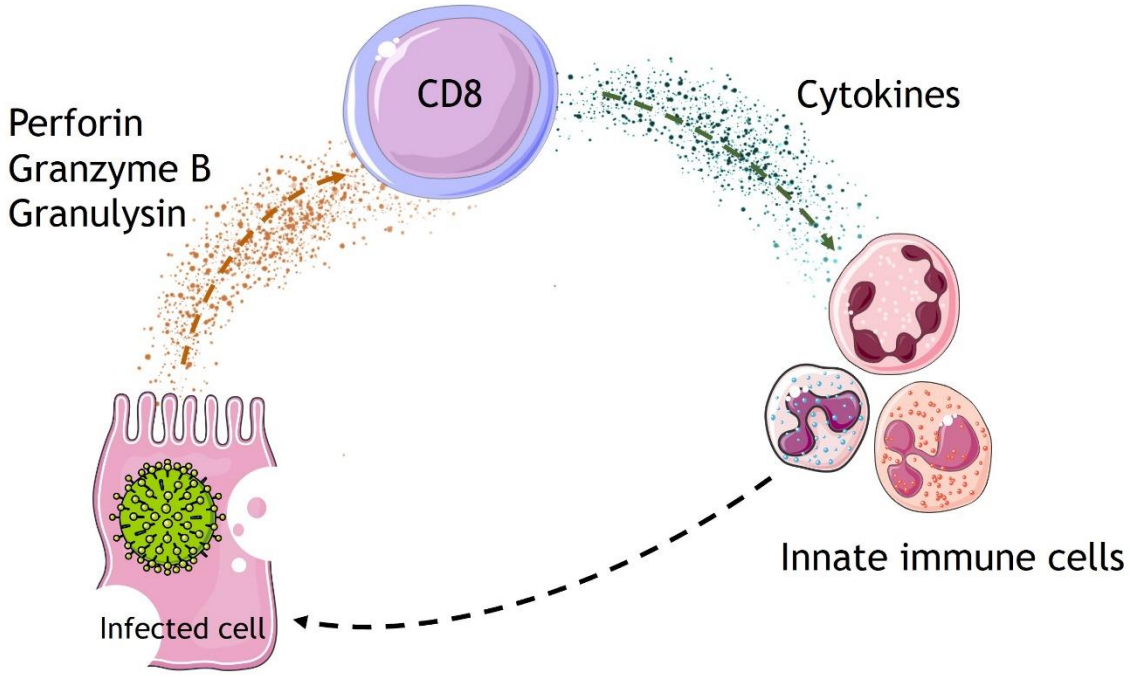

Figure 3 - Functions of CD8 T cells at the site of infection.

Cytotoxic CD8 T cells are known for inducing cell death of infected cells using perforin, granzyme and granulysin. They can also produce cytokines to attract and activate different immune cells.

1.4 Multifunctional T cells

Multifunctional T cells are CD4 or CD8 T cells that produce a number of different cytokines or effector molecules[22-24]. In my studies, we defined multifunctional cells as those that expressed at least three specific cytokines when activated: IFNγ, IL-2 and TNFα[25, 26](Figure 4). The CD4 T cells might also be able to produce a range of other cytokines including IL-4, and IL-10. Multifunctional CD8 T cells can secrete various cytokines and granzyme B and perforin.

IFNγ can activate anti-viral responses, IL-2 induces T cell proliferation but also survival, and TNFα stimulates incoming innate cells[27-31]. Due to this broad cytokine response, the multifunctional T cells are seen as very effective[22-24, 32, 33]. Differences between multifunctional and non-multifunctional T cells can also be observed once the infection has cleared and T cell memory has been generated[25].

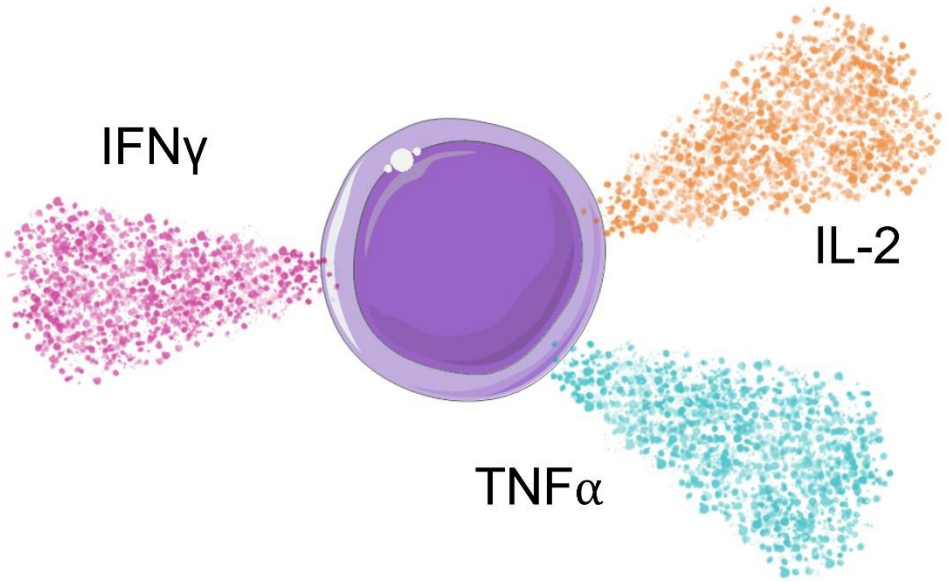

Figure 4 - A multifunctional T cell that has the ability to secrete IFNγ, IL-2 and TNFα.

Cytokine producing Tmem have been shown to provide protection against symptomatic influenza in humans[34-37]. A correlation has also been found between multifunctional CD4 T memory cells (Tmem) and protection against tuberculosis and leishmania in mice[23, 24]. Darrah *et al*. showed that the degree of protection a vaccine provides against *Leishmania major* infection in mice is predicted by the frequency of multifunctional CD4 T cells following vaccination[23]. Interestingly, multifunctional effector T cells generated by all vaccines tested in this study were unique in their capacity to produce high amounts of IFNγ.

A tuberculosis subunit vaccine investigated by Lindenstrøm *et al*. induced robust CD4 Tmem responses that were maintained at high levels for more than a year post-vaccination, and protected against a challenge infection[24]. Flow cytometry analysis of CD4 Tmem demonstrated that the long-lived memory population consisted almost exclusively of TNFα+ IL-2+ and IFNγ+ TNFα+ IL-2+ multifunctional T cells[24].

Multifunctional CD8 Tmem are associated with enhanced viral control[32, 33, 38]. Several studies in mice, macaques and humans show that multifunctional CD8 T

cells led to decreased viral loads or provided superior protection against HIV disease progression[22, 32, 33, 38].

Almeida at al. investigated T cells of HIV+ humans and showed that CD8 T cells that achieve optimal control of HIV-1 replication also display multifunctional capacities[22]. Chen *et al*. used mice and macaque models to compare vaccines, and concluded that the vaccine that supressed HIV most effectively produced a stronger, broader, and more multifunctional T cell response[38]. Genesca *et al*. also conducted a vaccine study in macaques, and found that the animals that do control viral replication after live attenuated HIV infection have multifunctional HIV-specific CD8 T cells with an increased survival potential[32]. Kwissa *et al*. showed that the frequency of multifunctional CD8 and CD4 T cells after challenge had an especially strong inverse correlation with the HIV viral loads[33].

Unfortunately, it remains unclear why these multifunctional T cells provide enhanced protection compared to other populations. A broader cytokine production could be key, but it could also be due to the larger amounts of cytokines produced by multifunctional T cells or their increased life span, or maybe a combination of some of these factors. Further research is needed to determine the exact cause of the enhanced protective capabilities of multifunctional T cells.

1.5 Memory T cells

Tmem are long lived cells that remain in the body to protect against a repeat infection[39-42]. These cells can give a faster and stronger response then naïve cells. This enhanced responses by memory cells provide the mechanistic basis for vaccination.

After T cell activation (see 1.2) the T cells, together with other immune cells will try to clear the pathogen. Once they succeed, T cells will go into the contraction phase; the majority of effector T cells will undergo apoptosis. The remaining cells are Tmem[39-42]. In mice, the half life of CD4 Tmem is approximately 50-100 days, whereas CD8 T cells will go into ultra-glide[43]. This means the CD8 memory population will stay fairly stable. Human CD4 Tmem have a half life of 8 to 12 years, and CD8 Tmem of 8 to 15 years[44].

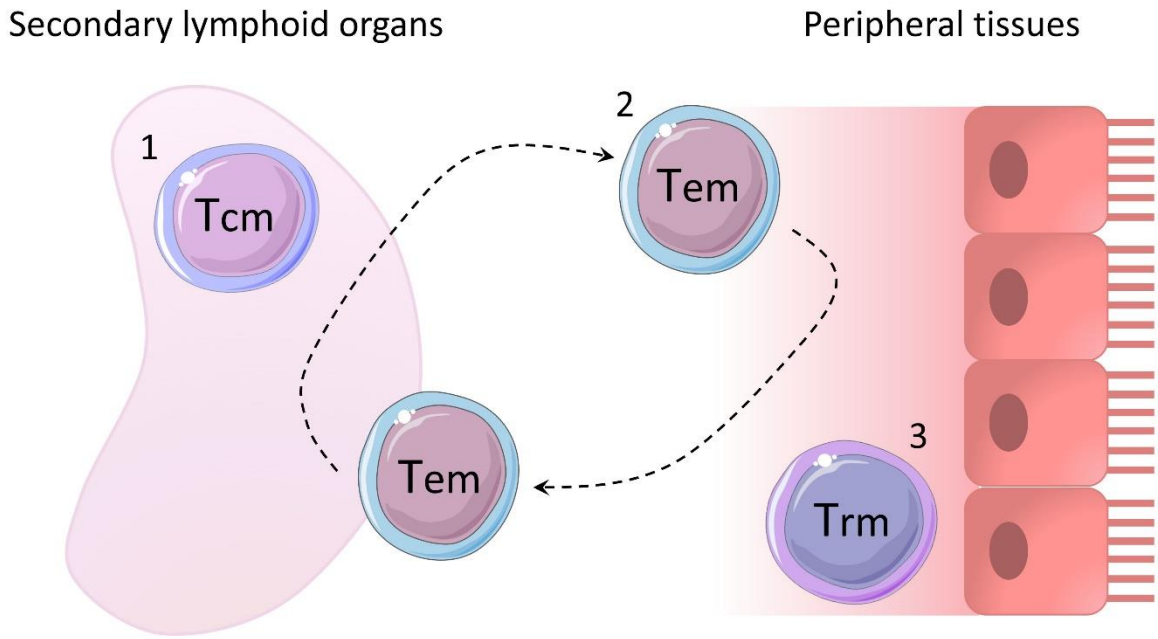

Figure 5 – The locations of Tcm, Tem and Trm.

Tcm circulate the blood and lymphoid organs, Tem circulate between lymphoid organs and other tissues and Trm remain near the site of the initial infection.

Tmem are a heterogeneous cell population[39-42]. They consist of central memory T cells (Tcm), effector memory T cells (Tem) and resident memory T cells (Trm) (Figure 5). Tcm, that recirculate through the blood and secondary lymphoid organs, proliferate upon reinfection to rapidly increase the pathogen-specific T cell population, Tem constantly circulate between lymphoid organs and other tissues, whereas Trm stay near the initial site of infection to ensure rapid protection from pathogens invading the tissue.

Both CD4 and CD8 Tmem populations contain cells from these three subgroups. They do however function differently. CD4 Tem produce cytokines to attract and/or activate other immune cells[20, 40, 42]. For example, it has been shown that during IAV infection, the IFNγ producing Tem activate an early innate response in the lung which reduces the infection[45]. IL-4 producing Tem can protect against *Heligmosoides polygyrus* in the gut[46]. CD4 Tem are also able to kill infected cells[47] and provide help to B cells[48]. IAV-specific CD4 Tcms have been shown to accelerate the B-cell antibody response in mice[49]. In humans these cells have been correlated with cross protective immunity[37].

CD8 Tem kill infected cells using granzyme B and perforin, and attract other immune cells through cytokine production[39, 41]. It has been shown that IAV-specific CD8 Tem in the lung can rapidly clear infected cells[50]. CD8 Tcm, like

CD4 Tcm, reside in secondary lymphoid organs and can rapidly proliferate to increase the number of pathogen-specific T cells[51]. These cells quickly move to areas of viral infection, to control the infection even more rapidly. The CD8 Tcm are known to have stem-cell-like characteristics; they can self renew and are multipotent, for example they are able to increase the memory population with both CD8 Tcms and Tems[52].

1.6 Influenza A virus

Influenza virus is an RNA virus with a large global impact. Each year, it causes between 250,000 and 500,000 deaths worldwide, and 3,000,000 to 5,000,000 severe infections[53, 54]. The WHO has estimated that around 20% of all children on earth experience an infection each year.

There are three strains of Influenza; A, B and C[55]. Influenza B and C have only been found in humans, they mostly infect children and the elderly and generally cause mild disease. These strains are less common and less variable than Influenza A. Influenza A can circulate through other animals like birds, this is the strain that causes pandemics.

The influenza A virus (IAV) is a rapidly mutating virus with highly variable surface proteins; hemagglutinin (H) and neuraminidase (N)[55]. Until now, 18 different H and 11 different N subtypes have been found. IAV H1N1 and H3N2 are the most common ones in transmission between humans. Due to this large variety of surface proteins, it is hard to build up immunity against many strains. For example, antibodies that were made during an IAV H1N1 infection will not be able to recognise IAV H3N2 surface proteins and therefore cannot prevent infection.

1.7 Influenza vaccines

Most vaccines rely on an antibody response for protection, which means Influenza vaccines have to be remade every year to protect against the dominant strains of that year[56]. The vaccines have to be produced before the annual strain is in wide-circulation. This is why the strains are predicted using mathematical modelling, unfortunately this only provides limited protection.

Some years the vaccine can work efficiently, but if the prediction is off, it might not protect well. Currently, two types of IAV-vaccines are available; trivalent inactivated and live attenuated[57]. The trivalent inactivated vaccine can sometimes contain an adjuvant to ensure an adequate immune response. It is administered intra muscularly in the arm. The live attenuated vaccine is an intranasal spray that is given to children. Both are updated annually to ensure they contain the strains that are predicted to circulate that year.

1.8 T cell response to IAV

Unlike Abs , cross-reactive T cells can reduce the consequences of a re-infection with a different Influenza strain, by recognising conserved parts of the virus[29, 35, 37, 48, 58, 59]. This causes IAV-specific Tmem to be able to be cross reactive and respond quickly to different serotypes of IAV despite the surface protein mutations.

A vaccine based on T cell protection might be a solution for yearly vaccinations that do not work optimally. It is not known yet how to create a vaccine that results in efficient Influenza-specific memory T cells. First more knowledge needs to be obtained about the protective T cells generated in infection, for example, to learn about the types of T cells that a future vaccine should induce for optimal protection. This has been a main aim of my research addressed via the questions listed below in chapter 1.9.

1.9 Key questions

- What is the phenotype of IAV-specific T cells in different organs over time post-infection?

- What is the cytokine production ability of IAV-specific T cells in different organs over time post-infection?

- What causes the higher percentage of multifunctional T cells in the memory pool than during active infection?

- What is the effect on the IAV-specific Tmem cells of a second IAV infection with a different strain?

1.10 Hypothesis

I have two main hypotheses. First based on what happens between the primary response and the formation of Tmem. Second, what happens to the Tmem after a second infection.

Formation of Tmem
I hypothesise that multifunctional Tmem are a distinct population, with distinct cellular processes and fate that leads to a proportional increase in multifunctional cells from the primary to the memory pool. This increased percentage of multifunctional IAV-specific T cells at memory could be due to increased survival of multifunctional Tmem, or, non-multifunctional T cells could gain an increased cytokine producing ability and become multifunctional over time.

Response of Tmem to second IAV infection
After a second IAV infection, I hypothesise that the proportion of multifunctional cells will not alter. This will be because the multifunctional Tmem will proliferate and respond at a similar pace as other Tmem.

1.11 Data obtained by others

The PI3kinase experiments were not performed by me, thus not a part of my PhD project, so these results will not be discussed here.

The RNAseq data was also not obtained or analysed by me. I performed ATAC-seq which unfortunately proofed to be unsuccessful. This led to the RNAseq experiments performed by others after I had finished the lab work of my PhD. As it is not part of my PhD this data will not be discussed here.

Chapter 2 Material and methods

2.1 Animals

2.1.1 Ethics statement

All mice were housed at the University of Glasgow and the animal research has been carried out at the University of Glasgow under licence P2F28B003 until July 2019, from July 2019 onwards licence PE1AF6E8B has been used. All protocols were conducted under the licenses issued by the U.K. Home Office under the Animals (Scientific Procedures) Act of 1986 and approved by the University of Glasgow Ethical Review Committee.

2.1.2 Mice

10 week old female C57BL/6 mice were purchased from Envigo (UK). They were maintained at the University of Glasgow under standard animal husbandry conditions. TRACE male and female mice were bred and maintained at the University of Glasgow mice and have been described previously[60].

2.2 Infections

2.2.1 Influenza A infection of mice

Mice were only selected to be infected if they weighed at least 18 grams. Following acclimatisation of a minimum of a week, the mice were briefly anesthetised using inhaled isoflurane and infected with 150-250 plaque forming units (PFU) of Influenza A virus (IAV) strain WSN in 20µl of PBS intranasally (i.n.). IAV was prepared and titered in MDCK cells. Infected mice were weighed daily between 4 and 12 days post-infection. In case a mouse had >15% weight loss, the entire cage received soft diet, and when any animal lost more than 20% of its initial weight it was removed from the study and euthanised. Group sizes were based on previous experiments considering the known variability of the anti-viral T cell response, animals that did not lose any weight following infection were excluded as these animals may not have been successfully infected.

2.2.2 Repeated IAV infection with X31

A number of mice have been (re)infected with 200 PFU X31 IAV, these mice were euthanised 5 or 35 days after the X31 infection. The mice were weighed daily from day 1 to 12 post-infection or until euthanised. None lost more than 20% of their starting weight.

2.3 Preparation of the tissues

2.3.1 Intravenous labelling

In order to distinguish tissue-derived T cells from those present in the peripheral blood we injected anti-CD45 antibody fluorescently labelled with Alexa Fluor 488 (BioLegend; 1 µg/mouse), or PE ThermoFisher 1 µg/mouse) in 200µl PBS, 3 minutes before being euthanised.

2.3.2 Euthanasia

All mice were euthanised using cervical dislocation of the neck.

2.3.3 Cell isolation

2.3.3.1 Lymphoid organs

Spleens and lymph nodes were mashed between two pieces of 45µm nitex mesh (Cadisch) in a small petri dish, washed in Hanks Balanced Salt solution (HBSS; Gibco) and transferred to 15ml tubes. Spleens were resuspended and 1ml of RBC lysis buffer (ThermoFisher) added for 2 minutes and then topped up with 8ml HBSS to stop the RBC lysis reaction. MedLNs were then resuspended in 1ml of complete (c)RPMI (RPMI with 10% foetal calf serum (FCS) (Gibco), 100µg/ml penicillin-streptomycin (Sigma Aldrich) and 2mM L-glutamine (Sigma Aldrich)) and spleens in 5ml of HBSS for cell counting. Spleens were then resuspended in complete media at $24x10^6$ cells per ml.

2.3.3.2 Lung

Lungs were extracted into 1ml of HBSS (ThermoFisher Scientific) in 5ml bijous. The tissues were chopped up and incubated in 2ml of HBSS containing

1.34mg/ml collagenase D (Roche) and 100µg/ml DNase (Sigma Aldrich) on a shaking incubator at 37°C, 160rpm for 40min. Subsequently they were mashed through a 70µm cell strainer (E & K Scientific) using the plunger of a 1ml syringe (BD Biosciences) into a small petri dish, washing with HBSS. Cells were then transferred to a 15ml tube and pelleted by centrifugation at 400g for 5min at 4°C and then red blood cell (RBC) lysed using 1ml Red Blood Cell lysis buffer (ThermoFisher), incubated at room temperature (RT) for 2 minutes. The samples were then topped up with 8ml HBSS to stop the RBC lysis reaction before washing in HBSS and resuspended in 2ml of cRPMI for cell counting.

2.3.3.3 Bone marrow

Femurs and tibias were cleaned of muscle and wiped with ethanol before transferring them into 5ml bijous with HBSS. The ends of the were cut off and the centre part was flushed through with sterile HBSS using a 26G needle. Cells were then pelleted by centrifugation at 400xg for 5min at 4°C. Cells were RBC lysed using 1ml RBC lysis buffer, incubated at RT for 2 minutes, then topped up with 8ml HBSS to stop the lysis reaction before washing in HBSS.

2.3.4 Cell counting

Cells were counted by mixing 10µl of homogenised cell sample with 10µl of 0.04% Trypan blue. 10µl of this solution was loaded on to a haemocytometer which held a glass cover slip attached by condensation. The number of cells were counted within the four corners and central square of the haemocytometer, if this number was <100 an additional 5 or 20 squares were counted. The total number of cells in the sample was calculated using the following formula:

$$n * \frac{25}{s} * 2 * v = number\ of\ cells\ in\ sample$$
$$n = number\ of\ cells\ counted$$
$$s = number\ of\ squares\ counted$$
$$v = volume\ of\ the\ sample\ (ml)$$

Cells from each sample were often split so that a portion could be used for co-culture(s) with bone marrow-derived dendritic cells (bmDCs) and a portion could be stained with MHC tetramers.

2.4 bmDC-T cell co-culture

2.4.1 Generations of bmDCs

In each well of a 6 well plate, $2*10^6$ cells were plated out in 3ml of cRPMI containing 5% granulocyte macrophage colony-stimulating factor (GM-CSF; prepared from X-63 supernatant) and cultured for at 37°C with 5% CO_2 [61]. Media was supplemented on day 2 with 2ml of fresh cRPMI + 5% GM-CSF and completely replaced with 3ml cRPMI+5% GM-CSF on day 5. Cells were harvested using 4mM EDTA in PBS incubated for 10 minutes at 4°C on day 7 (for incubation with IAV Ag) or 8 (for incubation with peptide). After the incubation the wells were flushed using a strippette, and the cells collected and washed in a 50ml tube.

2.4.2 Co-culture

2.4.2.1 IAV Ag-bmDCS

Sonicated IAV Ag preparation

The IAV Ag was generated using MDCK cells. A confluent flask of MDCKs was infected with IAV at an MOI of 0.001 diluted in PBS. The virus inoculum was removed after 1 hour, the cells washed with PBS and then 12 ml of OPTI-MEM (Gibco), supplemented with Pen/Strep and 1.0 µg/mL trypsin-TPCK, was added. The T75 flask was incubated at 37ºC and 5% CO_2. The cells were regularly checked for lysis and when 50% of the cells remained attached, the cells were harvested and pelleted by centrifugation at 1500rpm for 5 minutes. The supernatant was discarded and the cell pellet was resuspended in 500 µL glycine buffer (0.1 M glycine and 0.9% NaCl, pH 9.75). The lysate was shaken for 20 minutes at 4ºC, then sonicated four times for 10 seconds with a cooling period on ice between each burst. The lysate was centrifuged at 2000 rpm for 20 minutes at 4ºC. The supernatant was aliquoted into working volumes and stored at -80ºC. To normalise the IAV antigen between batches, the PFU per ml was tested.

IAV Ag loaded bmDCs

After harvesting the bmDCs on day 7, the cells were re-plated at $3*10^6$ cells in 3ml per well in a 6 well plate. The evening before the DCs were needed, IAV antigen was added at an MOI of 0.3. The DCs were harvested the following day and replated at $8*10^5$ cells/ml per well.

2.4.2.2 NP peptide loaded bmDCs

Once harvested, bmDCs were resuspended in 1ml of cRPMI and pulsed with 10µg/ml of NP311-325 and 10ug/ml of NP366-374 for 2 hours at 37°C. Peptide-pulsed bmDCs were subsequently plated out at a concentration of $8*10^5$ cells/ml per well.

2.4.2.3 Co-culture of bmDCs and ex vivo cells

The co-cultures were carried out in 48 well plates. The entire lymph node sample was used for the experiments, depending on the exact experiment the lymph node sample was used fully in one well or split up in 2 or 3 portions for different analysis methods. Lungs samples were resuspended in 500µl and 125µl per well. Spleens were resuspended at $24x10^6$ cells per ml and 125µl used per well.

250µl of Golgiplug (BD Bioscience) at a concentration of 2µg/ml were added to each well at the beginning of the experiment, unless stated otherwise.

2.5 Staining for flowcytometry

2.5.1 MHC Tetramer staining

The cells that were not used for co-culture with bmDCs were used for MHC class I and class II tetramer staining. PE-labelled IAb/NP311-325 and APC labelled Db/NP368-374 were provided by the NIH tetramer core.

All samples were stained with 25µl tetramer solution. The MHC II tetramer was diluted 1/200, and the MHC I tetramer 1/100 in three parts complete RPMI to two parts Fc block (homemade containing 24G2 supernatant and mouse serum) and incubated for 2 hours at 37°C 5% CO2 in the dark with agitation every 20 minutes. If the CX3CR1 BV711 antibody (BioLegend) was used in the staining panel, it was added in at this step at a 1/200 dilution.

2.5.2 Extracellular staining

2.5.2.1 Extracellular staining after co-culture

40µl of a 1:1 mixture of FC block and FACS buffer (PBS, 2% FCS, 1mM EDTA) was added to the cells and incubated at 4˚C in the dark for 10 mins. Subsequently, 40µl of surface antibody mix (Table 3), made up at 2x the concentration in PBS, was added and incubated for 20 minutes. Cells were subsequently washed twice in PBS.

2.5.2.2 Extracellular staining with MHC tetramers

Extracellular antibodies were made up at 3.5x the recommended concentration in 3:2 RPMI:Fc block. Following 2 hours of incubation with MHC tetramers, surface antibodies (Table 3) were added directly to cells in 10µl RPMI/Fc Block at a 3:2 ratio. Extracellular antibody staining for flow cytometry was conducted for 20 minutes at 4˚C. Cells were subsequently washed twice in PBS.

2.5.3 Viability staining

After two washes with PBS, 50µl of viability dye v506 (Thermofisher, UK) was added at 1/1000 in PBS for 20 minutes at 4˚C in the dark. Cells were then washed in FACS buffer for subsequent intracellular antibody staining. If intracellular staining was not required cells were washed and resuspended in FACS buffer or fixed with CytoFix&Perm (BD Bioscience) (see paragraph 2.5.4.1).

2.5.4 Intracellular staining

2.5.4.1 Fixation and permeabilization

After washing with FACS buffer, cells were fixed in Cytofix for 20 minutes and washed twice in Cytoperm diluted 1 in 10 in dH_2O (both BD Biosciences).

2.5.4.2 Cytokines and other intracellular antibodies

Intracellular antibodies (Table 3) were diluted in Cytoperm and added for 1 hour at room temperature in the dark. These cells were then washed twice in Cytoperm and resuspended in FACS buffer to be acquired on a Fortessa (BD Biosciences).

Table 3 - List of antibodies used for flow cytomery staining

Antibody	Company	Clone	Identifier
Anti-CD45 Alexa 488	ThermoFisher	30F11	Cat No: 53-0451-82; RRID: AB_2848416
Anti-CD45 PE	ThermoFisher	30F11	Cat No: 12-0451-82; RRID: AB_465668
Anti-CX3CR1 BV711	BioLegend	SA011F11	Cat No:149031; RRID: AB_2565939
Anti-CD4 APC-Alexa780	ThermoFisher	RM4-5	Cat No: 47-0042-82, RRID: AB_1272183
anti-CD8 BUV805	BD Bioscience	53-6.7	Cat No: 612898; RRID: AB_2870186
Anti-CD8 e450,	ThermoFisher	53-6.7	Cat No: 48-0081-82 RRID:AB_1272198
anti-CD44 BUV395	BD Bioscience	IM7	Cat No: 740215; RRID: AB_2739963
anti-CD44 PerCp-Cy5.5	ThermoFisher	IM7	Cat No: 45-0441-82 RRID:AB_925746
anti-PD-1 PeCy7	BioLegend	29F.1A12	Cat. No. 135215; RRID: AB_10696422
anti-PD1 BV605	BioLegend	29F.1A12	Cat. No. 135219; RRID: AB_11125371
anti-ICOS PerCP-Cy5.5	BioLegend	7E.17G9	Cat No. 117423; RRID: AB_2832418
anti-CD127 APC	ThermoFisher	A7R34	Cat No: 17-1271-82; RRID: AB_469435
Anti-CD103 PeCy7	BioLegend	2E7	Cat. No. 121425; RRID: AB_2563690
anti-CD69 PerCP-Cy5.5	ThermoFisher	H1.2F3	Cat No: 45-0691-82; RRID: AB_1210703
Anti-B220 eFluor-450	ThermoFisher	RA3-6B2	Cat No: 48-0452-82; RRID: AB_1548761
Anti-F4/80 eFluor-450	ThermoFisher	BM8	Cat No: 48-4801-82; RRID: AB_1548747
Anti-MHC II eFluor-450	ThermoFisher	M5114	Cat No: 48-5321-82; RRID: AB_1272204
Anti-IFN-g PE	ThermoFisher	XMG1.2	Cat No: 12-7311-82; RRID: AB_466193
Anti-IFN-g BV785	BioLegend	XMG1.2	Cat. No. 505837; RRID: AB_11219004
Anti-TNF Alexa-Fluor-488	ThermoFisher	MP6-XT22	Cat No: 53-7321-82; RRID: AB_469936
Anti-TNF BV605	BioLegend	MP6-XT22	Cat. No. 506329; RRID: AB_11123912
Anti-IL-2 APC	ThermoFisher	JES6-5H4	Cat No: 17-7021-82; RRID: AB_469490
Anti-IL-2 BV711	BioLegend	JES6-5H4	Cat. No. 503837; RRID: AB_2564225
Anti-Bcl2 PeCy7	BioLegend	Blc/10C4	Cat. No. 63351; RRID; AB_2565246

Anti-Ki67 PeCy7	BioLegend	16A8	Cat. No. 652426; RRID:AB_2632693
Anti-Myc, rabbit	Cell-Signalling Technology	D84C12	Cat No: 5605; RRID: AB_1903938
Anti-rabbit H+L PE	Cell-Signalling Technology	NA	Cat No: 79408, RRID:AB_2799931

2.6 Analysis and statistics

2.6.1 FlowJo

The flow cytometric data was analysed using FlowJo version 10. Analysis was conducted on single, live lymphocytes that were negative for MHCII and B220. For most figures, either the % of cells positive for a certain marker, or the total number of those cells in the organ, calculated with the initial cell count (see 2.3.4) was used. MFI was calculated by assessing the geometric mean of a desired marker.

2.6.2 GraphPad Prism

Data are expressed as individual mice from at least two independent experiments. Mean and standard error of mean (SEM) are also shown. Shapiro-Wilk was used to test for normalcy. Significance was calculated using the tests indicated in each figure legend. All statistical tests were carried out on GraphPad Prism software, version 6.0 (GraphPad software, San Diego, CA, USA). P values are determined as <0.05 = *, <0.01 = **, <0.001 = ***, <0.0001 = ****.

Chapter 3 Multifunctional cytokine production reveals functional superiority of memory CD4 T cells

Authors
Lotus M Westerhof (1,2), Kris McGuire (2$), Lindsay MacLellan (2), Ashley Flynn (1), Joshua I Gray (1), Matthew Thomas (3†), Carl S Goodyear (1,2), Megan KL MacLeod (1*)

Affiliations
1 - Centre for Immunobiology, Institute of Infection, Immunity and Inflammation, 120 University Place, University of Glasgow, Glasgow, UK, G12 8TA

2 - GLAZgo Discovery Centre, Institute of Infection, Immunity and Inflammation, University of Glasgow, Glasgow, UK

3 - Respiratory, Inflammation and Autoimmunity IMED, AstraZeneca, Gothenburg, Sweden

* Corresponding author, megan.macleod@glasgow.ac.uk

$ Current address: MRC Centre for Inflammation Research, University of Edinburgh

† Current address: Exploratory Innovation Department, Boehringer Ingelheim, Germany

3.1 Abstract

T cell protective immunity is associated with multifunctional memory cells that produce several different cytokines. Currently, our understanding of when and how these cells are generated is limited. We have used an influenza virus mouse infection model to investigate whether the cytokine profile of memory T cells is reflective of primary responding cells or skewed towards a distinct profile. We found that, in comparison to primary cells, memory T cells tended to make multiple cytokines simultaneously. Analysis of the timings of release of cytokine by influenza virus-specific T cells, demonstrated that primary responding CD4 T cells from lymphoid organs were unable to produce a sustained cytokine response. In contrast CD8 T cells, memory CD4 T cells, and primary responding CD4 T cells from the lung produced a sustained cytokine response throughout the restimulation period. Moreover, memory CD4 T cells were more resistant than primary responding CD4 T cells to inhibitors that suppress T cell receptor signalling. Together, these data suggest that memory CD4 T cells display superior cytokine responses compared to primary responding cells. These data are key to our ability to identify the cues that drive the generation of protective memory CD4 T cells following infection.

3.2 Introduction

Immunological memory provides superior immune protection from pathogens for two reasons. First, there are more pathogen-specific cells present in the memory as compared to the naïve compartment. Second, memory cells are intrinsically different from naïve cells: they are located in peripheral organs as well as secondary lymphoid organs; are more sensitive to activation signals; and provide a more tailored response[21, 62].

This tailored response is defined by the effector cytokines T cells express and is one of the main mechanisms of T cell-mediated immune protection. The ability to track antigen-specific T cells via their cytokine profile is essential to understand their protective potential. This cytokine profile is shaped by pathogen-triggered signals during the primary response[63]. These signals drive the effector cytokine production, such as interferon (IFN)γ, interleukin (IL)-4 or IL-17, most effective at co-ordinating pathogen control[62, 64].

Multiple studies demonstrate that memory T cells can develop from differentiated, effector cytokine producing cells[65-68]. However, there is also evidence that the least differentiated cells are more likely to enter the memory pool suggesting that these cells may dominate the memory pool[69-71]. Such cells may not, however, offer the best protection. The most effective memory T cells are thought to be cells that produce high levels of a range of different cytokines, termed poly or multifunctional T cells[22-24, 32]. While it is not yet clear why multifunctional memory T cells offer the most effective protection, their ability to produce cytokines, such as IFNγ, that activate innate immune cells, and IL-2, which aids T cell proliferation, means they both drive and sustain secondary responses.

Understanding the relationship between primary responding and memory T cells will aid in the design of vaccines that aim to drive protective immunological memory. A major hurdle in characterising pathogen-specific T cells is in their identification. Most studies use either monoclonal T cell receptor (TCR) transgenic CD4 T cells or identify endogenous T cells specific to a single epitope[72-76]. This narrow focus limits the research scope, especially as CD4 T cells are thought to respond to a diverse range of pathogen epitopes[77, 78].

Here we address how the cytokine profile of endogenous polyclonal pathogen-specific effector CD4 and CD8 T cells relates to that of subsequently generated memory T cells. We find that, in comparison to primary effector T cells, memory CD4 T cells have an increased tendency to be multifunctional, display a more sustained cytokine response, and are less sensitive to inhibitors of TCR signalling. Memory CD8 T cells are also more likely to be multifunctional than primary responding cells. However, primary and memory CD8 T cells are similar in the sustainability of the cytokine response and their sensitivity to TCR signalling inhibitors.

3.3 Results

3.3.1 Cytokine producing CD4 T cells decline most dramatically in the lung

The primary immune response is usually followed by a contraction phase in which most activated T cells undergo cell death[79]. Highly differentiated effector cytokine producing T cells are thought to be more likely to undergo apoptosis than less differentiated IL-2 producing cells[74].Moreover, memory cells in peripheral tissue are thought to be more differentiated than those in lymphoid organs and the bone marrow has been proposed as a site of memory T cell maintenance[80-85].

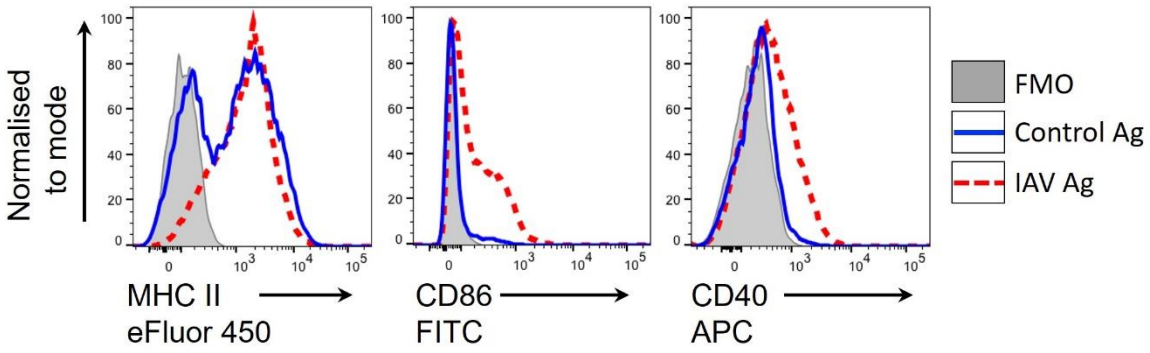

Figure 6 - IAV antigen causes some upregulation of MHC II and costimulatory molecule expression on bmDCs

Bone marrow derived DC were cultured overnight with sonicated IAV infected (red dotted line) or uninfected MDCK cells (blue line). The levels of MHC II, CD86 and CD40 were examined on CD11c+ cells with Frequency Minus One (FMO)s shown in grey. Data are representative of 3 experiments.

To address these assumptions, we examined the *ex vivo* cytokine responses of CD4 and CD8 T cells isolated from mice infected with influenza A virus (IAV) at the peak of the primary responses, day 9, and at two memory timepoints, days 30 and 75. We identified IAV-specific T cells by their ability to produce cytokine following *ex vivo* restimulation with bone marrow derived dendritic cells (bmDCs) incubated overnight with IAV. Incubation of bmDCs with IAV (IAV+ bmDCs) caused minor upregulation of MHC II and costimulatory molecules (Figure 6).

In all organs, we identified populations of IFNγ, TNFα, and IL-2 IAV-specific T cells (Figure 7 and Figure 8). Overall, the number of cytokine+ IAV-specific CD4 T cells declined from the peak response at day 9 and then numbers levelled out (Figure 9A). The decline in numbers of cytokine producing CD4 T cells was most

obvious in the lung for IFNγ+ cells and least obvious in the bone marrow for TNFα and IL-2+ cells, although this organ contained the smallest numbers of cytokine+ cells. Similarly, IAV-specific CD8 T cells declined from day 9 to day 30, although the small number of IL-2+ cells remained fairly constant. After the contraction phase, the numbers of cytokine+ CD8 T cells largely remained steady. For CD4 T cells, the memory cells were predominantly found in the spleen and mediastinal lymph node, while CD8 cytokine+ T cells were mainly found in the spleen.

The dramatic decrease of T cells in the lung could have been due to a large population of IAV-specific T cells within the lung vasculature at day 9. However, by labelling these cells in vivo with fluorescently labelled anti-CD45 shortly before the tissues were harvested[86], we found that more IAV-specific cytokine+ T cells were found in the blood at memory as compared to primary time points (Figure 9B).

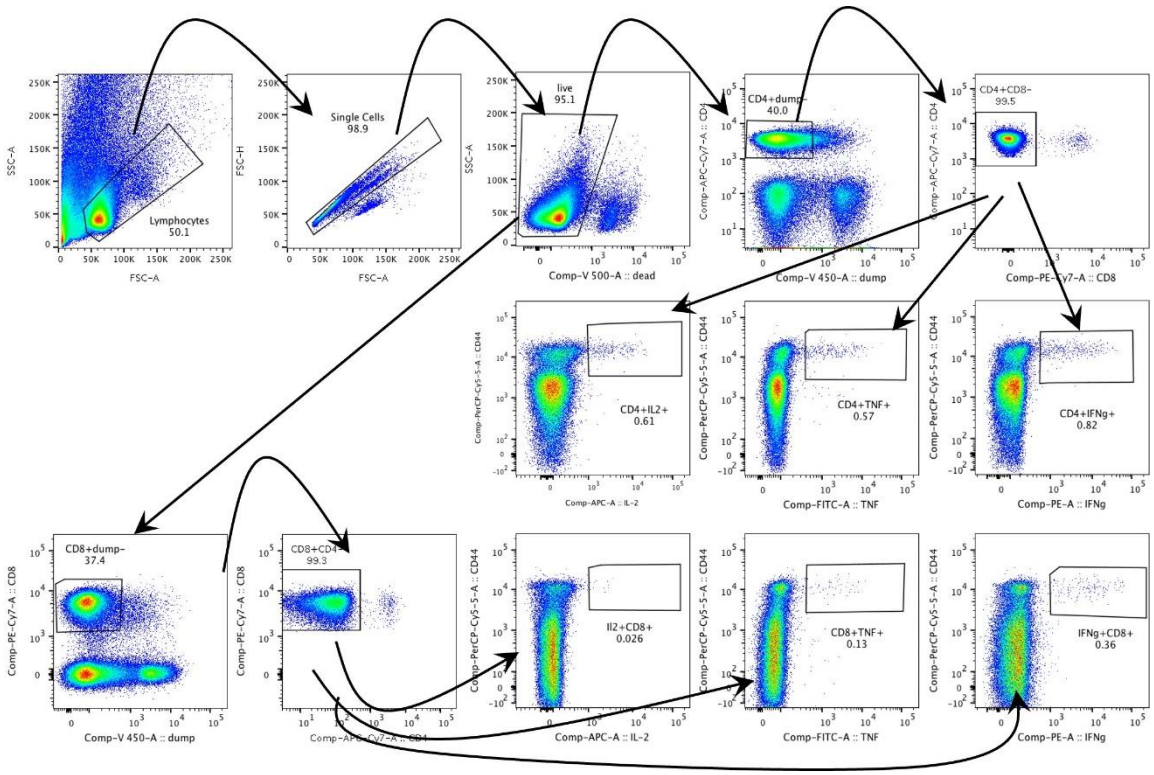

Figure 7 - Gating scheme for T cell cytokine analysis.

Cells are first gated through a lymphocyte gate, then on single cells and live cells. CD4 or CD8 T cells that do not express B220, or MHC II are then gated on before exclusion of cells that are CD8 or CD4 positive respectively. Cytokine positive cells are examined by plotting the cytokine versus the activation marker, CD44.

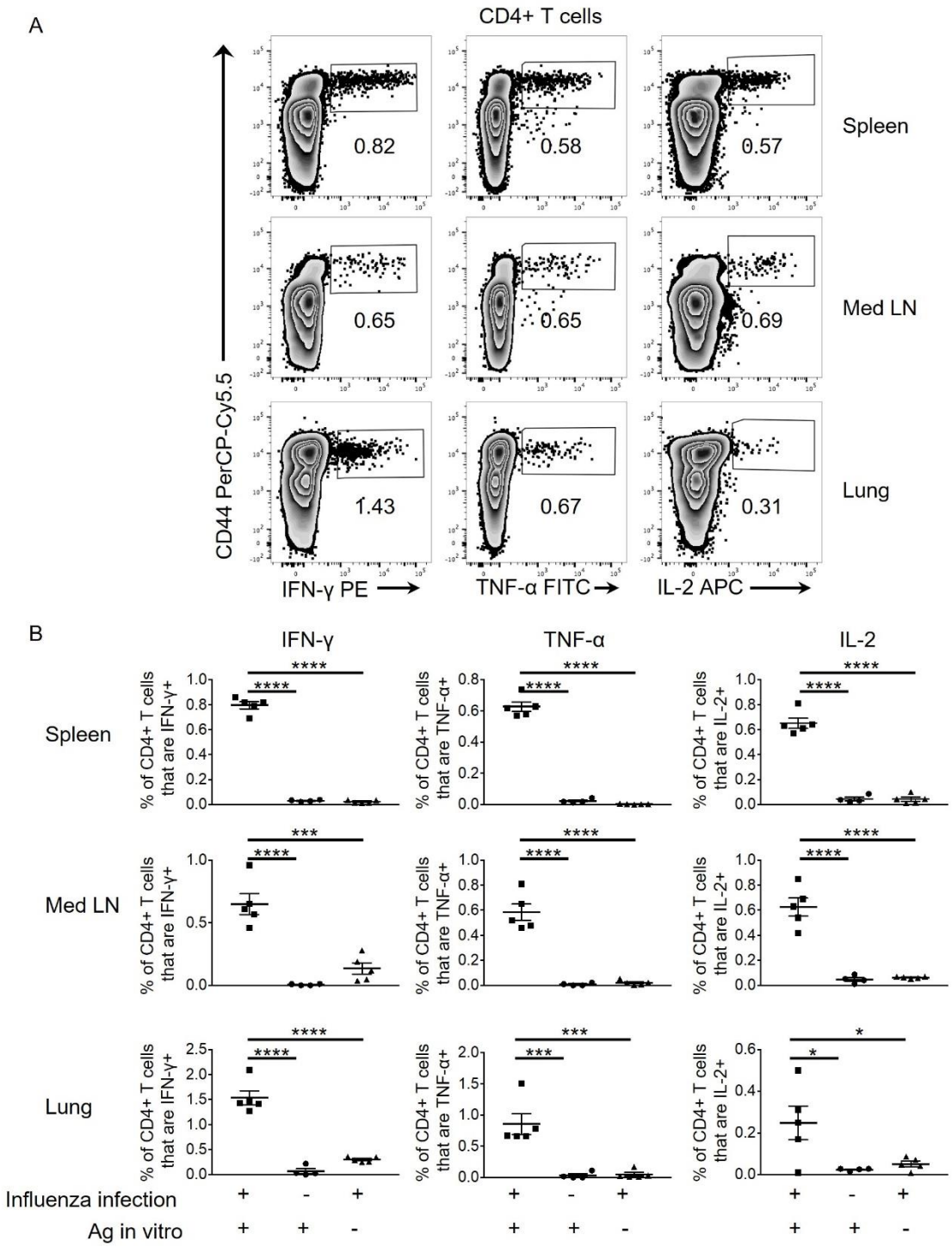
A
CD4+ T cells
Spleen
Med LN
Lung
0.82
0.58
0.57
0.65
0.65
0.69
1.43
0.67
0.31
CD44 PerCP-Cy5.5
IFN-γ PE
TNF-α FITC
IL-2 APC
B
IFN-γ
TNF-α
IL-2
Spleen
Med LN
Lung
% of CD4+ T cells that are IFN-γ+
% of CD4+ T cells that are TNF-α+
% of CD4+ T cells that are IL-2+
Influenza infection
Ag in vitro

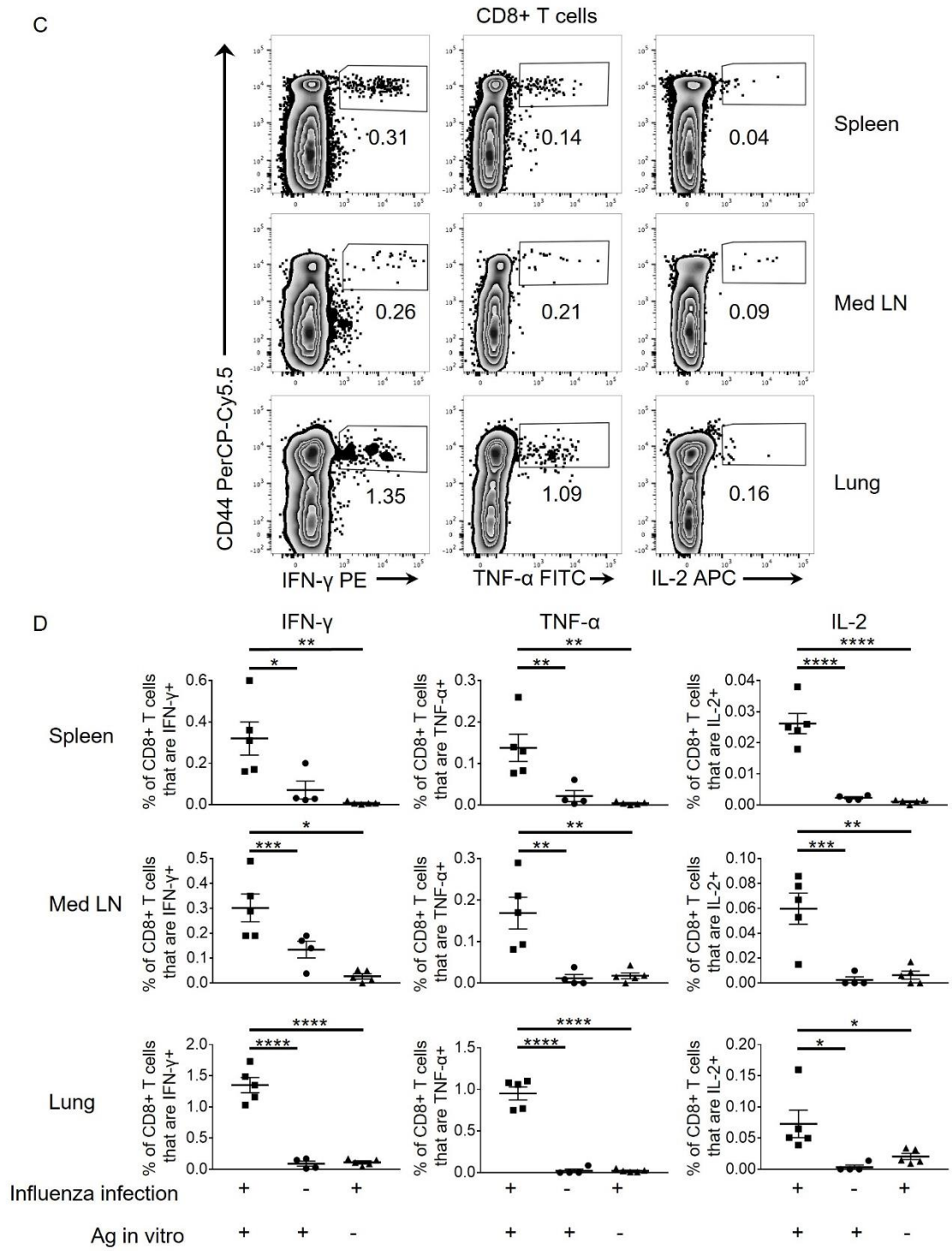

Figure 8 - Identification of influenza virus-specific cytokine producing CD4 and CD8 T cells.

C57BL/6 mice were infected with 200-300PFU of influenza virus (WSN) intranasally. 9 days later, the percentages of IFNγ, TNFα, and IL-2 producing CD4 T cells (A, B) or CD8 T ceslls (C, D) were analysed following a 6 hour co-culture of T cells isolated from the spleen, lymph nodes or lungs of the infected mice with IAV+ bmDCs. Data are representative of three experiments with 4-6 samples per timepoint. Cells are gated on live dump negative CD4 or CD8 T cells and the numbers show the percentages of cytokine positive cells in the indicated gates.

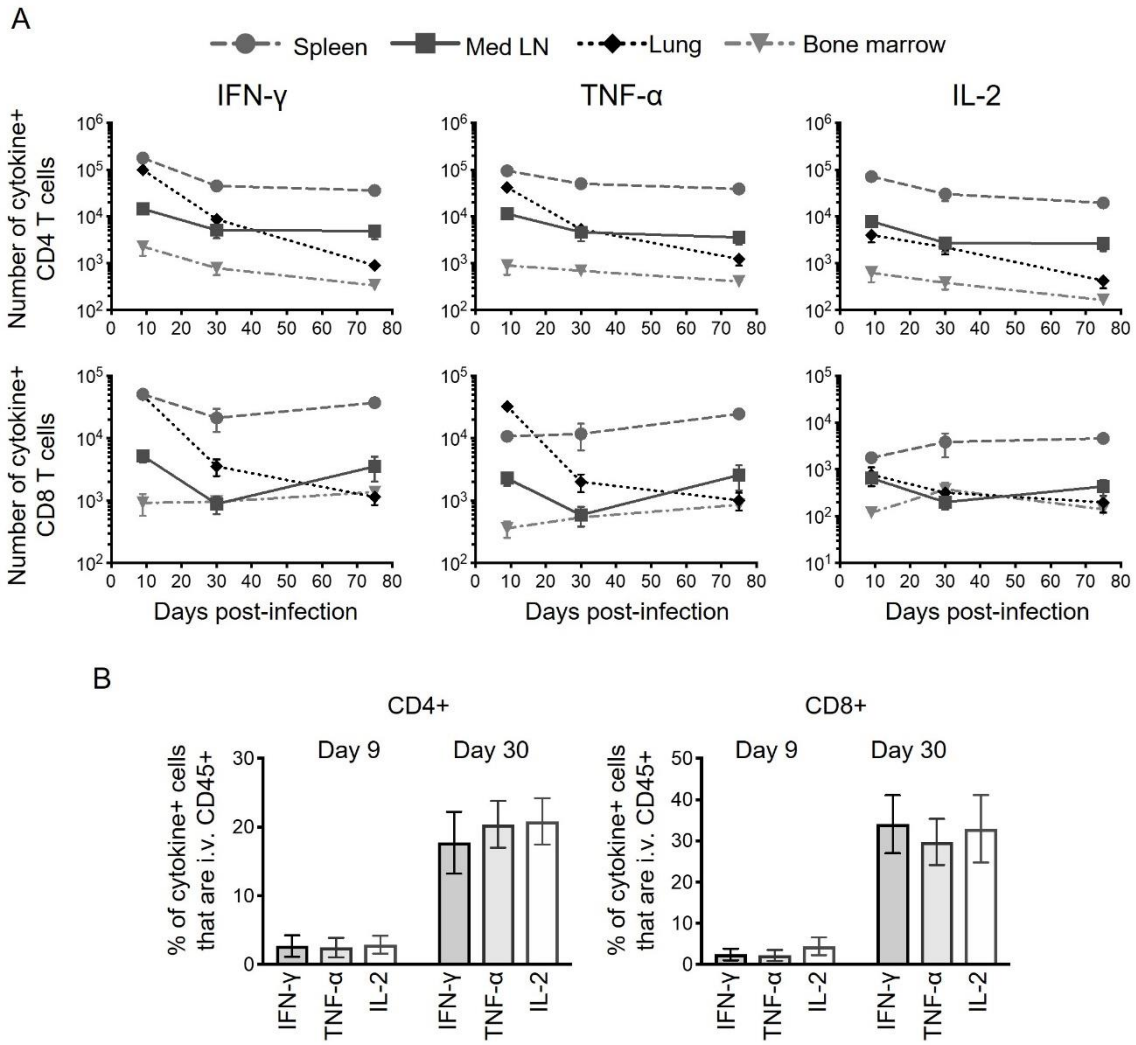

Figure 9 - Cytokine producing IAV-specific memory CD4 and CD8 T cell numbers stabilise in lymphoid organs but continue to decline in the lung.

C57BL/6 mice were infected with IAV and 9, 30 or 75 days later the IAV-specific cytokine+ T cells were examined by flow cytometry following 6 hours restimulation with IAV+ bmDCs. Mice were injected with fluorescently labelled anti-CD45 shortly before tissues were harvested. In A, each point represents the mean of 8-9 mice combined from two independent experiments; error bars are SEM and numbers are the absolute numbers of indicated cell types present in each organ. In B, the percentages of cytokine+ CD4 and CD8 T cells that bound to the injected anti-CD45+ and were IFNγ+ at days 9 and 30 are shown; each point represents one mouse and the line shows the mean of the group. Data are combined from 3 experiments with 3-4 mice per group.

Together these data confirm that, as expected, cytokine+ T cells contract from the peak of disease. However, our data suggests that cytokine+ memory T cells in lymphoid organs are just as likely as those from peripheral tissues to make effector cytokines. We did not observe preferential survival of memory CD4 or CD8 T cells in the bone marrow and, given the small numbers of memory CD4 T cells present in the bone marrow did not pursue these cells further.

3.3.2 Memory T cells are more likely to be multifunctional than primary responding T cells

Given that IL-2, particularly autocrine IL-2, is thought to support memory T cell development[74], we expected to see an increased proportion of IL-2 producing T cells in the memory pool. We did not observe a dramatic shift towards IL-2+ IAV-specific CD4 T cells within the memory pool (Figure 9). Rather, similar numbers of IAV-specific cells identified by any one of the three cytokines suggested that these may be the same cells that produce all three cytokines. To address this, we examined the combined cytokine producing capacity of individual cells in both the primary and memory response.

For CD4 T cells, we observed a consistent increase in the proportion of multifunctional cytokine+ cells that produced IFNγ, TNFα, and IL-2 in all three organs examined (Figure 10). This shift was associated with a reduction in single IFNγ+ cells. At day 9, minimal IL-2 was made by CD8 T cells. However, memory CD8 T cells are more likely to make IL-2 than primary responding cells[18, 71, 87]. We confirmed this and found that, as with the CD4 T cell response, the memory CD8 T cell pool was more likely to contain multifunctional CD8 T cells.

The increase in multifunctional T cells in the memory pool observed in the lung could have been due to the increased proportion of cells in circulation rather than a shift in multifunctionality in cells within the lung itself. However, for both CD4 and CD8 T cells we found similar proportions of multifunctional cells within the i.v. injected CD45 positive and negative fractions 30 days post-infection. This demonstrates that circulating and tissue resident populations displayed similar multifunctional characteristics and supports the idea that memory cells, regardless of location, shift towards increased multifunctionality (Figure 10D and Figure 11).

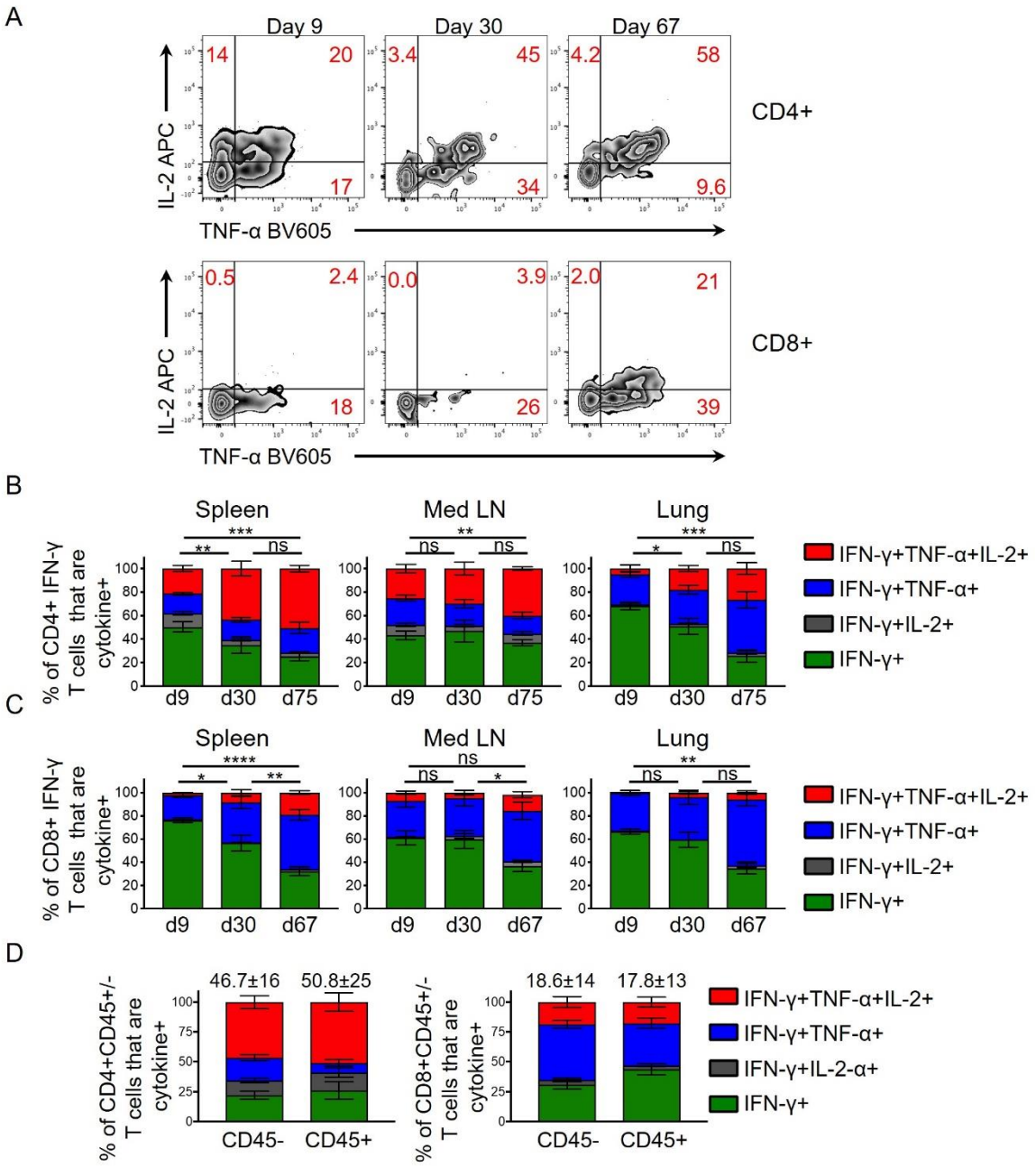

Figure 10 - Multifunctional CD4 and CD8 T cells increase in proportion from the primary to the memory pool.

Mediastinal lymph nodes, spleens and lungs were taken from C57BL/6 mice 9, 30 and 75 days post-infection with IAV. The percentages of IFNγ+ CD4 and CD8 T cells that also expressed IL-2 and/or TNF-α were determined following 6 hours stimulation with IAV+ bmDCs. In A, spleen cells are gated on live CD4 or CD8 dump negative lymphocytes that are IFNγ+; representative FACS plots from 3 experiments with 3-5 mice per group. In B and C data are from two time course experiment with a total of 8-9 mice/group/timepoint. In D, mice infected with IAV 30 days previously were injected i.v. with fluorescently labeled anti-CD45 3 minutes prior to euthanasia and lung cells stimulated and examined as in A. and numbers show mean+SD of the triple+ population. Data in D are from 3 experiments with a total of 10 mice. Samples were analysed by ANOVA followed by a Tukey's multiple comparison test: *: $p<0.05$; **$p<0.01$; ***$p<0.001$; ****$p<0.0001$.

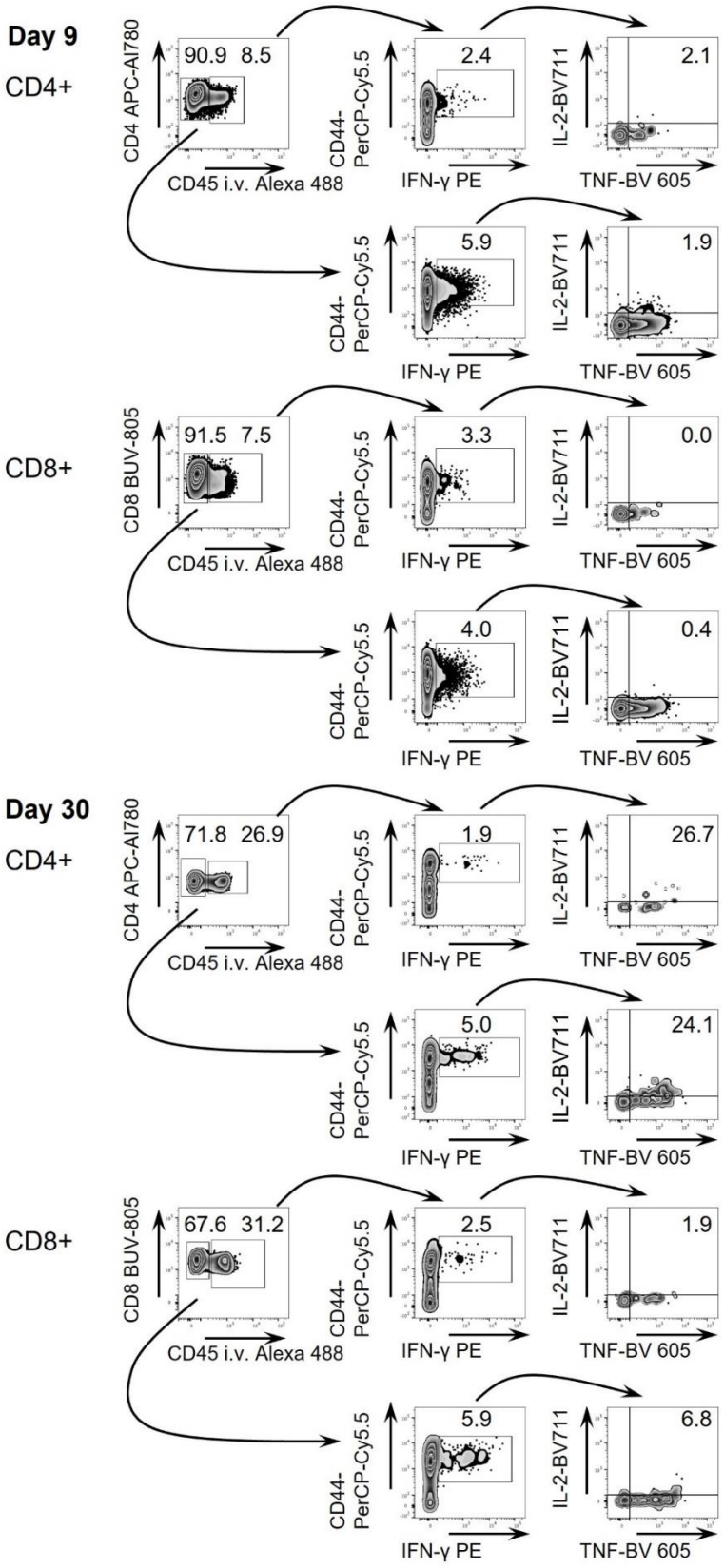

Figure 11 - The proportion of IAV-specific T cells that are present in lung vasculature increases from day 9 to day 30.

C57BL/6 mice were infected with IAV and 9 or 30 days later fluorescently labelled anti-CD45 was injected i.v. 3 minutes before tissues were harvested and single cell suspensions from the lung co-cultured with IAV+ bmDCs for 6 hours. Cells are gated as in SF2 and on CD4 or CD8 cells as indicated and then through subsequent gates as shown on either CD45+/- cells to determine the proportions of these cells that were IFNγ+, and the proportions of IFNγ+ cells that also expressed IL-2 and TNF-α. The numbers on the FACS plots show the percentages of cells in the indicated gates or quadrants. Data are from 3 experiments with 3-4 mice per group.

3.3.3 The dynamics of T cell cytokine release reveals functional maturation of CD4, but not CD8, T cells

To investigate the dynamics of cytokine production by T cells, we analysed the kinetics of cytokine secretion during the *ex vivo* restimulation. T cells from mice infected with IAV 9 or 30 days previously were activated with IAV+ bmDCs, and Golgi Plug added at the start of the incubation, two or four hours later. Cells were analysed two hours after the addition of Golgi Plug.

Primary responding and memory CD8 T cells produced sustained or increased levels of cytokine, most notably IFNγ, throughout the restimulation period. However, primary responding CD4 T cells from lymphoid organs produced less cytokine at 4-6 hours than at 2-4 hours post-stimulation (Figure 12: IFNγ and Figure 13: TNFα and IL-2). These data suggest that anti-viral CD4 T cells have a less sustained cytokine response than CD8 T cells.

In contrast, lung primary responding CD4 T cells produced sustained levels of cytokine suggesting that CD4 T cells from peripheral organs have altered regulation of their cytokine responses compared to those from lymphoid organs (Figure 12 and Figure 13). Interestingly, memory CD4 T cells, regardless of their source, displayed sustained cytokine responses with similar percentages of cells producing cytokine throughout the restimulation culture. These data suggest that memory CD4 T cells are functionally more superior than primary responding CD4 T cells.

An alternative explanation for this observation is that the primary responding pool contains a subset of T cells that only produce cytokine between 2-4 hours following restimulation but that this subset is missing from the memory pool. To investigate this, we calculated the proportion of the number of CD4 T cells producing IFNγ at 2-4 hours out of the number of IFNγ+ CD4 T cells found throughout the whole restimulation period (i.e. Golgi plug present from 0-6hours). These percentages were similar between the primary and memory CD4 T cells regardless of which organ was examined (Figure 14). These data suggest that there are similar proportions of the whole population responding at 2-4hours in the primary and memory CD4 T cells.

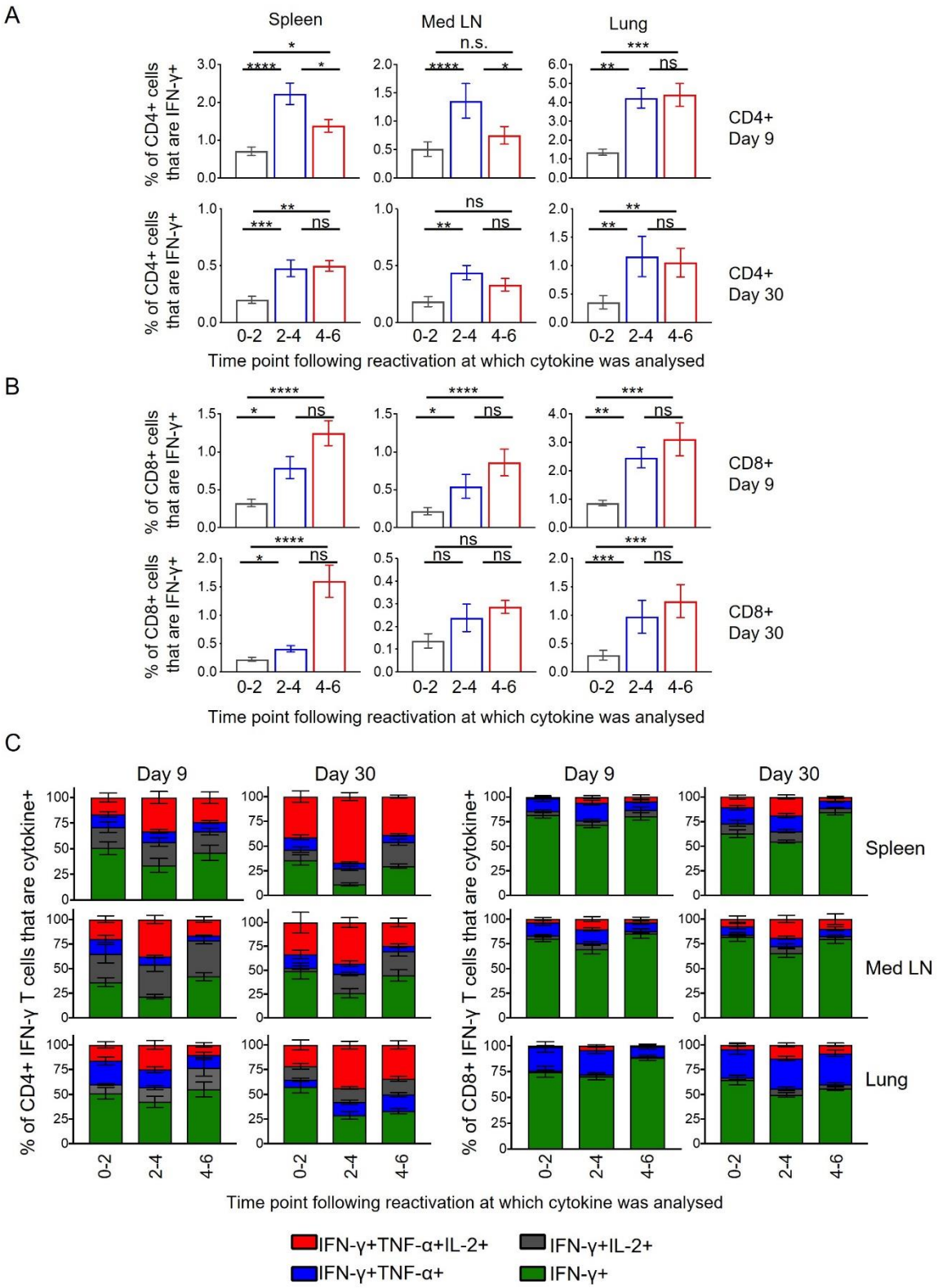

Figure 12 - Memory CD4 T cells demonstrate more sustained cytokine production than primary responding cells.

Mediastinal lymph nodes, spleens and lungs were taken from C57BL/6 mice 9 and 30 days post-infection with IAV and reactivated *in vitro* with IAV+ bmDCs for 2, 4 or 6 hours in the presence of Golgi plug for the last 2 hours of culture. The percentages of IFNγ+ CD4 (A) and CD8 T cells (B) or IFNγ+ CD4 and CD8 T cells that also expressed IL-2 and/or TNFα (C) were examined at the indicated time points. Error bars show SEM. Data are combined from 3 experiments/timepoint with 4 mice/timepoint. Samples were analysed using a Friedman's paired test followed by a Dunn's multiple comparison test *: $p<0.05$; **$p<0.01$; ***$p<0.001$; ****$p<0.0001$.

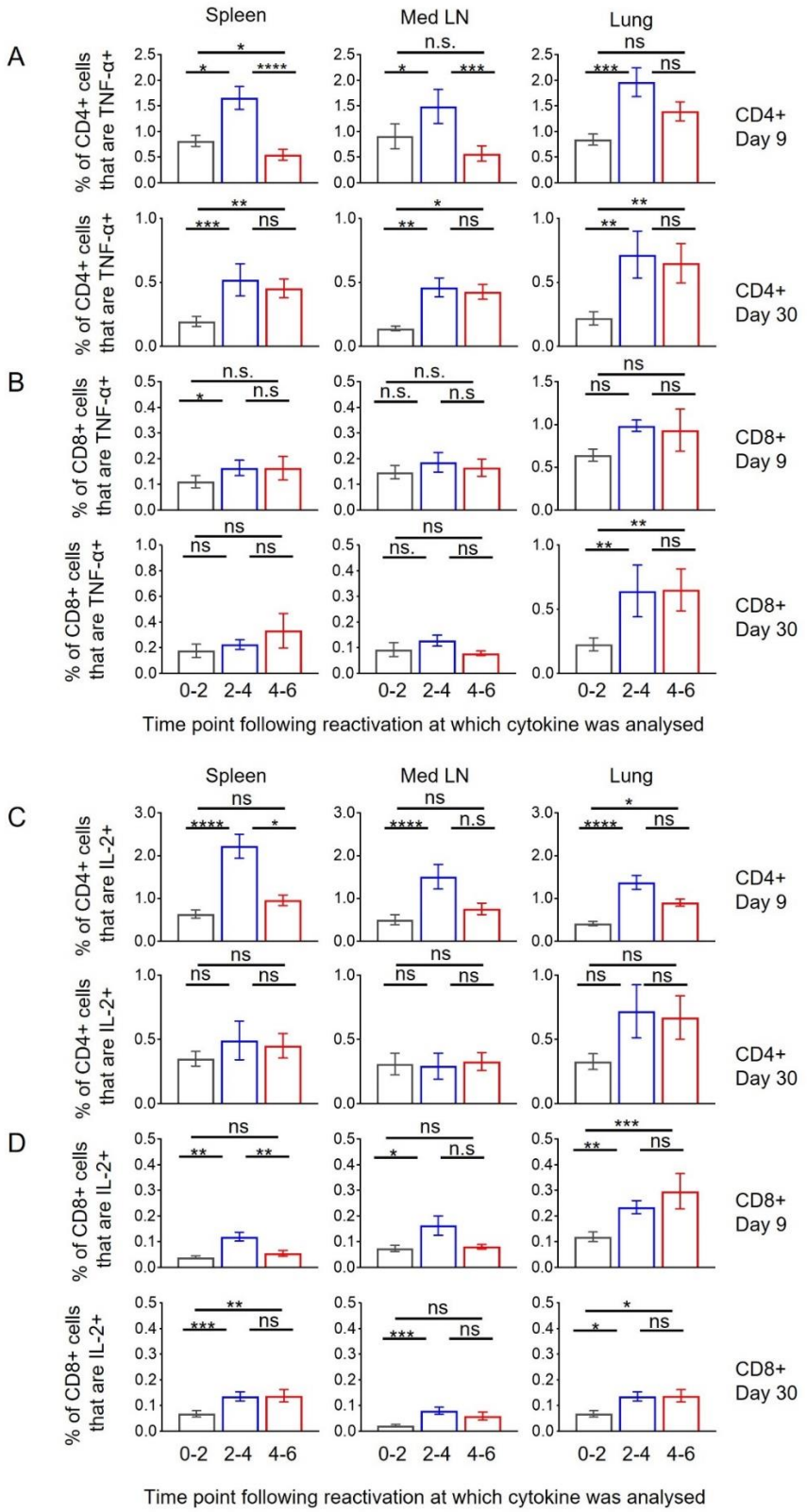

Figure 13 - Memory CD4 T cells demonstrate more sustained cytokine production than primary responding cells.

Mediastinal lymph nodes, spleens and lungs were taken from C57BL/6 mice 9 and 30 days post-infection with IAV and reactivated in vitro with IAV+ bmDCs for 2, 4 or 6 hours in the presence of Golgi plug for the last 2 hours of culture. The percentages of TNFα+ (A,B) and IL-2+ (C,D) CD4 (A, C) and CD8 T cells (B, D) were examined at the indicated time points. Error bars show SEM. Data are combined from 3 experiments per timepoint with 4 mice per timepoint in each experiment. Samples were analysed using a Friedman's paired test followed by a Dunn's multiple comparison test *: $p<0.05$; **$p<0.01$; ***$p<0.001$; ****$p<0.0001$.

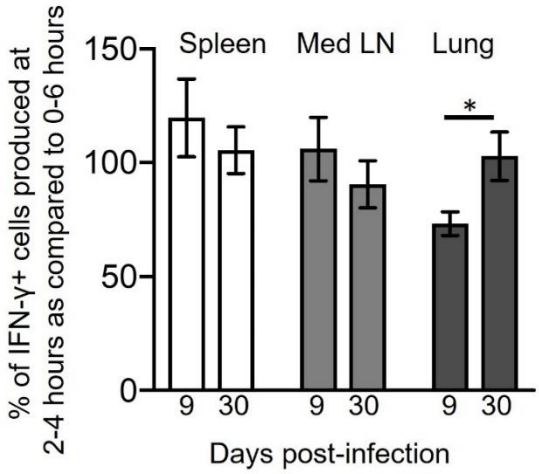

Figure 14 - Similar proportions of CD4 T cells producing IFNγ at 2-4 hours are present in the primary responding and memory T cell pools.

Mediastinal lymph nodes, spleens and lungs were taken from C57BL/6 mice 9 and 30 days post-infection with IAV and reactivated in vitro with IAV+ bmDCs for 4 or 6 hours with Golgi plug present either at 2-4 hours or the whole culture respectively. The numbers of IFNγ+ CD4 T cells present were calculated from the ex vivo counts and the flow cytometry data. The graph shows the percentages of CD4 IFNγ+ cells present at 2-4hours as compared to 0-6hours. Error bars show SEM. Data are combined from 3 experiments per timepoint with 4 mice per timepoint in each experiment. Samples were analysed using an unpaired t-test*: $p<0.05$.

By examining cytokine production across the restimulation culture, we were able to determine whether triple, double and single cytokine producing T cells had similar kinetics of cytokine production. This was the case for CD4 T cells, with all populations present at the three time points examined (Figure 12C). A similar pattern was found for CD8 T cells, although the percentages of multifunctional cells in the primary response were very low. These data show that multifunctional cells are indeed able to produce all three cytokines simultaneously and that these cells have similar kinetics of cytokine release as double and single cytokine producers at primary and memory time points.

3.3.4 PI3kinase inhibitors reveal altered cytokine responses by primary responding and memory CD4 T cells

The different cytokine profiles of IAV-specific CD4 T cells between organs and time points prompted us to investigate whether cytokine production was regulated distinctly in these cells. PI3Kinases (PI3K) play a key role in relating T cell activation to cytokine production [88]. Immune cells uniquely express two of the four isoforms of type I PI3K: PI3K-β, engaged by receptor tyrosine kinases, such as those stimulated by T or B cell receptor ligation; and PI3K-γ, usually activated by G-protein coupled receptors such as chemokine receptors [89]. These

differences in signalling pathways predict that inhibitors that target PI3K-ß, rather than PI3K-γ, are more likely to reduce T cell cytokine responses.

To test the requirement for different PI3K isoforms for cytokine production, we added PI3Kinase inhibitors that target either PI3K-γ or PI3K-ß to the restimulation co-culture. Cytokine responses by primary responding and memory IAV-specific CD4 and CD8 T cells from all organs were consistently reduced by the PI3K-ß inhibitor (Figure 15). In contrast, the PI3K-γ inhibitor had little or no effect on cytokine production.

To investigate whether the inhibitors affected the three different cytokines distinctly and whether these were different between primary and memory cells, we calculated the percentages of cytokine response for each organ from each sample to that in the relevant DMSO control (Figure 16). For both CD4 and CD8 T cells, IFNγ tended to be least affected and TNF-α most likely to be reduced for CD4 T cells and IL-2 most reduced for CD8 T cells. Memory CD4 T cells from the spleen and lung were less sensitive to the inhibitors than primary T cells. This pattern was much less apparent for memory CD8 T cells with only IL-2 responses in the lung and mediastinal lymph node less affected in the memory as compared to the primary response by the P3K-γ and PI3K-ß inhibitors respectively.

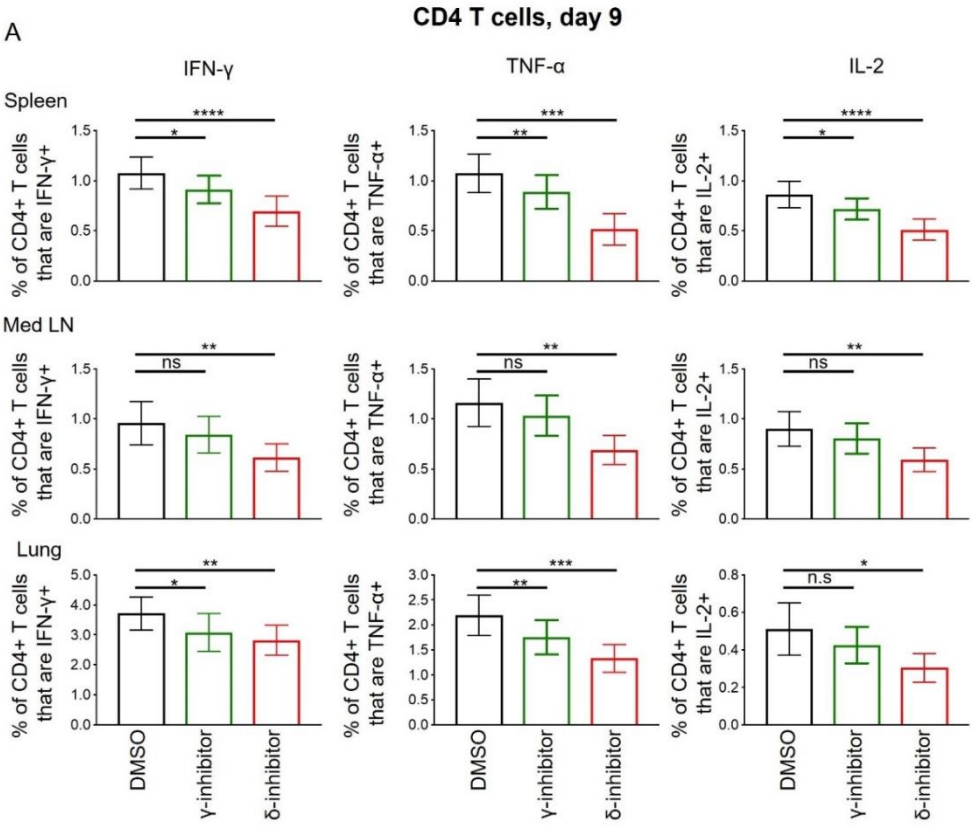
A
CD4 T cells, day 9
IFN-γ
TNF-α
IL-2
Spleen
Med LN
Lung
% of CD4+ T cells that are IFN-γ+
% of CD4+ T cells that are TNF-α+
% of CD4+ T cells that are IL-2+
DMSO
γ-inhibitor
δ-inhibitor

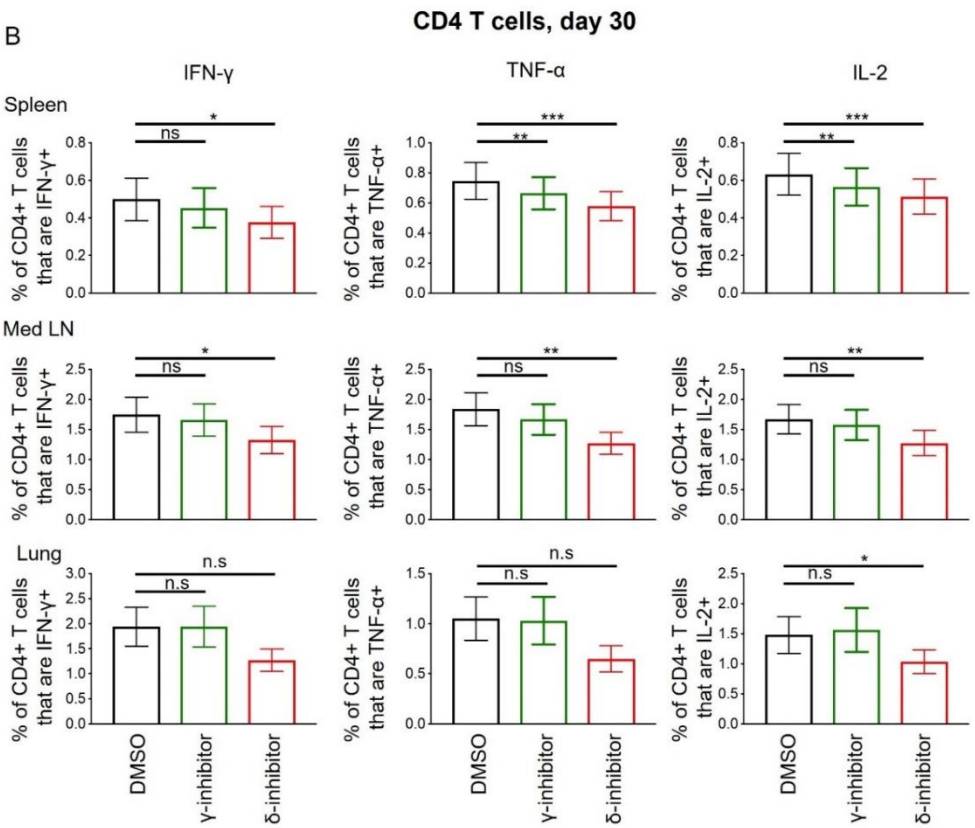
B
CD4 T cells, day 30
IFN-γ
TNF-α
IL-2
Spleen
Med LN
Lung
% of CD4+ T cells that are IFN-γ+
% of CD4+ T cells that are TNF-α+
% of CD4+ T cells that are IL-2+
DMSO
γ-inhibitor
δ-inhibitor

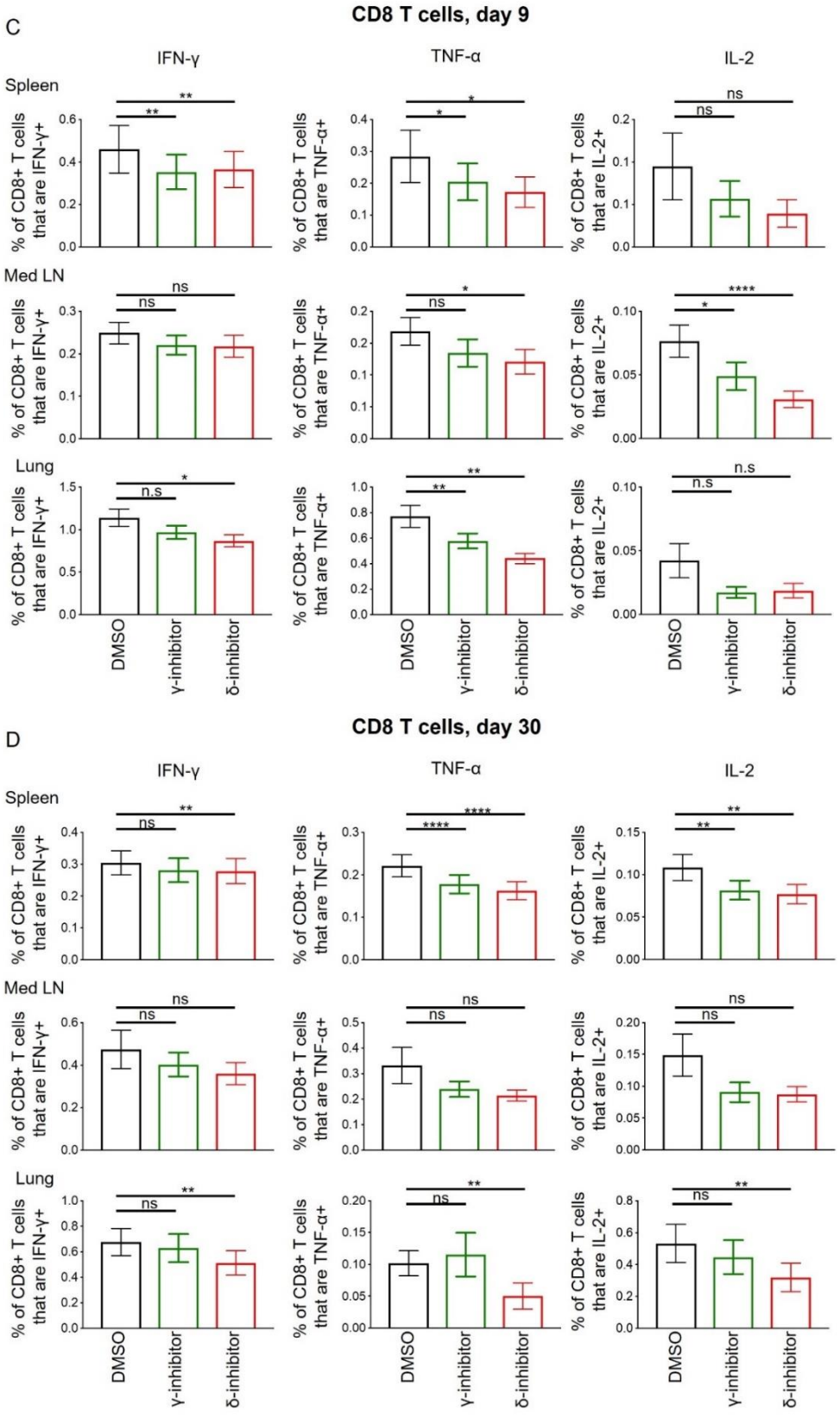

Figure 15 - PI3Kinase delta inhibitor reduces the proportion of cytokine producing T cells.

C57BL/6 mice were infected with IAV and 9 (A, C) or 30 (B, D) days later the percentages of IFNγ, TNFα, and IL-2 producing CD4 T cells (A, B) or CD8 T cells (C, D) were analysed following a 6 hour co-culture in the presence of the indicated PI3Kinase inhibitors of T cells isolated from the spleen, lymph nodes or lungs of the infected mice with bmDCs cultured overnight with sonicated influenza antigen. The data are combined from 3 independent experiments per time point with 4-5 samples per timepoint per experiment. Error bars are SEM and samples were analysed using paired ANOVA with Dunnett's multiple comparison test *: p<0.05; **p<0.01; ***p<0.0001; ****p<0.0001.

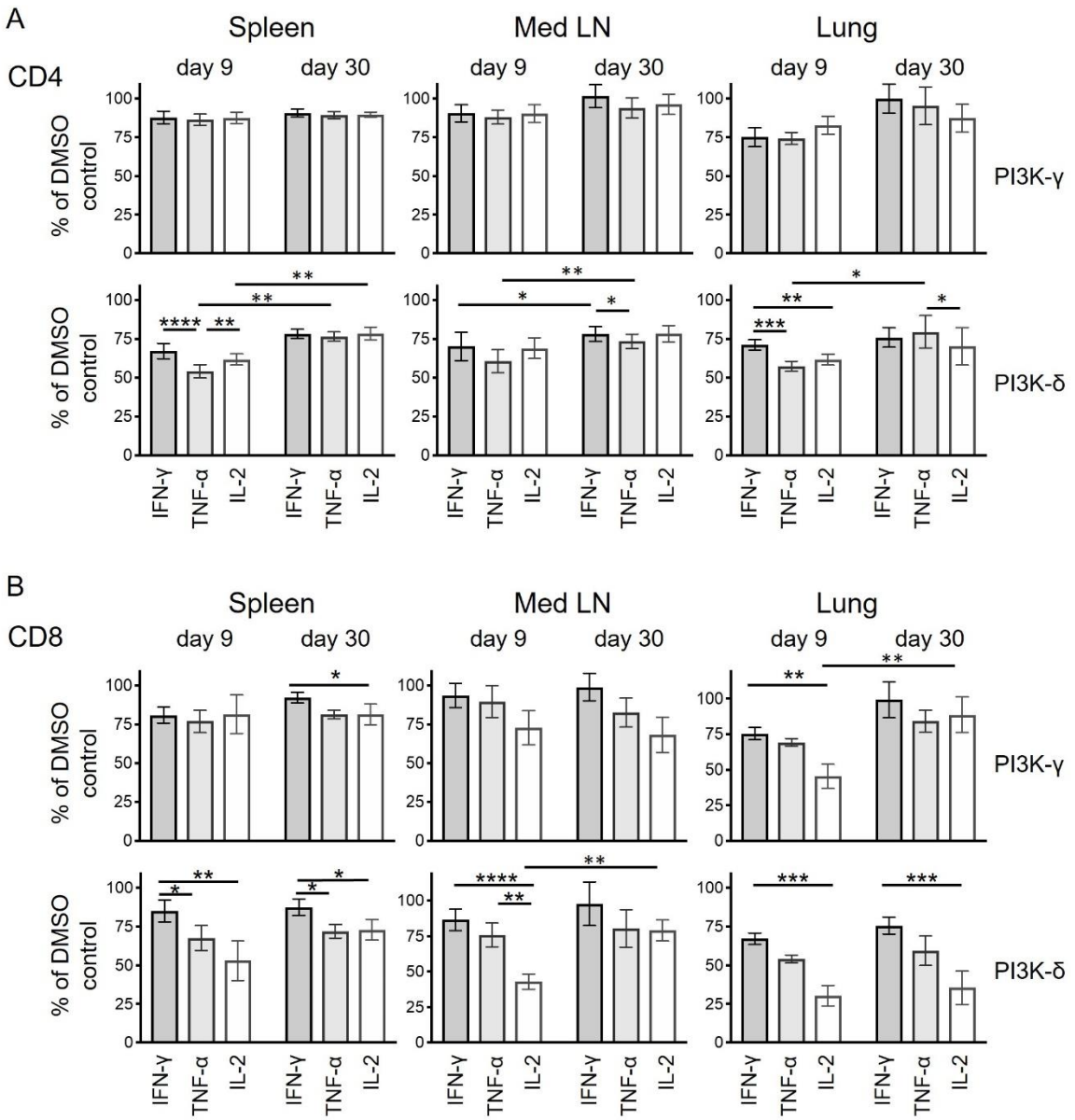

Figure 16 - Memory CD4 T cell cytokine production is less affected by PI3Kinase inhibitors than primary responding CD4 T cells.

T cells from the spleen, medLN and lung were isolated from C57BL/6 mice infected with IAV either 9 or 30 days previously and reactivated with IAV+ bmDCs for 6 hours in the presence of Golgi plug and the indicated PI3Kinase inhibitor. The percentages of cytokine+ CD4 (A) and CD8 (B) T cells in each sample in comparison to that sample's DMSO control was calculated. Data are combined from 3 independent experiments at each timepoint with 4-5 samples per experiment per timepoint, expect that some samples were removed from the primary responses due to lack of IL-2+ cells in the DMSO control: one sample removed from the CD4 T cell lung analysis; one sample removed from the CD8 medLN analysis; and two from the lung analysis. Comparisons between cytokines within a timepoint were made using paired Friedman test with Dunn's multiple comparison; comparisons between timepoints were calculated using a Kruskal-Wallis with Dunn's multiple comparison test. *: $p<0.05$; **$p<0.01$; ***$p<0.001$; ****$p<0.0001$.

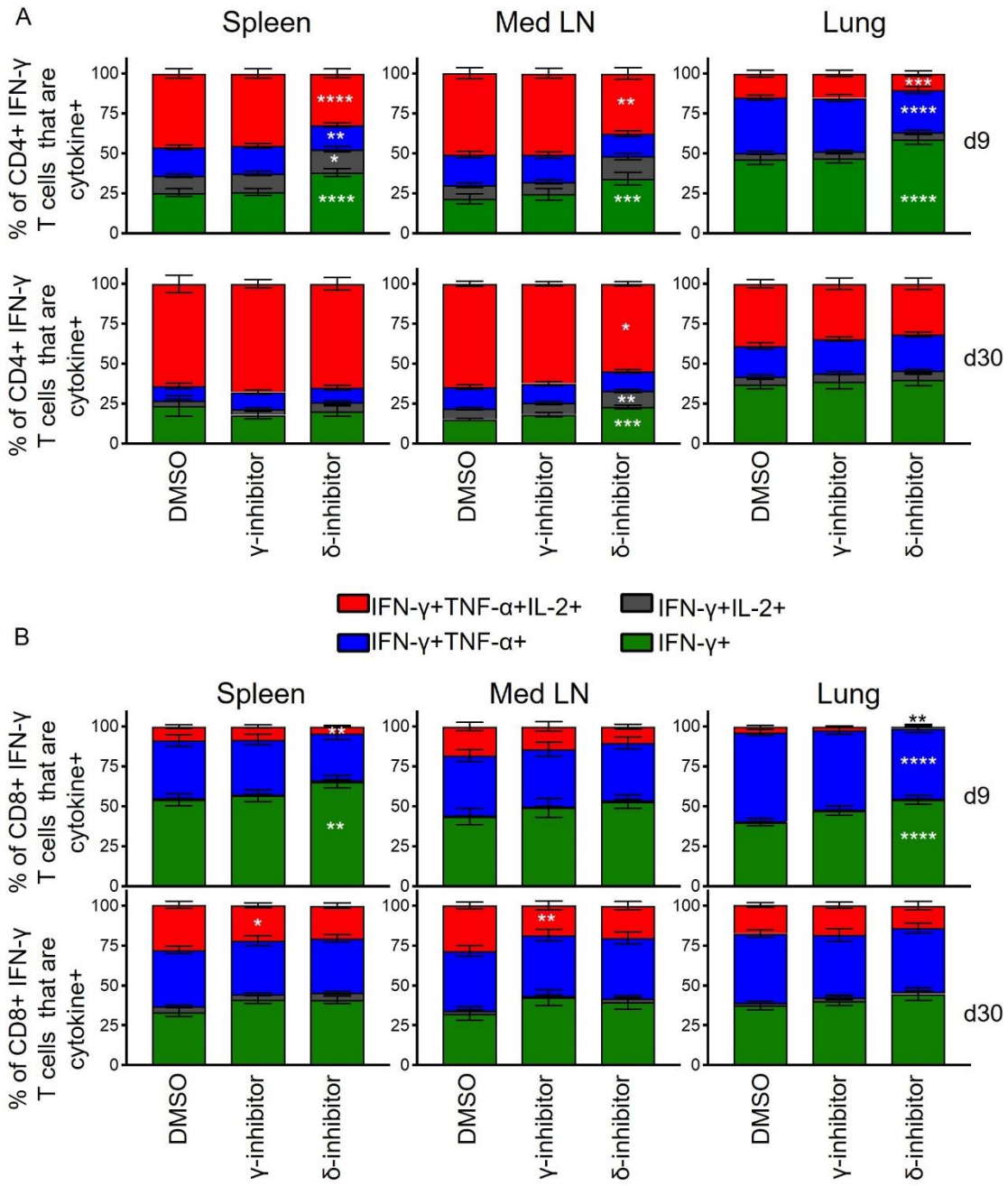

Figure 17 - Multifunctional memory CD4 T cells are less affected by PI3Kinase inhibitors than primary responding cells.

T cells from the spleen, medLN and lung were isolated from C57BL/6 mice infected with IAV either 9 or 30 days previously and reactivated with IAV+ bmDCs for 6 hours in the presence of Golgi plug and the indicated PI3Kinase inhibitor. The percentages of IFNγ+ CD4 (A) and CD8 (B) T cells that also produced TNF-α and/or IL-2 were examined. Data are combined from 3 independent experiments at each timepoint with 4-5 samples per experiment per timepoint. Samples were analysed using an ANOVA with Bonferroni's multiple comparison test comparing each inhibitor to the DMSO control *: $p<0.05$; **$p<0.01$; ***$p<0.001$; ****$p<0.0001$.

We also examined how the inhibitors affected the proportion of single, double and triple cytokine producing T cells (Figure 17). As IFNγ was least affected by the inhibitors, it was not surprising that the proportion of IFNγ single+ CD4 T cells increased in the presence of the PI3K-ß inhibitor. This pattern was apparent in all organs in the primary response but only slightly altered in

memory CD4 T cells from the mediastinal LN and not at all in memory CD4 T cells from the spleen and the lung.

In contrast, the effects of the inhibitors were less clearly distinct between primary and memory CD8 T cells. Triple cytokine producing cells were slightly reduced by the PI3K-ß inhibitor in spleen and lung in primary CD8 T cells and not at all in memory CD8 T cells. Surprisingly the PI3K-γ inhibitor reduced the triple cytokine positive population in in the memory T cells isolated from the spleen and mediastinal LN. Overall, these data again highlight the functional superiority of CD4, but not CD8, T cell cytokine production in the memory as compared to the primary pool.

3.4 Discussion

Our data demonstrate that memory cytokine producing IAV-specific CD4 T cells have distinct characteristics from the population of activated CD4 T cells from which they are generated. Memory CD4 T cells were much more likely to demonstrate characteristics of multifunctional T cells, produced sustained cytokine responses, and were less reliant on signals mediated by PI3Kinase-ß to produce cytokine. Interestingly, primary responding lung CD4 T cells did display a sustained cytokine response, suggesting that these cells may be regulated distinctly from those in lymphoid organs.

In contrast, while we confirm that CD8 memory T cells are more likely to produce IL-2[18, 71, 87], their sensitivity to PI3Kinase inhibitors was broadly similar to primary responding cells. Moreover, primary and memory CD8 T cells displayed similar kinetics in their cytokine secretion with a sustained or increasing response evident throughout the six hour restimulation. Together, these data show that, based on these parameters, memory CD4, but not CD8 T cells display superior behaviours than primary responding cells.

In all organs, we found that T cells could produce effector cytokines, indicating that effector memory T cells were as likely to be found in lymphoid as non-lymphoid organs. The increased proportion of triple cytokine+ CD4 and CD8 T cells suggests that these cells may preferentially survive. Alternatively, these cells may mature into this phenotype following contraction, or have improved

survival over time. This last hypothesis is supported by the continued increase in the proportion of multifunctional cells from day 30 to day 75 in some organs. It is experimentally difficult to discriminate between these possibilities. There are no surface markers that discriminate between the cytokine+ populations and neither cytokine secretion assays nor reporter mice can discriminate between single, double and triple producers.

It is not clear why multifunctional T cells increase within the memory pool. Potentially the production of IL-2 provides autocrine survival signals[74]. However, if autocrine IL-2 production was sufficient, we would expect an increased predominance of IL-2 single or double producing cells. This was not the case suggesting that other factors, potentially working with IL-2, promote memory T cell generation and/or survival. Whether these factors are directly linked to the co-production of these three cytokines or multifunctional cytokine production is merely a marker, is currently unclear. One potential explanation is that the repertoire of the memory pool is skewed towards specificities that are more likely to be multifunctional. However, there is little evidence for a loss of breadth within the IAV CD4 T cell response from the peak to day 60 post-infection[78].

Previous studies have compared the cytokine profiles of activated and memory CD4 T cells and found similar cytokine profiles between primary and memory populations[90, 91]. In these cases, T cells in lymphoid organs were analysed and only a single epitope examined. This limits the breadth of these analyses potentially explaining differences with our data. Indeed, precursor frequency and epitope specificity are likely to influence cytokine response[75].

We believe analysing a polyclonal antigen-specific population, rather than a single epitope response, is an advantage. It is likely, however, that our assay does not identify all responding IAV-specific T cells as some epitopes may not be generated by the bmDCs[92] and we are unable to identify IAV-specific T cells that do not produce cytokine. Our data on CD8 T cells do, however, correlate with findings from studies using immunodominant IAV epitopes[18, 71, 87]. A further caveat to our study is that the longest time period of *in vitro* reactivation examined was six hours. It will be important to examine longer reactivation periods enabling a greater understanding of the difference between primary

responding and memory T cells in terms of their ability to produce a sustained cytokine response.

The reduced sensitivity of memory CD4 T cells to the PI3K inhibitors and their more sustained cytokine response suggests that these cells are less reliant on strong activation signals than primary responding cells. This may be a consequence of increased expression of the key signalling molecule, Zap70[93], or altered association of signalling molecules within lipid rafts[94]. Previous studies demonstrated reduced T cell activation and cytokine responses in either the absence of PI3Ks or in the presence of inhibitors[95-99]. However, in these studies, the effect of the loss of PI3K signalling on cytokine production by CD4 T cells could not be uncoupled from initial effects on T cell priming. In contrast, we have directly demonstrated that inhibition of PI3K-ß reduces TCR driven cytokine responses.

Currently, PI3K inhibitors are being tested in clinical trials for chronic inflammatory lung diseases including chronic obstructive pulmonary disease and asthma[100]. IAV-triggered exacerbations are a major cause of hospitalisation in these patients[101]. As IFNγ+ IAV-specific memory CD4 and CD8 T cells have been associated with protection from disease following IAV infection in humans, it is unlikely that PI3K inhibitors will interfere with protective T cell memory[35, 37, 58, 84, 102]. In contrast, primary virus-specific immune responses may be more likely to be reduced by PI3K inhibitors and the cells most likely to be affected are those most associated with immune protection, multifunctional cytokine producing T cells. Choosing the most effective PI3K inhibitor that has the least impact on T cell cytokine production is an important clinical consideration. The PI3K-γ inhibitor had only a limited effect on T cell cytokine responses suggesting it offers a good compromise.

In summary, our data demonstrate that the memory T cell pool is not simply a mirror image of the primary response. While the location of these two populations is similar, memory CD4 and CD8 T cells have a greater capacity to make broader cytokine responses. CD4 T cells were also altered in their sensitivity to TCR signalling inhibitors and produced a more sustained cytokine response, suggesting functional maturation as these cells develop into memory

cells. These novel findings pave the way for an improved understanding of the signals that regulate memory CD4 T cell generation.

3.5 Materials and Methods

3.5.1 Animals and infections

10 week old female C57BL/6 mice were purchased from Envigo (UK). They were maintained at the University of Glasgow under standard animal husbandry conditions in accordance with UK home office regulations (Project License P2F28B003) and approved by the local ethics committee. Following one week of acclimatisation, the mice were briefly anesthetised using inhaled isoflurane and infected with 200-300 plaque forming units of IAV strain WSN in 20μl of PBS intranasally (i.n.). IAV was prepared and titred in MDCK cells. Infected mice were weighed daily. Any animals that lost more than 20% of their starting weight were removed from the study and humanely euthanised. Group sizes were based on previous experiments considering the known variability of the anti-viral T cell response, animals that did not lose any weight following infection were excluded.

3.5.2 Tissue preparation

Where indicated, mice were injected intravenously with 1μg of anti-CD45 (30-F11) labelled with Alexa 488 (eBioscience) and euthanised by cervical dislocation 3 minutes later. Alternatively, mice were euthanised with a rising concentration of carbon dioxide and perfused with PBS-5mM EDTA to remove blood cells from the lungs. Spleen and mediastinal lymph nodes were processed by mechanical disruption. Single cell suspensions of lungs were prepared by digestion with 1mg/ml collagenase and DNAse (Sigma) for 40 minutes at 37°C. At day 30, too few cells were recovered from the medLN for the analysis of PI3Kinase inhibitor sensitivity. Therefore, each of the organs from two mice that had lost similar amounts of weight were combined to provide one day 30 sample. In the PI3Kinase inhibitor experiments, T cells were isolated using Stemcell mouse T cell isolation kits following the manufacturer's recommendations.

3.5.3 Influenza virus and control antigen

The IAV antigen was prepared using a similar protocol as descried [103]. Briefly, T75 flasks of 80% confluent MDCK cells were incubated for one hour at 37°C 5% CO_2 with or without an MOI of 0.001 IAV WSN. Virus or control inoculums were removed and cells incubated for a further two days in 12ml of OPTI-MEM supplemented with Pen/Strep and 1.0 µg/mL trypsin-TPCK. 48 hours later, the cells were harvested, spun down, resuspended in 0.1M glycine buffer containing 0.9% NaCl, pH9.75 and shaken at 4°C for 20 minutes, incubated in a sonication bath for 10 seconds intervals 4 times before centrifugation at 2000rpm for 20 minutes at 4°C. Supernatant was aliquoted and frozen at -80°C.

3.5.4 Bone marrow DCs

bmDCs were prepared as described [61]. Briefly, bone marrow cells were flushed from the tibias and femurs of female C57BL/6 mice and red blood cells removed. Cells were cultured in complete RPMI (RPMI with 10% foetal calf serum, 100µg/ml penicillin-streptomycin and 2mM L-glutamine) at 37°C 5% CO_2 in the presence of GM-CSF (prepared from X-63 supernatant [104]) with media supplemented on day 2 and replaced on day 5. On day 7, DCs were harvested, incubated overnight with either control antigen or IAV antigen (MOI of 0.3).

3.5.5 Ex vivo restimulation

Single cell suspensions were co-cultured with bmDCs in complete RMPI at a ratio of approximately 10 T cells to 1 DC in the presence of Golgi Plug (BD Bioscience). Co-cultures were incubated at 37°C, 5% CO_2 for 6 hours unless stated. PI3K inhibitors were used at: PI3K-ß: 100nM; PI3K-γ: 300nM. These concentrations were selected as they are mid-range for the concentrations known to affect T cell responses. All inhibitors were 300-1000-fold selective over other PI3K family members.

3.5.6 Flow cytometry

Cells were harvested and following incubation with Fc block (homemade containing 24G2 supernatant and mouse serum) surface stained with anti-CD4 APC-Alexa 780 (eBioscience; clone: RM4-5), anti-CD44 PerCP-Cy5.5 (eBioscience;

clone: IM7), CD8 PeCy7 (eBioscience; clone: 53-6.7), and “dump” antibodies: B220 (clone: RA3-6B2) and MHC II (clone: M5114) both on eFluor-450 (eBioscience) for 20 minutes at 4°C. Cells were stained with a fixable viability dye eFluor 506 (eBioscience) as per the manufacturer’s recommendations. Cells were fixed with cytofix/cytoperm (BD Bioscience) for 20 minutes at 4°C and stained in permwash buffer with anti-cytokine antibodies for one hour at room temperature (anti-IFNγ PE (clone: XMG1.2;), anti-TNF Alexa-Fluor-488 (clone: MP6-XT22) anti-IL-2 APC (clone: JES6-5H4) all from eBioscience. Following washing with permwash buffer, samples were acquired on a BD LSR or Fortessa and analysed using FlowJo (version 10 Treestar). Data are presented as required for MIFlowCyt.

3.5.7 Statistical analysis

Data were analysed using Prism version 7 software (GraphPad). Differences between groups were analysed by paired or unpaired ANOVAs as indicated in figure legends. In all figures * represents a p value of <0.05; **: p<0.01, ***: p<0.001, ****: p<0.0001.

3.6 Acknowledgments

We thank the staff within the Institute of Infection, Immunity and Inflammation Flow Cytometry Facility and the Joint Research Facility at the University of Glasgow for technical assistance. We thank Drs Georgia Perona-Wright, Edward Hutchinson and David Withers for critically reading the manuscript.

3.7 Funding

This work was supported by an Arthritis Research UK Career Development Fellowship (19905) and a Marie Curie Fellowship (334430) to MKLM, by a DTP-MRC studentship to JIG (MR/JR50032X/1), and by the GLAZgo Discovery Centre.

3.8 Disclosures

MT was an employee of AstraZeneca during the study. CSG has received consulting fees from AstraZeneca (more than $10,000).

3.9 Competing Interest

PI3K inhibitor tools were generated as part of drug discovery projects aimed at modulating pulmonary immune responses. Any subsequent commercial interests had no influence on the design, performance or interpretation of any experiment presented in this body of work.

3.10 Author Contribution

LMW designed and performed experiments, analysed data and edited the manuscript, KM, LM, JIG, and AF performed experiments; MT provided reagents and edited the manuscript; CSG designed research and edited the manuscript, MKLM designed and performed the research, analysed data and wrote the manuscript.

Chapter 4 Multifunctional cytokine production marks influenza A virus-specific CD4 T cells with high expression of survival molecules

Authors
Lotus M Westerhof (1), Jonathan Noonan (2), Kerrie E Hargrave (1), Elizabeth T Chimbayo (1,3), Zhiling Cheng (1,‡), Thomas Purnell (1), Mark R Jackson (4), Nicholas Borcherding (5), Megan KL MacLeod (1*)

Affiliations
1 - School of Infection and Immunity, University of Glasgow, Glasgow, UK

2 - Baker Heart and Diabetes Institute & Baker Department of Cardiometabolic Health, University of Melbourne, Melbourne, Australia

3 - Malawi Liverpool Wellcome Centre, Blantyre, Malawi

4 - School of Cancer Sciences, University of Glasgow, Glasgow, UK

5 - Department of Pathology and Immunology, Washington University, St Louis, USA

‡ Current address: ZC: Pharmacology Research, BeiGene, Shanghai, China.

* Corresponding author: Megan KL MacLeod, B515 SGDB, 120 University Place, University of Glasgow, Glasgow, G12 8TA, megan.macleod@glasgow.ac.uk, ORCID: 0000-0003-1843-8580

4.1 Abstract

Cytokine production by memory T cells is a key mechanism of T cell mediated protection. However, we have limited understanding of the persistence of cytokine producing T cells during memory cell maintenance and secondary responses. We interrogated antigen-specific CD4 T cells using a mouse influenza A virus infection model. While CD4 T cells detected using MHCII tetramers declined in lymphoid and non-lymphoid organs, we found similar numbers of cytokine+ CD4 T cells at days 9 and 30 in the lymphoid organs. CD4 T cells with the capacity to produce cytokines expressed higher levels of pro-survival molecules, CD127 and Bcl2, than non-cytokine+ cells. Transcriptomic analysis revealed a heterogenous population of memory CD4 T cells with three clusters of cytokine+ cells. These clusters match flow cytometry data and reveal an enhanced survival signature in cells capable of producing multiple cytokines. Following re-infection, multifunctional T cells expressed low levels of the proliferation marker, Ki67, while cells that only produce the anti-viral cytokine, interferon γ, were more likely to be Ki67+. Despite this, multifunctional memory T cells formed a substantial fraction of the secondary memory pool. Together these data indicate that survival rather than proliferation may dictate which populations persist within the memory pool.

4.2 Introduction

Immunological memory protects against repeated infection with a strong and rapid pathogen-specific response with cytokine production often central to protection[22-24, 29, 48, 58, 59, 84, 105]. Improving our understanding of T cell memory is particularly important in the context of highly variable infections such as Influenza A Virus (IAV). While neutralising antibodies can prevent IAV infection, frequent mutations within viral surface proteins makes it difficult for strain-specific antibodies to recognise altered viruses[55].

In contrast, CD4 and CD8 T cells recognise conserved IAV epitopes[106, 107]. The presence of cytokine producing IAV-specific CD4 and CD8 T cells in human peripheral blood correlates with cross-strain protection against symptomatic influenza disease[34-37]. Mouse studies have demonstrated protection by CD4 and CD8 T cells, with the inflammatory T-helper (Th1) cytokine, interferon (IFN)γ, often essential[29, 48, 58, 84]. The cytokines TNFα and interleukin (IL-) 2 are also implicated in protection to IAV[27, 28]. These data support that the most effective memory T cells are those with the capacity to produce cytokines.

Multifunctional T cells, capable of producing a number of different cytokines, have been associated with effective immune protection in human disease and animal models[22-24, 105]. It remains unclear, however, why these cells provide enhanced protection compared to other populations. These data suggest that vaccines that drive cytokine producing T cells would be the most protective. However, while some studies found that cytokine producing T cells can become memory cells, other have described limited persistence of these cells[65, 108-110].

We previously showed that multifunctional CD4 and CD8 T cells expressing IFNγ, IL-2 and TNFα increase in predominance from the primary to the memory pool[25]. These data supported the conclusion that rapid production of cytokines does not limit long term immunity. Building on this, we have now tracked the characteristics of the IAV-specific T cell pool at multiple time points post-infection. Our data show that CD4 T cells with the capacity to produce cytokine express higher levels of pro-survival molecules than cells that do not produce cytokines. Multifunctional CD4 T cells, in particular, express a number of genes associated with cell survival. Following a re-challenge infection, multifunctional

T cells expressed low levels of Ki67, a marker of proliferation, compared to other cytokine+ T cell populations. Despite this, the proportion of cytokine+ cells that were multifunctional did not alter following the re-infection. Together these data demonstrate that the capacity to produce cytokine does not limit persistence of CD4 T cells into the primary or secondary memory pool.

4.3 Results

4.3.1 MHC tetramers and cytokine expression enable analysis of IAV-specific T cells

We used MHCI and MHCII tetramers (tet) containing immunodominant IAV nucleoprotein (NP) peptides (NP_{368-74} and $NP_{311-325}$) to identify and characterise responding T cells longitudinally following infection, Figure 18A-B; Figure 19. These peptides were also used to activate cells from the same mice to examine the anti-IAV T cell cytokine responses, Figure 1B, as optimal dual staining of MHC tetramers and cytokines was not possible.

IAV infected animals were injected with fluorescently labelled anti-CD45 shortly before euthanasia to label cells in the blood. The majority of lymphoid organ MHC tet+ and cytokine+ CD4 and CD8 T cells and lung CD4 T cells were negative for CD45iv, while around half of the lung IAV-specific CD8 T cells were within the blood, Figure 18C and cells gated as in Figure 19B.

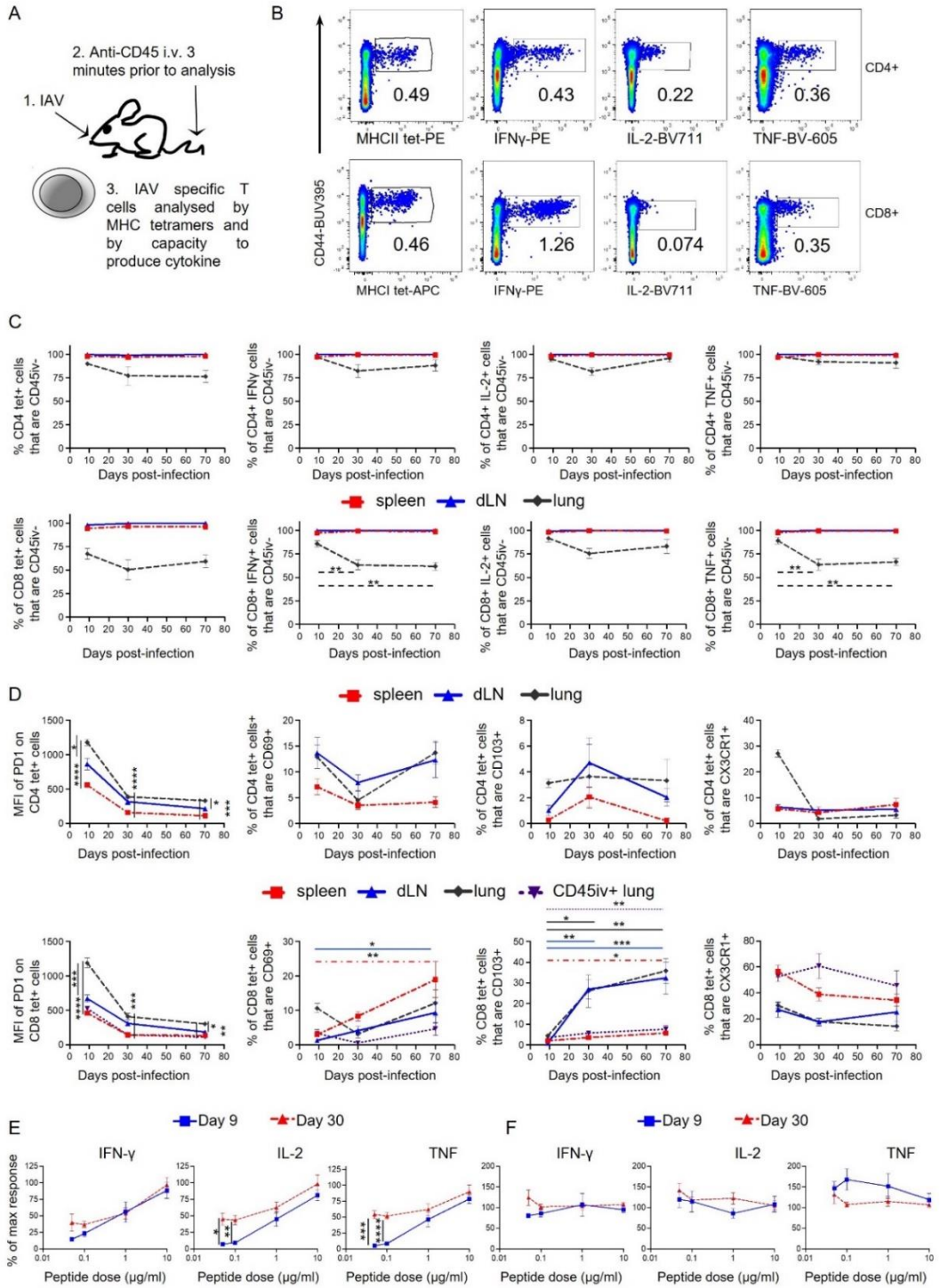

Figure 18 - MHC tetramers and cytokine expression enable analysis of IAV-specific T cells.

C57BL/6 mice were infected i.n. with IAV on day 0 and injected i.v. with fluorescently labelled anti-CD45 3 minutes prior to removal of organs (A). Single cell suspensions of spleens, mediastinal draining lymph node (medLN), and lung were examined 9, 30 or 70 days post-IAV infection. Cells were either stained with $IA^b/NP_{311-325}$ or $D^b/NP_{368-374}$ tetramers or cells were restimulated for 6hours with DCs presenting $NP_{311-325}$ and $NP_{368-374}$ peptides. Example flow cytometry plots of splenic IAV-specific cells as gated in Figure 19A (B). Percentages of IAV-specific cells that bound to the i.v. injected anti-CD45, cells gated as in Figure 19B (C). The phenotype of MHC tetramer+ CD4 and CD8 T cells (D). Spleen cells from IAV-infected mice restimulated with DCs cultured with 0.05, 0.1, 1, 10 or 100mg/ml of $NP_{311-325}$ and $NP_{368-374}$ (E-F). The percentage of max cytokine production as detected at 100mg/ml was calculated. In B-D, data are from two time course experiments with a total of 7-8 mice/time point. In C-D, symbols show the mean of the group and error bars are SEM. Statistical difference tested by ANOVA followed by a Dunnett's multiple comparison test for analyses between time points and by a Tukey's test between organs. In E-F, data are from two experiments with a total of 6-8 mice per timepoint. Significance between primary and memory tested by ANOVA followed by a Šídák's multiple comparison test. *: p<0.05, **:p<0.01, ***:p<0.001, ****:p<0.0001.

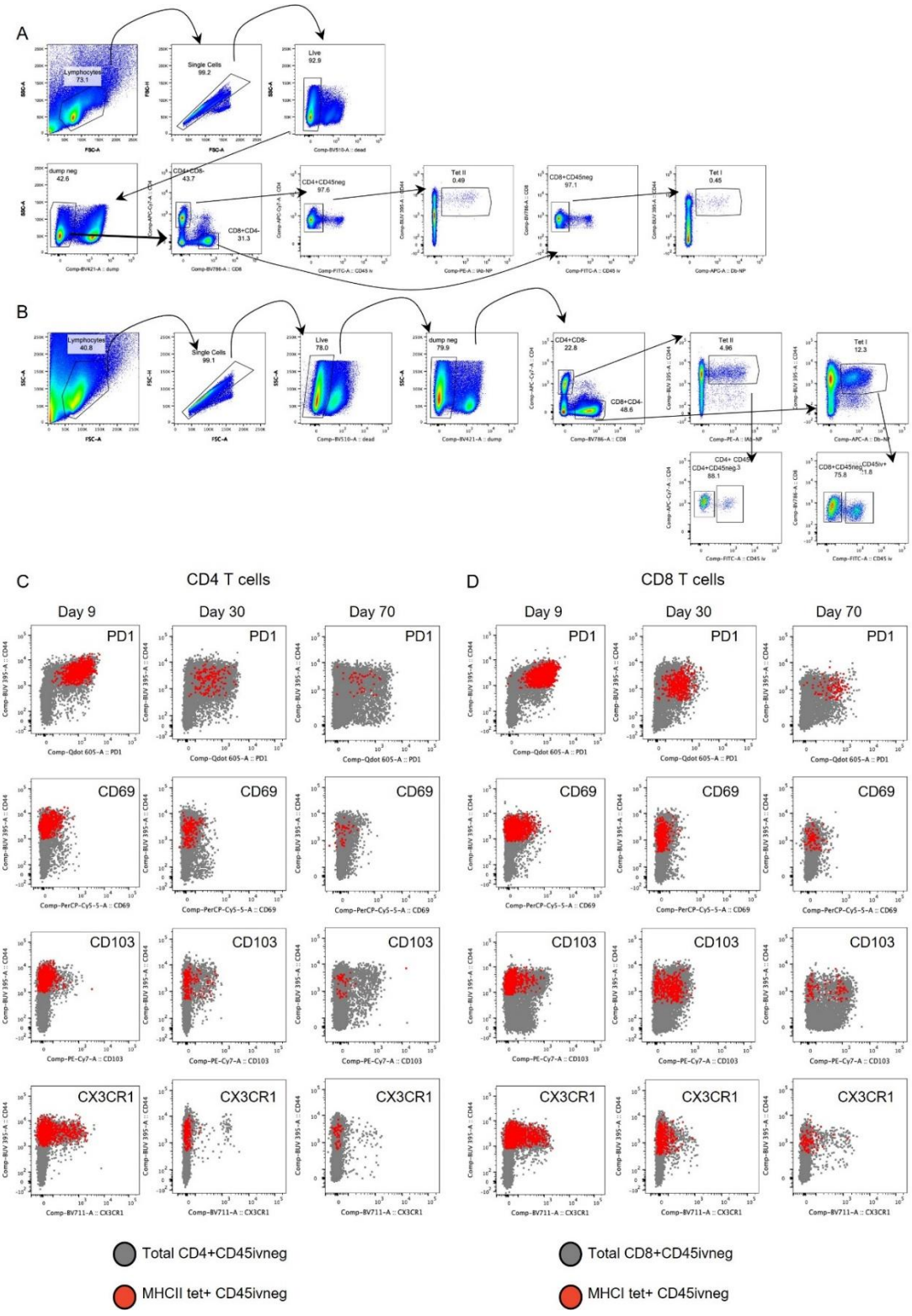

Figure 19 - Example gating of IAV-specific CD4 and CD8 T cells identified by MHC tetramers.

C57BL/6 mice were infected i.n. with IAV on day 0 and injected i.v. with fluorescently labelled anti-CD45 3 minutes prior to removal of organs for analysis. Single cell suspensions of spleen (A) and lung (B) are shown at day 9 of infection. A, shows example gating used in most figures in which we gate on CD45 i.v. negative tetramer+ or cytokine+ T cells. Example FACS plots of splenic CD45iv negative MHC tetramer+ cells CD4 (C) and CD8 (D) (shown in red) in comparison to total CD45iv negative T cells (grey).

While PD1 decreased on all the IAV-specific T cells after day 9, T cells in the lung expressed the highest levels at all timepoints, Figure 18D. Tissue resident memory (Trm) associated markers, CD69 and CD103[111], increased on CD8 MHCI tet+ cells in the lymphoid organs and lung CD45iv negative lung cells after day 9. However, very few CD4 MHCII tet+ cells expressed these markers.

While at day 9 some CD4 MHCII tet+ cells in the lung expressed CX3CR1, only a small minority of memory cells expressed this chemokine receptor. CX3CR1 was expressed by CD8 MHCI tet+ cells, most prominently in the spleen and on lung CD45iv+ cells suggesting that these are circulating effector memory cells[112].

In addition to phenotypic changes, cytokine+ memory CD4 T cells displayed increased sensitivity to peptide compared to primary responding cells, Figure 18E. In contrast, primary and memory CD8 T cell cytokine production was unaffected by peptide dose, Figure 18F.

4.3.2 While the number of IAV-specific CD4 T cells detected by MHC tetramer decline from day 9 to day 30, the numbers of cytokine+ CD4 T cells in the secondary lymphoid organs are stable

We examined the numbers of T cells detected by MHC tetramers or IFNγ production between days 9 and 30 post-infection. As MHC tetramers detect NP-specific T cells regardless of their ability to produce cytokines, altered dynamics between these and cytokine+ cells suggest differences between cells that can and cannot produce cytokine.

The numbers of IAV-specific CD4 T cells detected by MHCII tet were reduced between day 9 and 30 in all three organs, Figure 20A. In contrast, the numbers of CD4 T cell detected by cytokine production did not decline in the spleen and medLN, Figure 20A, Figure 21A. While the number of IFNγ+, and TNF+ cells were lower in the lung at day 30 than day 9, the numbers of IL-2+ cells were stable. In contrast, the numbers of IAV-specific CD8 T cells detected by either MHCI tetramers, IFNγ or TNF, remained stable in secondary lymphoid organs, although in all cases these cells declined in the lung (Figure 20B, Figure 21B). While the number of IL-2+ CD8 T cells were low, the cell numbers were unchanged in the spleen and lung, but did drop in the medLN between day 9 and 30.

These data suggest that CD4 T cells with the capacity to produce cytokine are more likely to enter the memory pool than those that cannot produce cytokine. To investigate this, we compared the phenotype and function of different memory CD4 T cell populations taking advantage of a reporter mouse we developed [60]. This reporter tool, TRACE, includes three transgenes to drive permanent expression of EYFP in activated T cells. The first transgene is the upstream 8.389kb of the *Il2* promoter which drives expression of rtTA. This promoter section was selected based on findings by Yiu *et al*. who characterised the *Il2* promoter, revealing DNase-1 hypersensitivity sites in this region following TCR stimulation[113]. Only in the presence of doxycycline, can rtTA drive expression at the tet-ON promoter. This leads to the production of Cre recombinase and subsequent removal of a stop codon at the ROSA locus. Removal of this stop codon enables permanent EYFP expression, Figure 22.

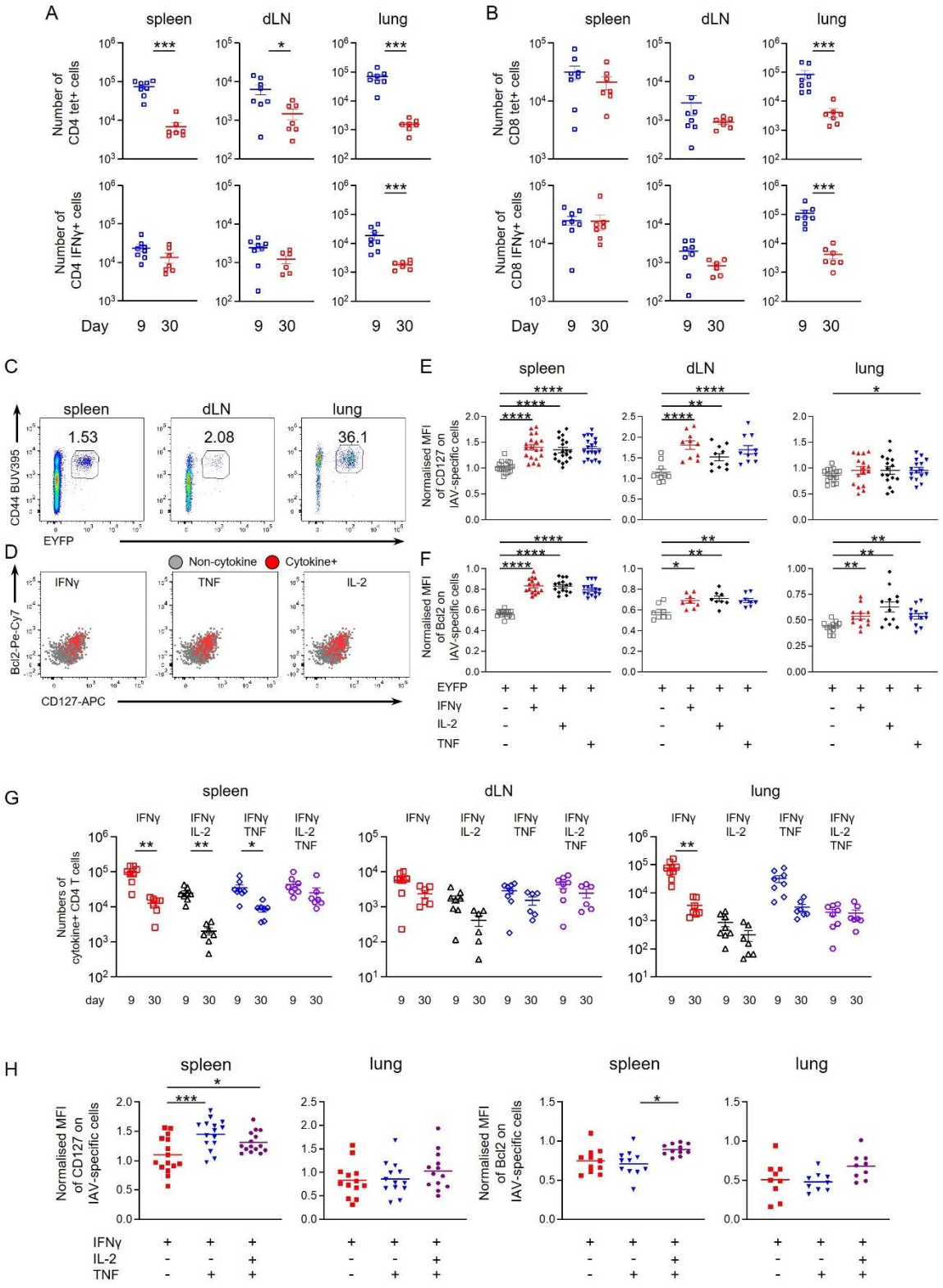

Figure 20 - Influenza virus-specific cytokine+ CD4 T cells are more likely to enter the memory pool than non-cytokine+ cells.

C57BL/6 (A-B, G) or TRACE (C-F, H) mice were infected i.n. with IAV on day 0 and injected i.v. with fluorescently labelled anti-CD45 (CD45iv) 3 minutes prior to removal of organs. Single cell suspensions of spleens, mediastinal draining lymph node (medLN), and lung were examined 9 or 30 days post-IAV infection and either stained with MHCII/NP or MHCI/ NP tetramers, or activated with IAV-peptide loaded DCs (A-B) or IAV-Ag loaded DCs (C-H). Numbers of MHC tetramer or IFNγ+ CD4 (A) or CD8 T cells (B). Example FACS plots from the indicated organs of TRACE mice (C) and the spleen (D) are gated on live CD4 dump negative, CD45i.v. negative cells (C) and on EYFP+ cytokine negative: grey; IFNγ, IL-2 and/or TNF+: red (D). In A-B and E-H, symbols represent a mouse and the lines shows the means, error bars are SEM. In A-B & G, data are from

two independent time course experiments with a total of 7-8 mice/time point, significance tested by a Mann-Whitney. In E-F, & H, data are from three independent experiments with a total of 5-8 mice and normalised by dividing the MFI on EYFP+ or cytokine+ cells by the MFI of naïve CD44^{lo} CD4 T cells from cells from the same mouse and organ. In E-H, samples from some medLNs and lungs were excluded as the numbers of cytokine+ cells collected were too low for analysis. Significance tested via a Friedman paired analysis with Dunn's multiple comparison test, *: p<0.05, **:p<0.01, ****:p<0.0001.

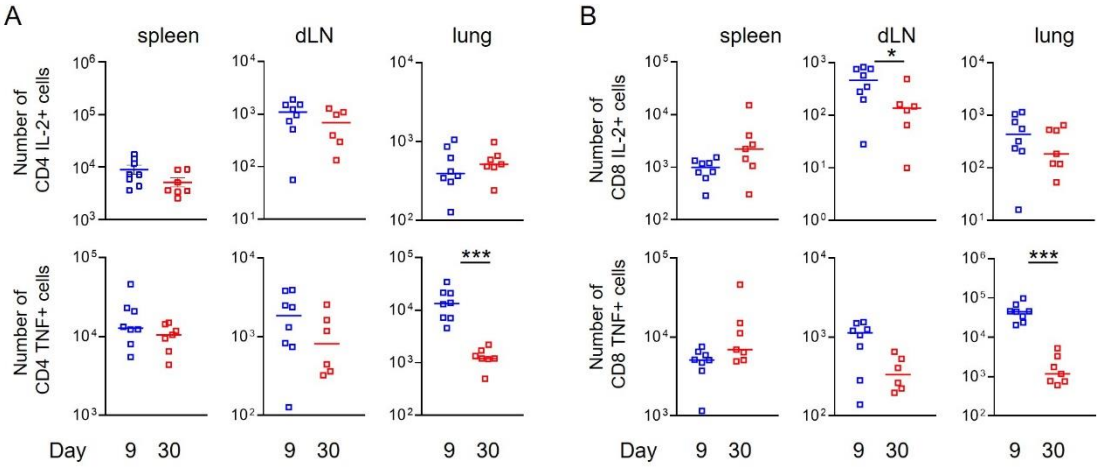

Figure 21 - IL-2 and TNF+ CD4 and CD8 T cells show minimal decline between day 9 and day 30 in secondary lymphoid organs.

C57BL/6 mice were infected i.n. with IAV on day 0 and injected i.v. with fluorescently labelled anti-CD45 (CD45iv) 3 minutes prior to removal of organs. Single cell suspensions of spleens, mediastinal draining lymph node (medLN), and lung were examined after 9 or 30 days and activated with IAV-peptide loaded DCs. Numbers of IL-2 or TNF+ CD4 (A) or CD8 T cells (B) were calculated. Data are from two independent time course experiments with a total of 7-8 mice/time point. The horizontal lines are the median. Significance tested by a Mann-Whitney, *: p<0.05, ***:p<0.001.

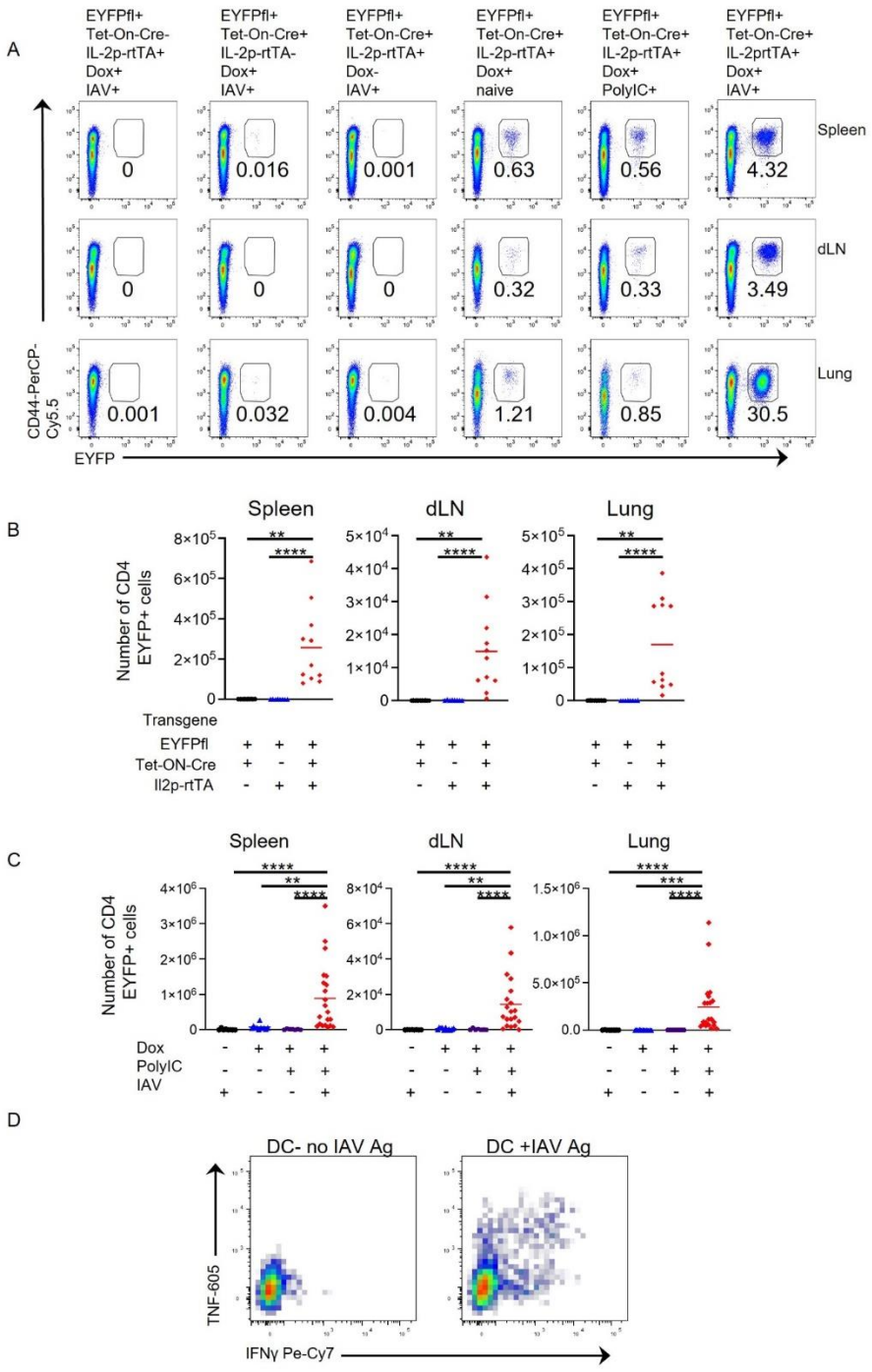

Figure 22 - TRACE mice enable identification of CD4 T cells responding to IAV infection.

TRACE mice that are positive for all three transgenes and double transgenic mice expressing STOP floxed EYFP (EYFPfl) and either tet-ON-Cre or the IL-2 promoter driving rtTA (IL-2p-rtTA) were given doxycycline (Dox) diet for a total of twelve days starting two days prior to intranasal infection with IAV or instillation of 20μg of PolyIC intranasally as indicated. In A, cells are gated as in Figure 19A on CD4 live lymphocytes that are negative for CD8, B220, MHCII and F4/80 in the indicated organ 8 days after infection/polyIC treatment and the numbers show the percentages of EYFP+ cells within the gate. In B, mice with the indicated transgenes were given dox diet and the numbers of EYFP+ CD4 T cells examined 8-12 days following treatment, data are combined from 3 independent experiments with 2-5 mice per experiment. In C, TRACE mice were treated/infected as indicated and the numbers of EYFP+ CD4 T cells examined 8-12 days following infection, data are combined from 4 independent experiments with 2-10 mice per experiment. Significance tested by a Kruskal-Wallis test followed by a Dunn's multiple comparison test: *: p<0.05, **:p<0.01, ***:p<0.001, ****:p<0.0001. D shows example staining from a day 8 IAV infected mouse, the cells on the left were co-cultured with DCs that had not received IAV-Ag, the plot on the right shows cells from the same mouse co-cultured with IAV-Ag+ DCs for 6 hours. Cells are gated on live single CD4 EYFP+ cells that are CD45iv negative.

As the EYFP+ CD4 T cells likely respond to an array of IAV antigens, we used bone marrow derived dendritic cells (DCs) cultured with a sonicated IAV antigen (IAV Ag) preparation to restimulate the T cells *ex vivo* for cytokine analysis [25]. EYFP+ CD4 T cells only produced cytokine following culture with DCs incubated with IAV Ag, demonstrating that cytokine production is antigen-specific, Figure 22D. By gating on CD4 T cells that produced either IFNγ, IL-2 or TNFα following the culture, we determined that between 49-69% of the cytokine+ cells were EYFP+, Figure 23A-B. This suggests that TRACE mice enable us to examine over half of the cytokine+ T cells that respond to IAV. Between 2-15% of the EYFP+ cells produced cytokine, a similar range as described to a model antigen inserted into IAV[114], Figure 23C-D. Importantly, the proportion of IFNγ+ CD4 T cells that also produce IL-2 and/or TNFα are similar when gating on total IFNγ+ or EYFP+ IFNγ+ cells, Figure 23E.

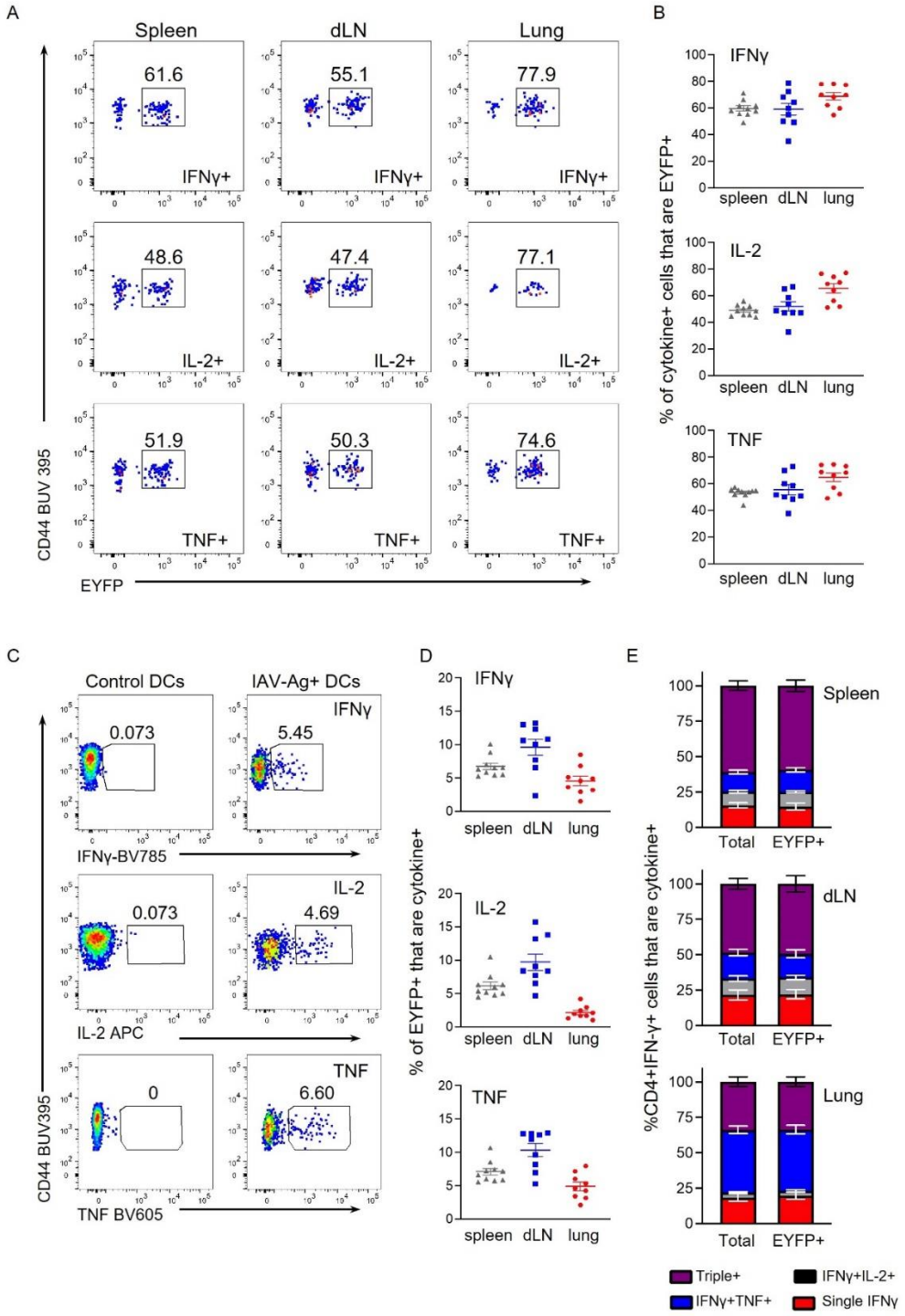

Figure 23 - TRACE mice enable identification of cytokine+ and negative CD4 T cells.

TRACE mice were infected i.n. with IAV on day 0 and injected i.v. with fluorescently labelled anti-CD45 3 minutes prior to removal of organs at day 14 post-infection. Single cell suspensions of spleens, mediastinal draining lymph node (medLN), and lung were activated by DCs incubated with IAV-Ag preparation or control DC. The percentages of CD45iv negative IFNγ, IL-2 and TNF+ cells that were EYFP were determined (A-B). Alternatively, the percentages of EYFP+ cells producing IFNγ, IL-2 or TNFα in response to control DC (no IAV Ag) or IAV-Ag+ DCs were analysed (C-D) and the percentages of total IFNγ+ or EYFP+ IFNγ+ CD4 T cells that also produced IL-2 and/or TNFα were determined (E). Some lymph nodes and lungs are excluded as the number of cytokine+ cells within the FACS plot was less than 10. A shows representative FACS plots gated on live CD45iv negative, CD4+cyokine+ and the numbers are the percentages of cells within the EYFP+ gate. C shows spleen cells gated on live CD454iv negative CD4+ EYFP+ cells and the numbers are the percentages of these cells that are cytokine+. In B and D, data are combined from two experiments with 4-6 mice, each point is a mouse and the horizontal line is the mean, errors are SEM. In E, data are from the same experiments and error bars are SEM.

The expression of the pro-survival molecules CD127 and Bcl2[115] was examined in EYFP+ cytokine negative CD4 T cells and those expressing IFNγ, IL-2 or TNFα 40 days post-infection, Figure 20C-F. In the secondary lymphoid organs, the cytokine+ EYFP+ T cells expressed higher levels of both molecules compared to cytokine negative cells. These differences were less clear in the lung, potentially reflecting the reduced survival of cytokine+ and negative cells in this organ. These data are consistent with the hypothesis that CD4 T cells with the capacity to produce cytokines have an enhanced survival capacity compared to non-cytokine+ T cells.

Additionally, we analysed CD4 IFNγ+ cells that were also positive for IL-2, TNF, all three cytokines, or only expressed IFNγ. The numbers of triple cytokine+ CD4 T cells did not change in any of the organs between days 9 and 30, Figure 20G. The numbers of all other populations declined significantly in at least one of the organs. While triple cytokine+ cells in the spleen expressed high levels of CD127 and Bcl2, no differences in expression of these survival molecules were found in lung cytokine+ CD4 T cells, Figure 20H. These data suggest that survival, at least based on these two molecules alone, may not explain the differences in stability of the cytokine+ cell populations between days 9 and 30.

4.3.3 Single IFNγ+ CD4 and CD8 T cells are more likely to be in cell cycle than multifunctional T cells

An alternative explanation for the stability of the numbers of triple cytokine+ T cells could be increased proliferation in comparison to other cytokine+ populations. We gated on IFNγ+ Ki67+ cells to examine whether these cells were producing one or more cytokine, Figure 24. IFNγ single+ CD4 and CD8 T cells were more likely to be in cell cycle compared to triple+ cells at both day 9 and 30, Figure 25A-B. These data suggest that enhanced proliferation by multifunctional T cells does not explain their increase predominance in the memory pool [25] nor the lack of decline in the numbers of these cells between day 9 and 30 post-infection, Figure 20G.

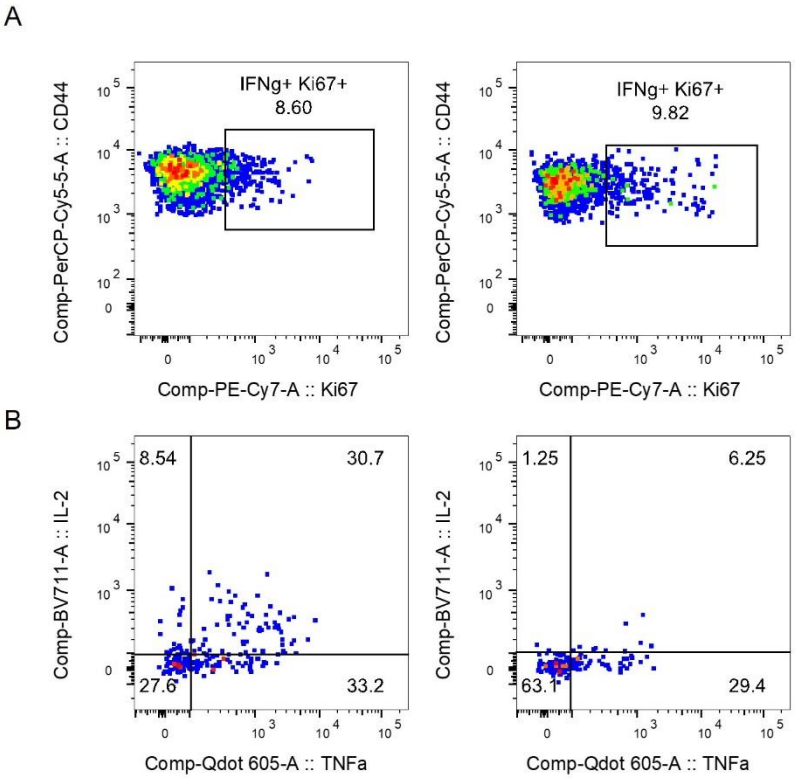

Figure 24 - Detection of IFNγ Ki67+ cells by flow cytometry.

C57BL/6 mice were infected i.n. with IAV on day 0 and injected i.v. with fluorescently labelled anti-CD45 (CD45iv) 3 minutes prior to removal of organs. At day 9 post-infection, single cell suspensions of spleens were co-cultured with IAV-Ag+ DCs for 6 hours. In A, cells are gated as in Figure 19A and on CD4 or CD8 T cells that are IFNγ+. In the bottom panel, cells are also gated on the Ki67+ population shown in A. The numbers show the percentage within the indicated gates or quadrants. Data are representative of the experiments shown in Figure 25.

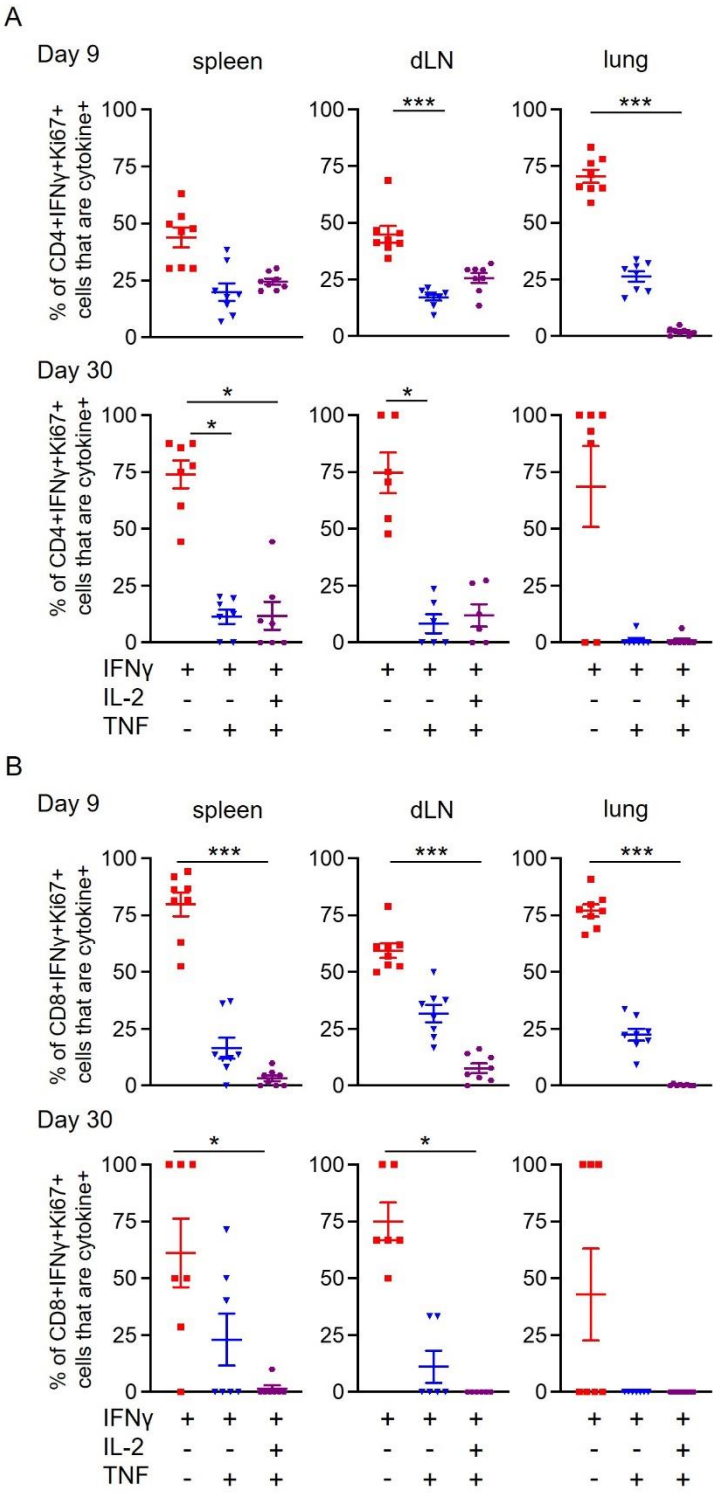

Figure 25 - Single IFNγ+ CD4 and CD8 T cells are more likely to be in cell cycle 9 and 30 days after IAV infection than T cells producing multiple cytokines.

C57BL/6 mice were infected i.n. with IAV on day 0 and injected i.v. with fluorescently labelled anti-CD45 3 minutes prior to removal of organs at the indicated time point. Single cell suspensions of spleens, mediastinal draining lymph nodes (medLN), and lungs from IAV infected mice were activated by IAV-Ag+ DCs for 6 hours. Data are from two independent time course experiments with a total of 7-8 mice/time point. Each symbol represents a mouse and the horizontal line shows the mean of the group and significance tested via paired Friedman analysis with Dunn's multiple comparison test *: $p<0.05$, ***:$p<0.001$.

4.3.4 scRNAseq analysis reveals heterogeneity in cytokine+ and cytokine negative memory CD4 T cells

To obtain a more detailed understanding of differences between the cytokine+ and negative memory T cell populations, we performed single-cell gene transcription analysis. TRACE mice were infected with IAV and after 40 days the mice were injected with anti-CD45 i.v. 3 minutes prior to tissue harvest. CD45 iv negative spleen and lung CD4 T cells were isolated and activated with IAV-Ag+ DCs for 4 hours to drive cytokine mRNA expression. We sorted EYFP+ cells from the spleens and lung and, to provide a base line level of gene expression, naïve, $CD44^{lo}$ EYFP-negative CD4 T cells from the spleen, Figure 26. Cells from 4 infected TRACE mice were combined with oligo tagged antibodies used to distinguish each animal and organ.

Initial clustering produced 19 different clusters, including 8 naïve clusters, 10 memory clusters and one Treg cluster, Figure 28A. To focus on the differences between the memory clusters, we reduced the complexity of the naïve population into a single population, Figure 29A; all clusters remained transcriptionally distinct, Figure 28B; Table 4. Of the 10 memory clusters, 7 expressed little to no *Ifng*, *Tnf or Il2*, Figure 28C. Cells from all memory clusters were found in both the spleen and lung, with the spleen contributing most cells in all but the *Ifng*+ cluster, Figure 27A & Figure 28D. Naïve and Treg clusters cells were almost entirely from the spleen, consistent with their origin from the naïve sort gate (Figure 26).

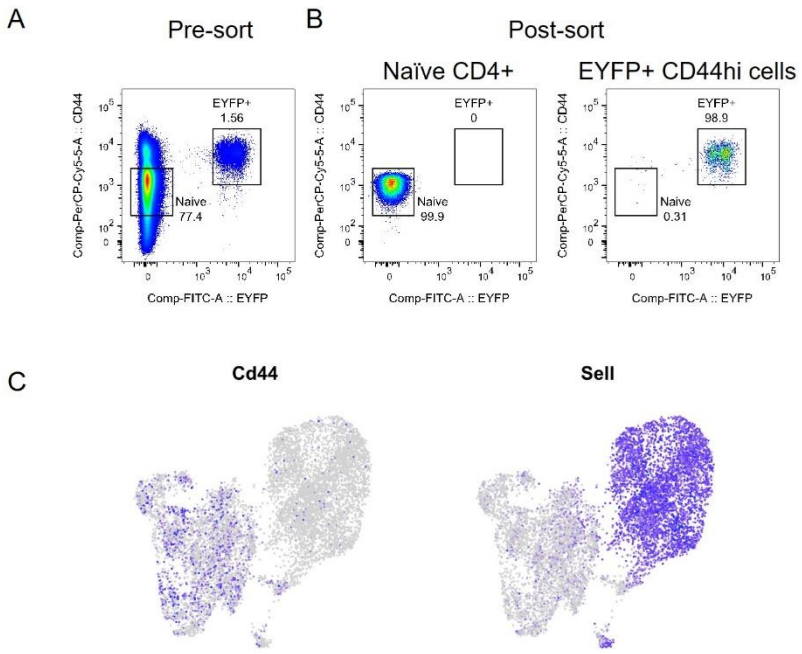

Figure 26 - Example data from sorted EYFP negative naïve and EYFP+ memory CD4 T cells.

TRACE mice were infected with IAV and injected with anti-CD45 3 minutes prior to removal of spleens and lungs. Isolated CD4 T cells were activated for 4 hours by co-culture with IAV-Ag DCs and the CD45iv negative CD4+CD44^{hi}EYFP+ cells (spleens and lung) and CD4+CD44^{lo}EYFPnegative (spleens) cells were FACS sorted. In A, FACS plots are gated on live CD4+ single lymphocytes negative for CD45iv, B220 and MHCII and show cells prior to the sort with sort gates shown. In B, cells are gated on the indicated cells post-sort. A-B are from a practice sort prior to isolation of the cells for scRNAseq transcriptomic analysis. In C, the expression of *Cd44* and *Sell* (which codes for CD62L) are shown overlaid on the UMAP described in Figure 27A.

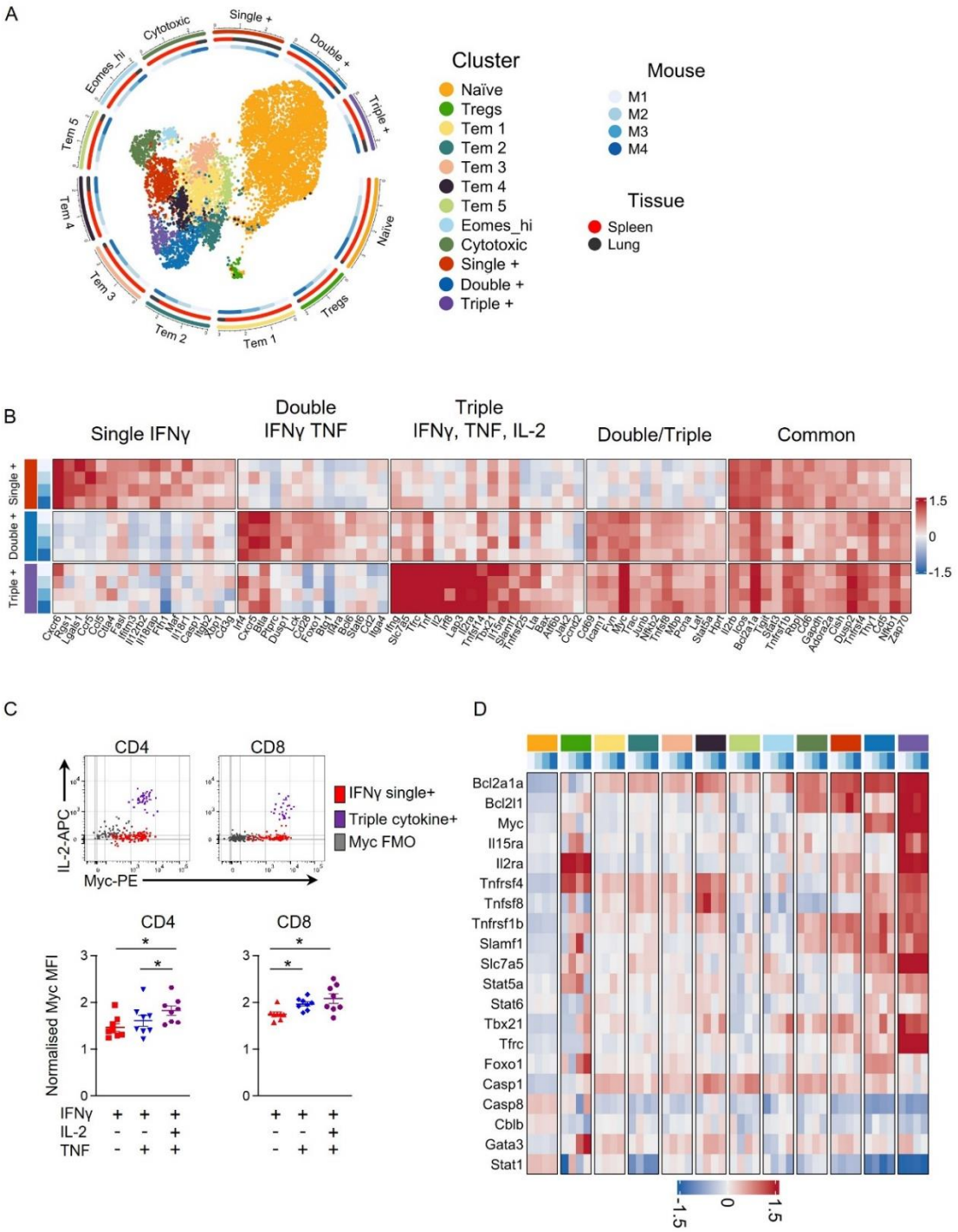

Figure 27 - Triple cytokine+ CD4 T cells have a pro-survival transcriptional signature.

TRACE mice were infected with IAV and 40 days later injected with anti-CD45 3minutes prior to removal of spleens and lungs. Isolated CD4 T cells were activated for 4 hours with IAV-Ag DCs and the CD45iv negative CD4+CD44^{hi}EYFP+ cells (spleens and lung) and CD4+CD44^{lo}EYFPnegative (spleens) cells were FACS sorted and their transcriptomes examined by scRNAseq. UMAP of one naïve cluster, one Treg cluster, and 10 memory clusters. The radial tracks around the UMAP reflect the numerical representation of each cluster, and the mouse/tissue origin within each cluster on a logarithmic axis (A). DEGs in single, double, and triple cytokine+ clusters identified by comparison between the indicated populations and all other clusters (B). The normalised MFI of Myc by single, double, and triple cytokine+ cells in CD4 and CD8 T cells from C57BL/6 IAV infected mice examined at day 40 post-infection; expression was normalised by dividing each sample's MFI by the MFI on naïve CD4+ cells in the same sample (C). Expression of mRNA for cell survival molecules from the scRNAseq analysis (D, legend as in A). Data in A, B, D, are from one experiment with cells from 4 mice. In C, data are from 2 independent experiments with each symbol representing one mouse and the horizontal line showing the mean of the groups; significance tested by paired ANOVA with Tukey's multiple comparison test, *: $p<0.05$.

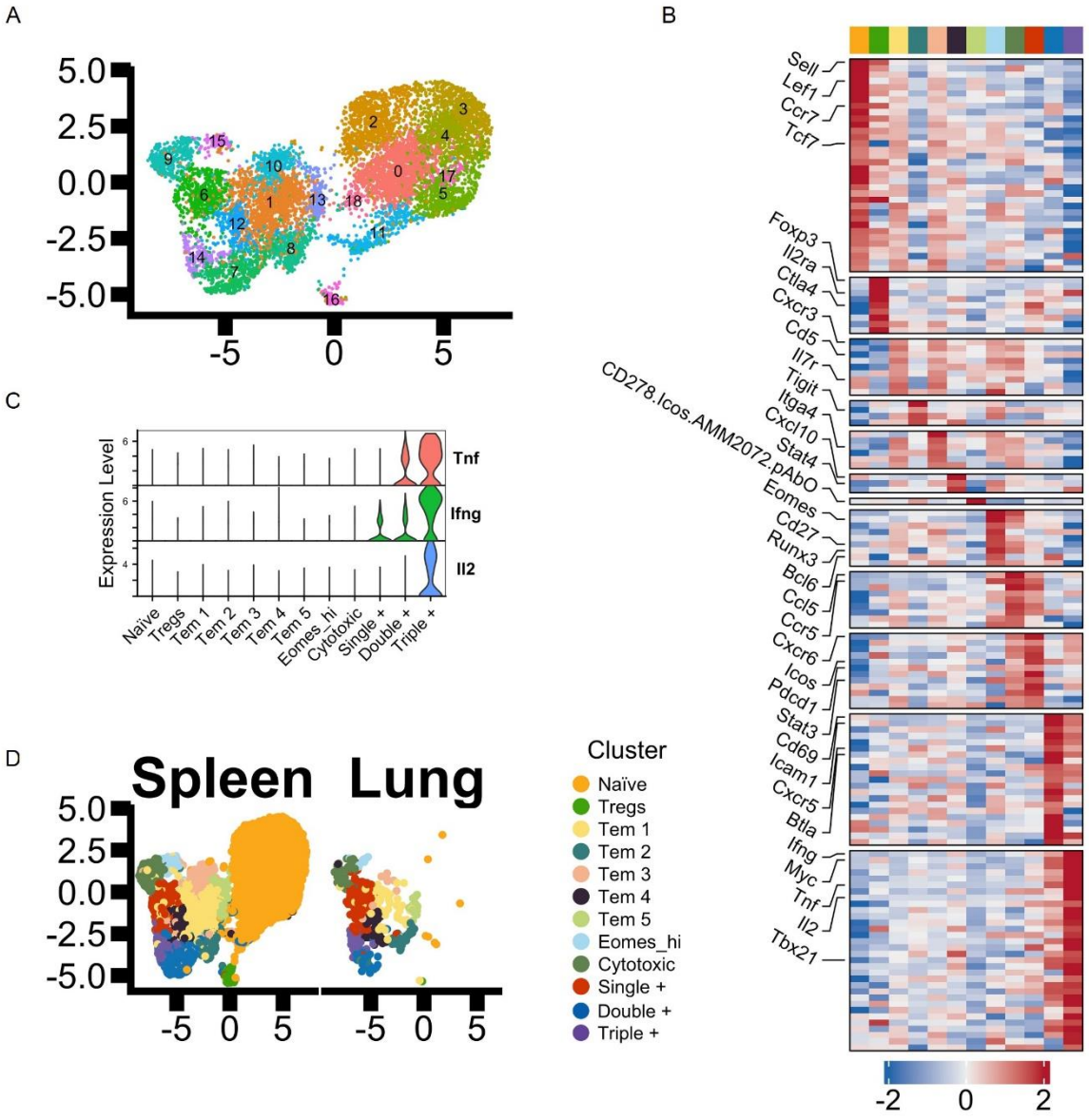

Figure 28 - scRNAseq reveals heterogeneity in the memory CD4 T cell pool.

TRACE mice were infected with IAV and injected with anti-CD45 3 minutes prior to removal of spleens and lungs. Isolated CD4 T cells were activated for 4 hours by co-culture with IAV-Ag DCs and the CD45iv negative CD4+CD44hiEYFP+ cells (spleens and lung) and CD4+CD44loEYFPnegative (spleens) cells were FACS sorted and their transcriptomes examined by scRNAseq. UMAP of eight naïve clusters, one Treg cluster, and 10 memory clusters (A). DEGs in main clusters identified by comparison between the indicated populations and all other clusters (B). Where genes were differentially expressed in multiple clusters, the gene was visualised in the cluster with the highest fold change; for a list of all DEGs see Table 4. Expression of *Tnf*, *Ifng* and *Il2* by each cluster (C). UMAP of analysed cells displaying cells from the spleen and lung separately (D).

Table 4 - Gene expression and clustering

gene	p_val	avg_log2 FC	pct.1	pct.2	p_val_adj	cluster
Sell	0	3,87402	0,961	0,257	0	Na√Øve
Ly6c1	0	3,61567	0,745	0,246	0	Na√Øve
Oas2	0	3,21438	0,875	0,248	0	Na√Øve
Lef1	0	2,51805	0,615	0,168	0	Na√Øve
Trib2	0	2,51644	0,911	0,453	0	Na√Øve

Txk	0	2,51501	0,582	0,154	0	Na/Øve
Pik3ip1	0	2,43825	0,444	0,11	0	Na/Øve
Ccr7	0	2,236	0,936	0,456	0	Na/Øve
Itk	0	1,2734	0,979	0,887	0	Na/Øve
Casp8	0	1,2728	0,9	0,691	0	Na/Øve
Cd247	0	1,23632	0,973	0,8	0	Na/Øve
Lgals9	0	1,07832	0,936	0,745	0	Na/Øve
Irf7	0	1,02978	0,997	0,944	0	Na/Øve
Tcf7	0	0,92314	0,955	0,79	0	Na/Øve
Stat1	0	0,79564	0,974	0,853	0	Na/Øve
H2.K1	0	0,27426	1	1	0	Na/Øve
Selplg	1,03E-303	0,93678	0,92	0,732	4,23E-301	Na/Øve
Bach2	1,87E-301	1,75276	0,555	0,245	7,66E-299	Na/Øve
Cd274	2,12E-275	1,20324	0,756	0,528	8,67E-273	Na/Øve
Birc3	1,14E-265	1,05295	0,795	0,609	4,67E-263	Na/Øve
Ddx58	8,70E-246	0,81424	0,911	0,768	3,56E-243	Na/Øve
Ifngr1	7,89E-245	0,61394	0,969	0,8	3,23E-242	Na/Øve
Socs1	1,01E-204	1,20862	0,598	0,392	4,14E-202	Na/Øve
Trbc2	1,70E-136	0,45314	0,995	0,975	6,95E-134	Na/Øve
Btg1	7,78E-128	0,29747	0,999	0,995	3,18E-125	Na/Øve
Cblb	5,64E-122	0,68029	0,759	0,67	2,31E-119	Na/Øve
Il4ra	3,31E-117	0,84125	0,647	0,505	1,35E-114	Na/Øve
Vps28	5,42E-111	0,61293	0,657	0,582	2,22E-108	Na/Øve
Myd88	6,76E-111	0,63704	0,626	0,552	2,76E-108	Na/Øve
Tmem173	5,51E-101	0,89193	0,445	0,328	2,25E-98	Na/Øve
Ltb	3,18E-96	0,7099	0,63	0,493	1,30E-93	Na/Øve
Mcm4	1,83E-92	0,716	0,434	0,366	7,50E-90	Na/Øve
Ifnar1	2,15E-86	0,63521	0,53	0,444	8,81E-84	Na/Øve
Ccnd2	1,81E-83	0,65597	0,507	0,417	7,40E-81	Na/Øve
Cd3d	4,14E-77	0,4534	0,722	0,665	1,69E-74	Na/Øve
Cxcl10	3,96E-62	0,36305	0,7	0,556	1,62E-59	Na/Øve
Stat6	2,60E-57	0,25438	0,544	0,569	1,06E-54	Na/Øve
Lamp1	3,70E-57	0,38669	0,607	0,572	1,51E-54	Na/Øve
Il7r	9,82E-56	0,46815	0,678	0,532	4,02E-53	Na/Øve
Foxp3	1,19E-229	6,97594	0,982	0,016	4,88E-227	Tregs
Lrrc32	7,42E-133	5,91779	0,755	0,016	3,04E-130	Tregs
Il2ra	1,52E-62	4,0743	0,618	0,063	6,22E-60	Tregs
Tnfrsf4	2,13E-50	2,14855	0,955	0,5	8,73E-48	Tregs
Tnfrsf18	1,50E-46	1,73955	0,927	0,647	6,15E-44	Tregs
Ctla4	7,33E-40	2,29255	0,8	0,29	3,00E-37	Tregs
Tnfrsf9	3,51E-39	2,91317	0,673	0,223	1,44E-36	Tregs
Cish	6,43E-26	1,37012	0,9	0,591	2,63E-23	Tregs
Il2rb	2,70E-23	1,42294	0,855	0,427	1,10E-20	Tregs
Rgs1	7,59E-22	1,80577	0,736	0,352	3,11E-19	Tregs
Cd2	9,88E-22	0,95698	0,991	0,899	4,04E-19	Tregs

Nt5e	9,22E-09	1,5422	0,436	0,196	3,77E-06	Tregs
Xbp1	2,55E-06	0,967	0,564	0,384	0,001044	Tregs
Socs1	7,90E-06	0,66908	0,718	0,498	0,003232	Tregs
CD279.RMP1.30.Pdcd1.AMM2138.pAbO	4,73E-05	0,45087	1	0,992	0,019364	Tregs
Cxcr3	5,42E-227	2,03524	0,695	0,238	2,22E-224	Tem 1
Cd4	2,51E-148	1,06713	0,912	0,685	1,03E-145	Tem 1
Cd5	2,21E-136	1,4752	0,726	0,403	9,06E-134	Tem 1
Gapdh	2,96E-112	0,6695	0,993	0,937	1,21E-109	Tem 1
Il2rb	1,03E-90	0,80268	0,714	0,391	4,21E-88	Tem 1
Cd3g	1,82E-87	0,98772	0,809	0,59	7,44E-85	Tem 1
Cd6	6,02E-86	1,13691	0,721	0,459	2,46E-83	Tem 1
Cd28	1,73E-77	0,82999	0,789	0,54	7,09E-75	Tem 1
Itga4	5,43E-75	1,1751	0,583	0,343	2,22E-72	Tem 1
Tigit	2,55E-65	0,63047	0,648	0,374	1,04E-62	Tem 1
Cd3e	6,27E-64	0,76111	0,834	0,686	2,56E-61	Tem 1
Casp1	2,35E-62	1,24214	0,461	0,232	9,63E-60	Tem 1
Thy1	2,13E-59	0,73191	0,669	0,417	8,72E-57	Tem 1
Stat4	1,10E-50	0,58931	0,89	0,757	4,48E-48	Tem 1
Fth1	4,18E-47	0,58748	0,999	0,998	1,71E-44	Tem 1
Pdcd1	2,13E-44	1,07198	0,495	0,287	8,72E-42	Tem 1
Tnfrsf4	1,90E-41	0,54207	0,684	0,48	7,79E-39	Tem 1
Tnfrsf18	9,78E-41	0,55717	0,802	0,629	4,00E-38	Tem 1
Trac	2,38E-39	0,52892	0,945	0,881	9,73E-37	Tem 1
Lat	8,74E-39	0,54732	0,857	0,728	3,58E-36	Tem 1
Cd9	1,43E-38	0,82177	0,532	0,345	5,84E-36	Tem 1
Hif1a	1,19E-37	0,48918	0,914	0,821	4,86E-35	Tem 1
Fyn	7,75E-36	0,48561	0,797	0,63	3,17E-33	Tem 1
S100a10	1,34E-35	0,70676	0,669	0,526	5,49E-33	Tem 1
Adora2a	6,31E-31	0,75337	0,478	0,305	2,58E-28	Tem 1
Cd27	1,60E-29	0,69076	0,613	0,471	6,56E-27	Tem 1
Ctla4	2,12E-27	0,3419	0,443	0,275	8,68E-25	Tem 1
Il7r	1,06E-24	0,55076	0,708	0,595	4,32E-22	Tem 1
Trbc2	1,61E-21	0,33755	0,993	0,984	6,60E-19	Tem 1
Dusp2	8,96E-21	0,31999	0,446	0,301	3,66E-18	Tem 1
Bin2	2,53E-19	0,49418	0,568	0,436	1,04E-16	Tem 1
Lck	4,31E-19	0,3572	0,843	0,753	1,76E-16	Tem 1
Fyb	2,62E-13	0,4901	0,435	0,336	1,07E-10	Tem 1
Icos	4,94E-12	0,25554	0,533	0,418	2,02E-09	Tem 1
Ctsd	1,33E-08	0,37289	0,456	0,372	5,45E-06	Tem 1
Ikbkb	1,45E-06	0,35074	0,469	0,394	0,000593	Tem 1
Mapk1	3,88E-06	0,27785	0,504	0,442	0,001587	Tem 1
CD279.RMP1.30.Pdcd1.AMM2138.pAbO	0	2,71309	1	0,992	0	Tem 2

Pdcd1	9,73E-105	1,87617	0,816	0,291	3,98E-102	Tem 2
Tigit	3,52E-85	1,8777	0,8	0,391	1,44E-82	Tem 2
Cd9	4,27E-73	1,6737	0,753	0,351	1,75E-70	Tem 2
Il2rb	4,88E-57	0,78253	0,818	0,414	2,00E-54	Tem 2
Hif1a	5,85E-53	1,00181	0,974	0,826	2,39E-50	Tem 2
Bcl2a1a	1,61E-42	0,36755	0,761	0,433	6,57E-40	Tem 2
Cxcr4	6,36E-42	1,38331	0,453	0,15	2,60E-39	Tem 2
CD278.Icos.AMM2072.pAbO	1,07E-37	0,59573	1	1	4,39E-35	Tem 2
Itgb2	8,88E-37	0,81625	0,545	0,246	3,63E-34	Tem 2
Dusp2	2,48E-36	0,61528	0,621	0,306	1,01E-33	Tem 2
Adora2a	2,16E-33	0,95955	0,624	0,313	8,83E-31	Tem 2
Cd44	5,62E-32	1,06273	0,411	0,155	2,30E-29	Tem 2
Dusp1	9,29E-32	1,32707	0,542	0,252	3,80E-29	Tem 2
Cd6	6,91E-29	0,53806	0,768	0,48	2,83E-26	Tem 2
Tnfrsf9	7,84E-28	1,02207	0,482	0,217	3,21E-25	Tem 2
Cd5	4,45E-26	0,74823	0,711	0,431	1,82E-23	Tem 2
Tnfsf8	6,32E-26	0,94255	0,642	0,383	2,58E-23	Tem 2
Tnfrsf4	1,50E-25	0,64532	0,763	0,494	6,15E-23	Tem 2
Ybx3	2,60E-23	0,51528	0,463	0,24	1,06E-20	Tem 2
Fyn	6,20E-22	0,61543	0,866	0,642	2,54E-19	Tem 2
Cxcr3	3,13E-18	0,35619	0,479	0,288	1,28E-15	Tem 2
Cd28	1,02E-15	0,52261	0,771	0,563	4,19E-13	Tem 2
Trac	2,00E-13	0,57137	0,958	0,886	8,20E-11	Tem 2
Rbpj	4,16E-12	0,43425	0,437	0,282	1,70E-09	Tem 2
Trbc1	3,46E-200	2,10417	1	0,653	1,41E-197	Tem 3
Cxcr3	2,89E-59	1,64899	0,685	0,28	1,18E-56	Tem 3
Cd3g	4,80E-45	1,05052	0,866	0,607	1,96E-42	Tem 3
Itga4	1,64E-39	1,25224	0,673	0,361	6,72E-37	Tem 3
Lat	7,55E-34	0,87767	0,912	0,737	3,09E-31	Tem 3
Cd4	6,68E-32	0,78121	0,884	0,707	2,73E-29	Tem 3
Itgb2	4,94E-24	1,39859	0,443	0,252	2,02E-21	Tem 3
Thy1	9,49E-24	0,89618	0,688	0,439	3,88E-21	Tem 3
Gapdh	3,50E-23	0,48934	0,983	0,942	1,43E-20	Tem 3
Trac	1,19E-22	0,63751	0,952	0,887	4,85E-20	Tem 3
Cd5	1,23E-22	0,85699	0,682	0,434	5,02E-20	Tem 3
Cd28	1,13E-21	0,75944	0,776	0,563	4,62E-19	Tem 3
Cd9	5,42E-20	0,94872	0,591	0,36	2,22E-17	Tem 3
Lck	8,93E-20	0,56327	0,909	0,759	3,65E-17	Tem 3
Tigit	2,52E-18	0,44234	0,639	0,399	1,03E-15	Tem 3
Fyn	5,42E-17	0,61958	0,807	0,645	2,22E-14	Tem 3
Tnfrsf18	1,30E-16	0,55536	0,832	0,643	5,31E-14	Tem 3
Bcl2a1a	1,04E-15	0,37114	0,662	0,439	4,23E-13	Tem 3
Casp1	3,29E-15	0,89013	0,449	0,253	1,35E-12	Tem 3
Il2rb	6,71E-15	0,44305	0,639	0,423	2,75E-12	Tem 3

Stat4	1,30E-13	0,51843	0,875	0,77	5,31E-11	Tem 3
Cd6	1,82E-13	0,64793	0,673	0,485	7,42E-11	Tem 3
Cd3e	2,90E-13	0,49711	0,835	0,699	1,19E-10	Tem 3
Lgals1	3,50E-13	1,01556	0,44	0,261	1,43E-10	Tem 3
S100a10	5,42E-13	0,68476	0,69	0,538	2,22E-10	Tem 3
Bin2	2,45E-10	0,64482	0,594	0,447	1,00E-07	Tem 3
Pdcd1	1,47E-09	0,26142	0,46	0,308	6,01E-07	Tem 3
Dusp2	5,63E-09	0,71658	0,457	0,314	2,30E-06	Tem 3
Tnfrsf4	3,05E-07	0,25138	0,648	0,5	0,000125	Tem 3
Ctsd	4,02E-07	0,42842	0,523	0,377	0,000164	Tem 3
Hif1a	1,28E-06	0,30881	0,915	0,829	0,000525	Tem 3
Il7r	1,37E-06	0,48432	0,707	0,605	0,000559	Tem 3
Cd52	3,17E-06	0,39894	0,764	0,698	0,001298	Tem 3
Bax	5,61E-06	0,3268	0,645	0,513	0,002295	Tem 3
Fyb	5,05E-05	0,43463	0,455	0,344	0,02065	Tem 3
Cd27	6,25E-05	0,43626	0,599	0,484	0,025544	Tem 3
Cxcl10	5,54E-158	2,41034	0,94	0,621	2,27E-155	Tem 4
Tnfsf8	1,37E-97	2,47201	0,789	0,38	5,62E-95	Tem 4
Tnfrsf4	2,59E-70	1,76826	0,869	0,493	1,06E-67	Tem 4
Bcl2a1a	1,58E-46	0,87025	0,846	0,434	6,45E-44	Tem 4
Il2rb	5,66E-43	0,71145	0,815	0,418	2,31E-40	Tem 4
Hif1a	7,47E-41	0,83653	0,983	0,828	3,05E-38	Tem 4
Tnfrsf9	7,42E-33	1,75862	0,52	0,218	3,03E-30	Tem 4
Casp1	2,27E-31	0,99627	0,577	0,249	9,30E-29	Tem 4
Pdcd1	7,86E-30	0,98441	0,634	0,302	3,22E-27	Tem 4
Stat4	1,31E-29	0,82891	0,946	0,768	5,35E-27	Tem 4
Tigit	2,02E-29	0,76111	0,728	0,397	8,24E-27	Tem 4
Tnfrsf18	6,10E-28	0,94317	0,856	0,644	2,50E-25	Tem 4
Cd5	1,44E-25	0,65023	0,742	0,433	5,90E-23	Tem 4
Cish	4,46E-24	0,58214	0,862	0,586	1,82E-21	Tem 4
Maf	8,98E-24	0,92246	0,436	0,18	3,67E-21	Tem 4
Jak2	9,49E-22	0,76468	0,839	0,596	3,88E-19	Tem 4
Nfkb2	3,82E-19	0,52097	0,856	0,611	1,56E-16	Tem 4
Adora2a	1,68E-17	0,81699	0,57	0,318	6,86E-15	Tem 4
Lgals1	1,71E-16	0,27101	0,46	0,262	6,97E-14	Tem 4
Dusp1	6,18E-16	1,02543	0,487	0,257	2,53E-13	Tem 4
Cxcr3	6,88E-16	0,4855	0,513	0,288	2,81E-13	Tem 4
Gapdh	4,78E-15	0,41785	0,99	0,942	1,96E-12	Tem 4
Tnfrsf1b	1,03E-14	0,58591	0,577	0,346	4,20E-12	Tem 4
Nfkb1	3,06E-14	0,47684	0,896	0,739	1,25E-11	Tem 4
Itga4	1,14E-13	0,40032	0,57	0,367	4,66E-11	Tem 4
Icos	1,19E-13	0,25779	0,631	0,426	4,86E-11	Tem 4
Ybx3	1,47E-13	0,48274	0,433	0,243	6,02E-11	Tem 4
Ctla4	2,67E-13	0,3887	0,497	0,289	1,09E-10	Tem 4
Tnfrsf25	2,74E-13	0,28899	0,56	0,375	1,12E-10	Tem 4

Cd6	3,63E-13	0,46564	0,705	0,485	1,48E-10	Tem 4
Cd4	1,44E-12	0,42199	0,883	0,708	5,88E-10	Tem 4
CD279.RMP1.30.Pdcd1.AMM2138.pAbO	3,11E-10	0,30732	1	0,992	1,27E-07	Tem 4
Icam1	3,60E-10	0,25529	0,416	0,267	1,47E-07	Tem 4
Cd52	1,03E-06	0,34485	0,829	0,697	0,000421	Tem 4
Stat3	2,81E-06	0,35566	0,93	0,875	0,001151	Tem 4
Rbpj	3,14E-06	0,59721	0,423	0,284	0,001284	Tem 4
CD278.Icos.AMM2072.pAbO	8,37E-196	1,97702	1	1	3,42E-193	Tem 5
Cxcr3	7,74E-19	0,89431	0,609	0,289	3,17E-16	Tem 5
Casp1	2,36E-18	0,65336	0,542	0,254	9,65E-16	Tem 5
Cd28	2,65E-15	0,34569	0,833	0,566	1,08E-12	Tem 5
Ctla4	6,92E-15	0,39474	0,557	0,29	2,83E-12	Tem 5
Tigit	8,30E-15	0,25543	0,667	0,403	3,39E-12	Tem 5
Icos	1,05E-13	0,57397	0,703	0,426	4,28E-11	Tem 5
CD279.RMP1.30.Pdcd1.AMM2138.pAbO	9,77E-13	0,35271	1	0,992	4,00E-10	Tem 5
Cd5	1,07E-12	0,50873	0,703	0,438	4,39E-10	Tem 5
Cd6	4,26E-12	0,27006	0,734	0,487	1,74E-09	Tem 5
Il18r1	5,90E-10	0,87034	0,453	0,236	2,41E-07	Tem 5
Trbc1	3,42E-05	0,26329	0,812	0,664	0,013967	Tem 5
S100a10	5,61E-05	0,32978	0,698	0,54	0,022932	Tem 5
Gzmk	5,74E-154	5,07516	0,965	0,056	2,35E-151	Eomes_hi
Eomes	5,88E-75	4,37997	0,655	0,053	2,40E-72	Eomes_hi
Tigit	7,01E-35	1,83416	0,876	0,402	2,87E-32	Eomes_hi
Ccr5	1,71E-30	2,90348	0,469	0,068	6,98E-28	Eomes_hi
Cxcr4	7,30E-27	2,27434	0,54	0,158	2,98E-24	Eomes_hi
Lat	1,34E-25	1,27183	0,938	0,742	5,50E-23	Eomes_hi
Pdcd1	1,63E-23	1,65057	0,743	0,308	6,68E-21	Eomes_hi
Cxcr3	8,74E-22	1,4504	0,726	0,29	3,57E-19	Eomes_hi
Fyn	2,79E-19	1,04536	0,903	0,648	1,14E-16	Eomes_hi
Fyb	4,62E-17	1,39662	0,646	0,345	1,89E-14	Eomes_hi
Ybx3	1,25E-16	1,6061	0,602	0,245	5,12E-14	Eomes_hi
Stat3	2,04E-15	1,02684	0,956	0,876	8,36E-13	Eomes_hi
Cd6	6,50E-15	1,09158	0,805	0,488	2,66E-12	Eomes_hi
Cd27	5,66E-14	1,20432	0,77	0,485	2,32E-11	Eomes_hi
Gapdh	4,23E-12	0,66588	0,991	0,943	1,73E-09	Eomes_hi
Cd5	4,36E-12	1,01398	0,761	0,439	1,78E-09	Eomes_hi
Cd9	1,02E-11	1,22673	0,611	0,366	4,17E-09	Eomes_hi
Runx3	1,15E-09	1,14538	0,558	0,293	4,72E-07	Eomes_hi
Tnfrsf9	1,12E-08	0,9452	0,487	0,225	4,60E-06	Eomes_hi
Stat4	1,46E-08	0,704	0,912	0,772	5,97E-06	Eomes_hi

Adora2a	1,90E-08	1,01594	0,566	0,324	7,76E-06	Eomes_hi
Gimap7	3,52E-08	0,89871	0,602	0,332	1,44E-05	Eomes_hi
Dusp1	4,12E-08	1,21869	0,469	0,262	1,69E-05	Eomes_hi
Il2rb	2,25E-07	0,2999	0,664	0,429	9,21E-05	Eomes_hi
Bcl6	2,86E-07	0,99612	0,522	0,289	0,000117	Eomes_hi
Cd4	2,89E-07	0,5429	0,894	0,711	0,000118	Eomes_hi
Cd28	7,46E-07	0,6682	0,779	0,569	0,000305	Eomes_hi
CD279.RMP1.30.Pdcd1.AMM2138.pAbO	2,20E-06	0,50528	1	0,992	0,000898	Eomes_hi
Itgb2	5,89E-06	0,86849	0,451	0,257	0,002407	Eomes_hi
Bcl2a1a	7,13E-06	0,41924	0,673	0,445	0,002915	Eomes_hi
Fth1	1,15E-05	0,56337	1	0,998	0,00471	Eomes_hi
Ctsd	4,98E-05	0,663	0,575	0,38	0,020387	Eomes_hi
Cd3e	5,30E-05	0,57781	0,841	0,703	0,021676	Eomes_hi
Cd3g	5,91E-05	0,56006	0,779	0,616	0,024186	Eomes_hi
Trbc1	7,14E-05	0,72725	0,796	0,666	0,0292	Eomes_hi
Thy1	8,25E-05	0,3998	0,646	0,446	0,03374	Eomes_hi
Ccl5	0	6,02391	0,997	0,126	0	Cytotoxic
Gzmk	3,67E-133	3,76249	0,496	0,049	1,50E-130	Cytotoxic
Ccr5	2,78E-103	3,62519	0,432	0,057	1,14E-100	Cytotoxic
Cxcr6	1,70E-95	1,95159	0,635	0,147	6,95E-93	Cytotoxic
Lilrb4a	1,48E-90	2,07645	0,633	0,159	6,06E-88	Cytotoxic
Ccr2	2,71E-86	3,10972	0,418	0,059	1,11E-83	Cytotoxic
Il2rb	5,98E-85	1,39463	0,882	0,412	2,45E-82	Cytotoxic
Cd6	2,41E-76	1,49155	0,866	0,476	9,85E-74	Cytotoxic
Maf	4,09E-72	2,14728	0,563	0,172	1,67E-69	Cytotoxic
Il18rap	5,35E-63	2,06613	0,496	0,133	2,19E-60	Cytotoxic
Tigit	6,49E-63	1,19005	0,815	0,39	2,66E-60	Cytotoxic
Fasl	1,70E-62	2,0444	0,483	0,124	6,97E-60	Cytotoxic
Bcl2a1a	1,34E-60	0,85519	0,853	0,43	5,47E-58	Cytotoxic
Ybx3	1,04E-47	1,48149	0,584	0,234	4,25E-45	Cytotoxic
Rgs1	5,12E-46	1,54375	0,668	0,343	2,10E-43	Cytotoxic
Pdcd1	1,15E-45	1,32399	0,66	0,298	4,69E-43	Cytotoxic
Bcl2l1	9,12E-44	1,52105	0,475	0,157	3,73E-41	Cytotoxic
Stat3	1,20E-38	0,94617	0,938	0,874	4,90E-36	Cytotoxic
Cxcr3	1,87E-37	0,98974	0,614	0,282	7,67E-35	Cytotoxic
Cd5	1,97E-33	0,91743	0,74	0,43	8,07E-31	Cytotoxic
Cd4	1,02E-32	0,71537	0,92	0,704	4,19E-30	Cytotoxic
Casp1	1,79E-31	1,15601	0,539	0,248	7,31E-29	Cytotoxic
Cxcr4	2,77E-30	1,41369	0,408	0,152	1,13E-27	Cytotoxic
Tnfrsf9	6,23E-26	0,62914	0,464	0,218	2,55E-23	Cytotoxic
Lgals1	3,06E-25	1,123	0,512	0,258	1,25E-22	Cytotoxic
Tnfrsf1b	6,14E-24	0,73587	0,611	0,342	2,51E-21	Cytotoxic
Cd3e	4,10E-23	0,68995	0,866	0,697	1,67E-20	Cytotoxic
Adora2a	1,43E-22	0,70391	0,574	0,316	5,86E-20	Cytotoxic

Fth1	2,09E-22	0,53619	1	0,998	8,56E-20	Cytotoxic
Gapdh	1,54E-21	0,51777	0,992	0,942	6,32E-19	Cytotoxic
Cd3g	7,81E-21	0,63385	0,815	0,609	3,20E-18	Cytotoxic
Cd48	2,93E-20	0,96179	0,466	0,237	1,20E-17	Cytotoxic
Gimap7	9,99E-20	0,91803	0,563	0,326	4,09E-17	Cytotoxic
Icos	7,88E-19	0,67037	0,654	0,423	3,22E-16	Cytotoxic
Ctla4	4,56E-18	0,82713	0,507	0,287	1,86E-15	Cytotoxic
Il18r1	1,48E-15	0,99952	0,41	0,233	6,06E-13	Cytotoxic
Itgb2	8,05E-15	0,74819	0,448	0,251	3,29E-12	Cytotoxic
Cd27	2,77E-14	0,85872	0,633	0,482	1,13E-11	Cytotoxic
Itga4	6,53E-14	0,61478	0,568	0,365	2,67E-11	Cytotoxic
Tnfrsf18	7,66E-11	0,44222	0,796	0,644	3,13E-08	Cytotoxic
Ifngr1	1,48E-09	0,25086	0,949	0,886	6,05E-07	Cytotoxic
Runx3	4,75E-09	0,74535	0,432	0,29	1,94E-06	Cytotoxic
Cd28	7,11E-09	0,27334	0,721	0,565	2,91E-06	Cytotoxic
Il7r	2,40E-08	0,4376	0,633	0,608	9,83E-06	Cytotoxic
Fyb	3,00E-08	0,5112	0,493	0,342	1,23E-05	Cytotoxic
Stat4	2,23E-07	0,3707	0,85	0,77	9,12E-05	Cytotoxic
S100a10	6,14E-07	0,26994	0,676	0,538	0,000251	Cytotoxic
Bin2	3,19E-06	0,31548	0,576	0,447	0,001303	Cytotoxic
Gimap5	3,26E-06	0,45865	0,517	0,386	0,001333	Cytotoxic
Dusp2	1,56E-05	0,3118	0,432	0,314	0,006395	Cytotoxic
Ctsd	5,55E-05	0,43293	0,493	0,378	0,022679	Cytotoxic
Cxcr6	0	3,95041	0,875	0,121	0	Single +
Il2rb	5,52E-214	1,93704	0,956	0,397	2,26E-211	Single +
Tnfrsf9	2,70E-190	2,44542	0,776	0,192	1,10E-187	Single +
Lilrb4a	6,95E-188	2,95169	0,686	0,146	2,84E-185	Single +
Rgs1	1,77E-182	2,62957	0,818	0,327	7,23E-180	Single +
Icos	1,06E-163	2,07772	0,864	0,404	4,32E-161	Single +
Bcl2a1a	2,28E-162	1,71501	0,912	0,417	9,32E-160	Single +
Pdcd1	6,56E-142	1,94154	0,785	0,282	2,68E-139	Single +
Lgals1	6,84E-135	2,43344	0,676	0,242	2,80E-132	Single +
Ccr5	1,03E-129	2,61734	0,426	0,05	4,21E-127	Single +
Tigit	4,12E-127	1,46873	0,869	0,378	1,68E-124	Single +
Bcl2l1	5,69E-123	1,74783	0,603	0,142	2,33E-120	Single +
Stat3	1,13E-107	1,1772	0,95	0,872	4,63E-105	Single +
Ybx3	6,48E-100	1,77481	0,654	0,222	2,65E-97	Single +
Ccl5	4,86E-91	0,7284	0,526	0,139	1,99E-88	Single +
Tnfrsf1b	6,65E-91	1,46657	0,754	0,327	2,72E-88	Single +
Ctla4	8,67E-82	2,26175	0,642	0,273	3,54E-79	Single +
Rbpj	4,08E-76	1,76624	0,616	0,267	1,67E-73	Single +
Cd6	3,95E-75	1,23103	0,829	0,47	1,62E-72	Single +
Gapdh	2,52E-71	0,85393	0,985	0,941	1,03E-68	Single +
Adora2a	7,05E-67	1,16373	0,678	0,304	2,88E-64	Single +
Fasl	1,11E-63	1,53521	0,425	0,121	4,56E-61	Single +

Ifitm3	2,60E-60	2,03433	0,465	0,195	1,06E-57	Single +
Il12rb2	1,80E-59	1,26417	0,48	0,167	7,34E-57	Single +
Cish	2,62E-59	0,86831	0,881	0,576	1,07E-56	Single +
Il18rap	2,28E-58	1,60964	0,426	0,13	9,34E-56	Single +
Fth1	4,92E-55	0,75004	1	0,998	2,01E-52	Single +
Dusp2	3,36E-50	1,07148	0,623	0,299	1,37E-47	Single +
Maf	8,37E-48	1,43489	0,454	0,171	3,42E-45	Single +
Cd44	3,41E-41	1,39605	0,403	0,15	1,39E-38	Single +
Hif1a	7,34E-41	0,56197	0,965	0,824	3,00E-38	Single +
Il18r1	2,64E-37	1,30617	0,485	0,224	1,08E-34	Single +
Tnfrsf4	3,03E-34	0,54264	0,754	0,49	1,24E-31	Single +
Tnfrsf18	1,23E-33	0,54225	0,871	0,636	5,01E-31	Single +
Thy1	1,35E-31	0,5711	0,693	0,433	5,51E-29	Single +
Casp1	7,37E-27	0,49701	0,447	0,248	3,02E-24	Single +
Cd5	3,20E-26	0,49889	0,664	0,429	1,31E-23	Single +
Cxcr3	2,12E-25	0,34277	0,476	0,284	8,66E-23	Single +
Itgb2	4,29E-23	0,54648	0,441	0,247	1,76E-20	Single +
Gimap5	4,79E-18	0,44074	0,564	0,38	1,96E-15	Single +
Xbp1	3,67E-15	0,35655	0,539	0,377	1,50E-12	Single +
Nfkb1	2,26E-14	0,34247	0,875	0,736	9,26E-12	Single +
Cd3g	3,58E-13	0,29164	0,765	0,608	1,47E-10	Single +
Stat4	9,55E-12	0,29799	0,886	0,766	3,91E-09	Single +
Zap70	1,04E-10	0,42301	0,8	0,667	4,25E-08	Single +
Cd69	2,60E-192	2,41939	0,851	0,462	1,06E-189	Double +
Bcl2a1a	1,65E-168	1,98214	0,911	0,42	6,77E-166	Double +
Nfkb1	5,88E-167	1,66626	0,946	0,732	2,41E-164	Double +
Icam1	3,87E-149	2,77907	0,622	0,251	1,58E-146	Double +
Fyn	3,04E-129	1,54962	0,893	0,637	1,24E-126	Double +
Irf4	1,11E-124	3,27497	0,403	0,051	4,56E-122	Double +
Thy1	1,29E-122	2,24697	0,791	0,429	5,28E-120	Double +
Myc	1,56E-100	2,57715	0,539	0,153	6,37E-98	Double +
Cxcr5	2,92E-94	2,59398	0,452	0,089	1,20E-91	Double +
Btla	4,45E-94	2,63945	0,403	0,076	1,82E-91	Double +
Ptprc	5,01E-85	0,89437	0,95	0,973	2,05E-82	Double +
Tnfrsf1b	7,46E-85	1,86216	0,64	0,337	3,05E-82	Double +
Cish	3,22E-83	1,6117	0,793	0,584	1,32E-80	Double +
Trac	9,60E-73	1,01967	0,952	0,886	3,92E-70	Double +
Dusp1	6,09E-69	1,94287	0,525	0,249	2,49E-66	Double +
Zap70	3,27E-67	1,06456	0,845	0,666	1,34E-64	Double +
Dusp2	5,71E-64	1,85952	0,616	0,302	2,34E-61	Double +
Junb	3,92E-61	1,23197	0,897	0,751	1,60E-58	Double +
Lck	9,64E-58	0,91746	0,913	0,756	3,94E-55	Double +
Adora2a	7,27E-54	1,6071	0,574	0,312	2,97E-51	Double +
Icos	5,11E-52	1,34214	0,694	0,417	2,09E-49	Double +
Nfkb2	1,36E-51	1,00732	0,824	0,607	5,57E-49	Double +

Tnfrsf4	9,58E-48	1,27188	0,707	0,494	3,92E-45	Double +
Cd28	2,28E-46	1,14578	0,764	0,561	9,31E-44	Double +
Tnfsf8	4,68E-39	1,60389	0,556	0,385	1,91E-36	Double +
Cd5	6,87E-38	0,94258	0,721	0,427	2,81E-35	Double +
Tigit	2,97E-33	1,11105	0,655	0,394	1,21E-30	Double +
Mbp	1,61E-32	1,14235	0,568	0,338	6,58E-30	Double +
Foxo1	2,18E-32	1,23165	0,442	0,204	8,91E-30	Double +
Btg1	6,94E-31	0,56756	0,996	0,998	2,84E-28	Double +
Il4ra	1,16E-29	1,02621	0,748	0,57	4,76E-27	Double +
Il2rb	3,66E-27	0,73676	0,674	0,418	1,50E-24	Double +
Pcna	2,77E-23	0,86591	0,612	0,433	1,13E-20	Double +
Tnfrsf18	4,12E-22	0,77993	0,791	0,643	1,69E-19	Double +
Bcl6	5,18E-18	0,98155	0,446	0,283	2,12E-15	Double +
Stat3	1,74E-16	0,45862	0,928	0,874	7,12E-14	Double +
Lat	3,99E-16	0,57861	0,826	0,739	1,63E-13	Double +
Stat5a	3,88E-15	0,73608	0,603	0,463	1,59E-12	Double +
Gapdh	1,84E-14	0,37812	0,969	0,942	7,51E-12	Double +
Stat6	1,05E-08	0,45222	0,674	0,549	4,31E-06	Double +
Cd6	1,47E-08	0,3729	0,624	0,485	6,00E-06	Double +
Cd2	3,11E-08	0,37617	0,911	0,899	1,27E-05	Double +
Rbpj	3,33E-07	0,48373	0,401	0,282	0,000136	Double +
Hif1a	2,20E-06	0,44161	0,878	0,83	0,000901	Double +
Hprt	6,87E-06	0,45999	0,517	0,434	0,002811	Double +
Stat4	1,19E-05	0,35217	0,822	0,771	0,004884	Double +
Itga4	0,0001145	0,4475	0,421	0,371	0,04683	Double +
Ifng	1,85E-255	6,1537	0,755	0,145	7,58E-253	Triple +
Myc	2,67E-208	4,52495	0,915	0,158	1,09E-205	Triple +
Nfkb1	3,18E-192	2,52779	0,979	0,739	1,30E-189	Triple +
Slc7a5	3,73E-167	3,79185	0,888	0,138	1,53E-164	Triple +
Tfrc	1,10E-147	3,95323	0,782	0,076	4,51E-145	Triple +
Tnf	6,62E-134	4,88174	0,729	0,097	2,71E-131	Triple +
Bcl2l1	3,52E-131	3,39424	0,819	0,156	1,44E-128	Triple +
Il2	1,97E-129	6,07456	0,495	0,024	8,04E-127	Triple +
Bcl2a1a	9,03E-124	2,38674	0,984	0,436	3,69E-121	Triple +
Irf8	4,65E-110	3,41852	0,755	0,183	1,90E-107	Triple +
Lap3	2,71E-103	3,336	0,622	0,043	1,11E-100	Triple +
Dusp2	6,30E-98	2,74565	0,899	0,307	2,58E-95	Triple +
Tnfrsf4	4,10E-97	2,59597	0,926	0,497	1,68E-94	Triple +
Il2ra	3,74E-96	3,49871	0,633	0,057	1,53E-93	Triple +
Ybx3	1,66E-87	2,77352	0,798	0,237	6,80E-85	Triple +
Tnfsf14	4,17E-81	3,74364	0,447	0,022	1,70E-78	Triple +
Rbpj	2,43E-60	2,28055	0,771	0,278	9,95E-58	Triple +
Tnfsf8	2,11E-55	2,49609	0,745	0,387	8,64E-53	Triple +
Cish	3,32E-50	1,38824	0,947	0,587	1,36E-47	Triple +
Il2rb	1,10E-47	1,43052	0,91	0,421	4,48E-45	Triple +

Tbx21	2,13E-41	2,32051	0,537	0,12	8,72E-39	Triple +
Nfkb2	6,74E-41	1,25127	0,926	0,613	2,76E-38	Triple +
Il15ra	9,04E-41	1,9367	0,441	0,077	3,70E-38	Triple +
Tnfrsf1b	7,55E-40	1,37424	0,819	0,344	3,09E-37	Triple +
Cd44	1,10E-38	1,95434	0,585	0,157	4,49E-36	Triple +
Zap70	3,52E-38	1,15101	0,931	0,67	1,44E-35	Triple +
Slamf1	7,62E-36	2,02288	0,511	0,122	3,12E-33	Triple +
Mbp	3,19E-35	1,7928	0,638	0,344	1,31E-32	Triple +
Stat5a	6,79E-34	1,55376	0,761	0,465	2,78E-31	Triple +
Pdcd1	6,60E-33	0,28613	0,686	0,305	2,70E-30	Triple +
Thy1	9,61E-32	1,4831	0,819	0,441	3,93E-29	Triple +
Tnfrsf9	6,31E-31	1,72564	0,617	0,22	2,58E-28	Triple +
Gapdh	6,51E-29	0,87408	0,995	0,943	2,66E-26	Triple +
Tnfrsf25	1,04E-27	1,56881	0,702	0,374	4,25E-25	Triple +
Fyn	1,16E-25	0,92858	0,936	0,645	4,74E-23	Triple +
Adora2a	4,00E-25	0,83325	0,691	0,319	1,63E-22	Triple +
Lta	5,96E-23	1,776	0,441	0,135	2,44E-20	Triple +
Hprt	3,15E-22	0,56942	0,761	0,431	1,29E-19	Triple +
Cd5	2,17E-20	1,00241	0,777	0,436	8,86E-18	Triple +
Trac	2,94E-20	0,70702	0,979	0,887	1,20E-17	Triple +
Cd6	1,02E-19	1,09636	0,798	0,486	4,17E-17	Triple +
Tigit	1,20E-19	0,80325	0,739	0,401	4,89E-17	Triple +
Pcna	4,45E-19	0,65734	0,755	0,436	1,82E-16	Triple +
Icam1	1,41E-15	1,21732	0,553	0,266	5,78E-13	Triple +
Lilrb4a	1,06E-14	1,41789	0,426	0,174	4,33E-12	Triple +
Bax	1,28E-12	0,719	0,777	0,513	5,25E-10	Triple +
Lat	3,84E-12	0,56547	0,931	0,74	1,57E-09	Triple +
Icos	9,82E-12	0,85353	0,686	0,427	4,02E-09	Triple +
Cxcr3	2,94E-10	0,39514	0,484	0,292	1,20E-07	Triple +
Atf6b	3,03E-10	0,65944	0,521	0,302	1,24E-07	Triple +
Gimap5	4,83E-09	0,56885	0,601	0,387	1,98E-06	Triple +
Jak2	1,44E-08	0,57471	0,803	0,6	5,89E-06	Triple +
Cd69	3,09E-08	0,81073	0,681	0,479	1,27E-05	Triple +
Junb	4,46E-08	0,43731	0,915	0,756	1,83E-05	Triple +
Ccnd2	7,09E-07	0,32967	0,628	0,461	0,00029	Triple +
Stat3	2,84E-06	0,44159	0,968	0,875	0,001163	Triple +

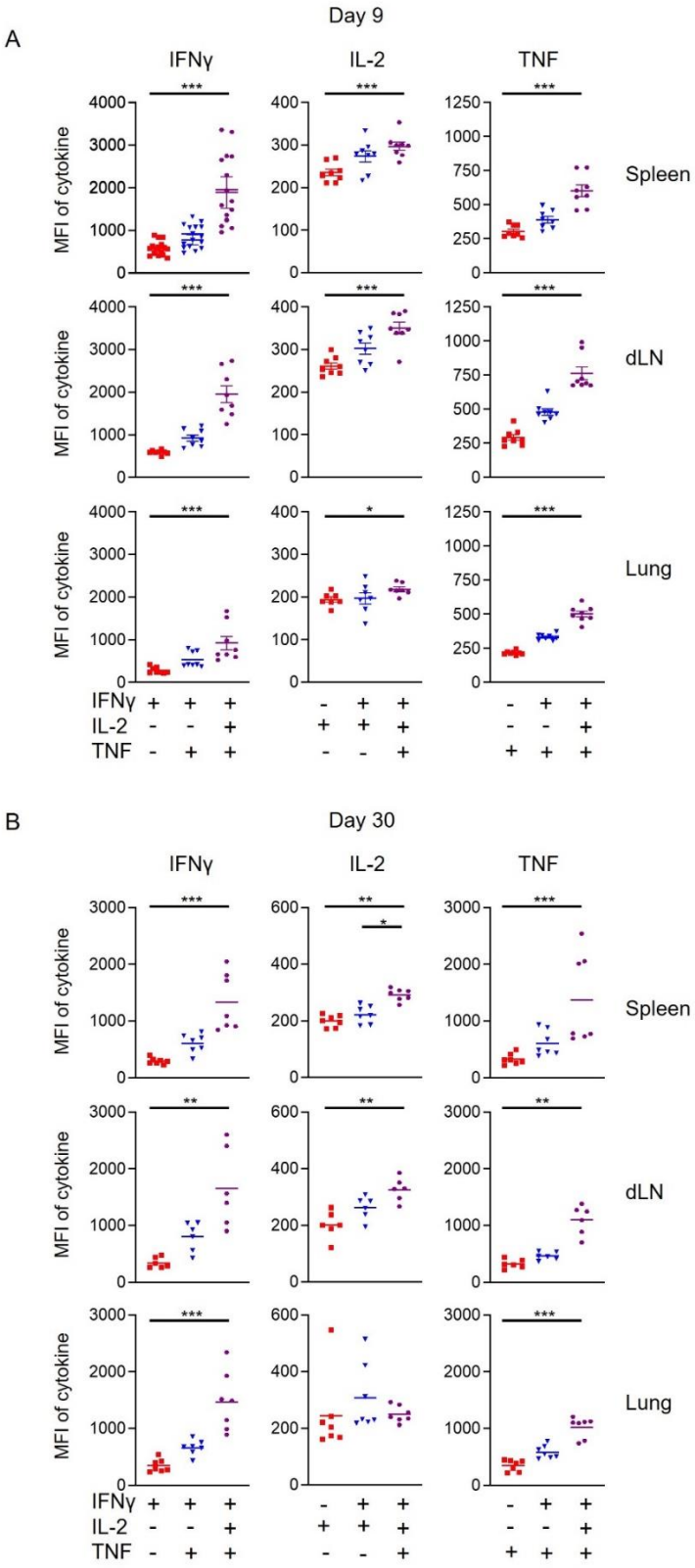

Figure 29 - Triple cytokine+ CD4 T cells produce more cytokine on a per cell basis than single cytokine+ T cells.

C57BL/6 mice were infected i.n. with IAV on day 9 or day 30 and injected i.v. with fluorescently labelled anti-CD45 3 minutes prior to removal of organs for analysis. Single cell suspensions of spleens, mediastinal draining lymph node (medLN), and lung were activated by DCs incubated with IAV-Ag. CD45iv negative IAV-specific CD4 T cells cytokine+ at day 9 (A) or day 30 (B) T cells were detected by flow cytometry. Each symbol represents a mouse and the line shows the mean of the group with SEM shown. Significant differences were assessed by Friedman's multiple comparison test followed by multiple comparisons with Dunn's multiple comparison test; *: $p<0.05$, **:$p<0.01$, ***:$p<0.001$.

Triple+ cells were uniquely enriched for *Il2* and, while the single+ and double+ clusters clearly expressed *Ifng* +/- *Tnf*, these transcripts were only significantly enriched (versus all other cells) within the triple+ cluster. Previous studies have demonstrated that multifunctional T cells produce more IFNγ on a per cell basis than single IFNγ+ T cells [22-24]. We also found that triple cytokine+ T cells express the greatest amounts of IFNγ by flow cytometry, Figure 29. Moreover, by gating on total IL-2+ or TNF+ T cells, we found that triple cytokine+ CD4 T cells also expressed more of these cytokines than single IL-2+ or TNF+ cells respectively.

4.3.5 Triple cytokine+ memory CD4 T cells express a pro-survival gene signature

We focussed on the transcriptional signatures of the three cytokine producing clusters: single+ (*Ifng*) double+ (*Ifng* & *Tnf*), and triple+ (*Ifng*, *Tnf* & *Il2*) cells, Figure 27B. The single+ CD4 T cells expressed the highest levels of *Icos* and *Pdcd1* (PD1), which we confirmed at protein level, Figure 30. Genes uniquely upregulated in the double+ cells included *Cxcr5*, *Bcl6*, *Irf4* and *Foxo1*, indicating a Tfh-like phenotype [116-118].

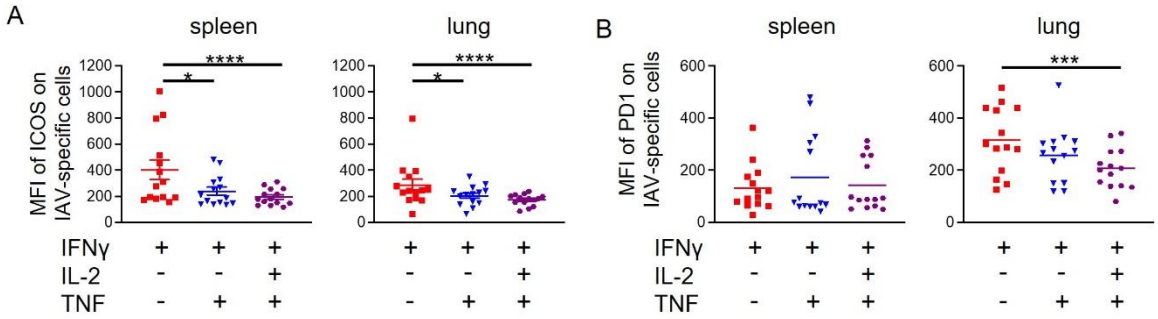

Figure 30 - Single IFNγ+ CD4 memory T cells express higher levels of PD1 and ICOS than triple cytokine+ cells.

C57BL/6 mice were infected i.n. with IAV on day 0 and injected i.v. with fluorescently labelled anti-CD45 3 minutes prior to removal of organs at day 40. Single cell suspensions of spleens and lung were activated by DCs incubated with IAV-Ag. CD45iv negative cytokine+ CD4 T cells were detected by flow cytometry to detect ICOS (A) and PD1 (B) expression. Data are from two separate experiments. Each symbol represents a mouse and the horizontal line shows the mean of the group. Significance tested via paired Friedman analysis with Dunn's multiple comparison test *: $p<0.05$, ***:$p<0.001$, ****:$p<0.0001$.

We also observed genes commonly enriched across some or all cytokine+ clusters. Strikingly, the double and triple cytokine+ cells expressed high levels of the transcription factor *Myc*; we confirmed increased Myc protein expression in triple+ cells by flow cytometry, Figure 27C. The triple cytokine+ memory CD4 T cells also expressed high levels of molecules associated with survival, Figure 27D. These included Bcl2 family members (*Bcl2a1a* and *Bcl2l1*(Bclx)), receptors

for pro-survival cytokines (*Il2ra*, *Il15ra*) and costimulatory molecules (*Tnfrsf4* (OX40), *Tnfsf8* (CD30L))[53, 119-124].

4.3.6 TCR clones are found in multiple memory T cell clusters but are not shared between different animals

We used CDR3 sequencing to address whether clones were restricted to particular memory T cell clusters. We found expanded clones within each of the memory populations, with the relative absence of these in the naïve and regulatory populations, Figure 31A-B. Few expanded clones appeared cluster specific, with most represented across multiple clusters, Figure 31C-D. These data suggest that TCR CDR3 sequence does not dictate T cell fate. Finally, analysis of expanded clonotypes derived from each animal demonstrated little evidence of public T cell clones, Figure 31E.

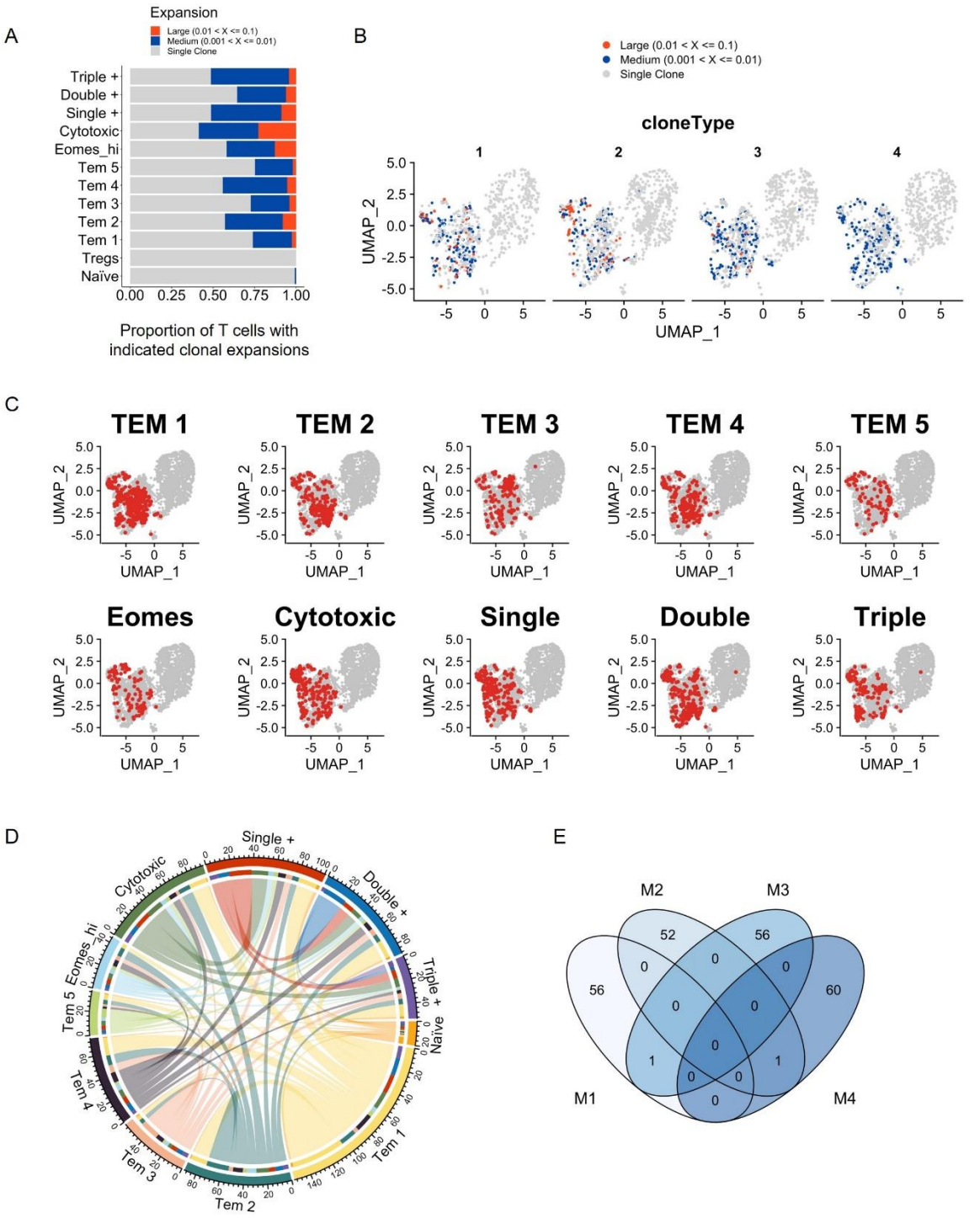

Figure 31 - TCR clones are found in multiple memory T cell clusters but are not shared between different animals.

scRNAseq analysis described in Figure 31 was integrated with single cell TCR CDR3 analysis. Large, medium and single clones identified by TCR CDR3 sequencing are displayed for each cluster and the proportion of T cells with the indicated clonal expansions shown (A). Enriched clones are overlaid on the scRNAseq UMAP for each animal and coloured by the magnitude of expansion (B). To highlight the extent to which clones were shared across clusters, clones found within each memory cluster were identified and displayed on the UMAP (C). To provide higher resolution these data are presented as a chord diagram, highlighting the inter-cluster relationship of individual clones (D). The limited overlap of identified clones between mice is displayed as a Venn diagram (E).

4.3.7 Single IFNγ+ T cells dominate the proliferative response during re-infection

Our data above and the relationship between T cell multifunctionality, persistence into the memory pool, and protection from disease, suggest that triple cytokine+ T cells should dominate a secondary response to IAV [22-25, 32, 33]. To test this, we re-infected IAV-memory mice with a distinct strain of IAV, X31. In this model, T cell responses are associated with immune protection [29], and re-challenged mice lost less weight than primary infected animals, Figure 32A.

Re-infection led to an increase in the percentages of cytokine+ CD4 and CD8 T cells that expressed Ki67, most notably in cells in the spleen and medLN, Figure 33A-B. The IFNγ+ Ki67+ CD4 and CD8 T cells present in the re-infected animals were most likely to be within the single IFNγ+ population, especially in the medLN and the lung, Figure 33C-D.

The low levels of Ki67 in triple cytokine+ cells may suggest that this population would be less prevalent following re-infection and that single or double positive T cells may become a more prominent population. This was not the case. The percentages of IFNγ+ cells that were also expressing IL-2 and/or TNFα were the same before and at day 5, Figure 32B, and day 35 following re-infection, Figure 33E-F. These data are consistent with the hypothesis that multifunctional T cells have an ability to survive within the memory pool.

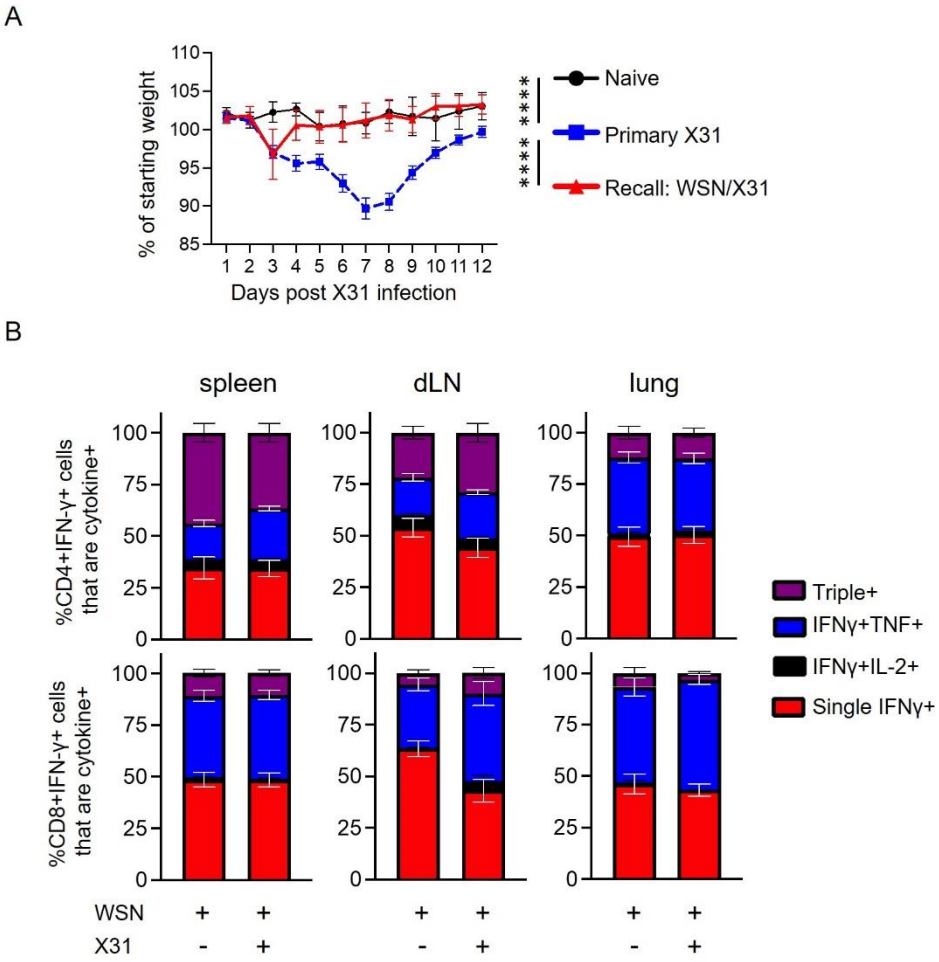

Figure 32 - Previous infection with IAV leads to a protective response following re-challenge infection but no changes in the proportion of cytokine+ populations.

C57BL/6 mice were infected i.n. with WSN IAV on day -30 and then infected with X31 on day 0. Controls were age-matched naïve animals or naïve mice infected with X31 IAV on day 0. Mice were weighed and the difference in weight loss calculated by measuring the area and the curve (A). On day 5 after the challenge infection, a separate cohort of mice were injected i.v. with fluorescently labelled anti-CD45 3 minutes prior to removal of organs for analysis. Single cell suspensions of spleens, mediastinal draining lymph node (medLN), and lung were activated by bmDCs incubated with IAV-Ag. The proportions of IFNγ+ CD4 and CD8 T cells expressing IL-2 and TNFα were calculated (B). In A, naïve animals are from one experiment (4 naïve animals) and infected animals combined from two experiments with a total of 12 primary infected animals and 9 re-infected animals. The areas under the curves were compared by ANOVA followed by a Tukey's multiple comparison test with ****:p<0.0001. In B, data are from two experiments with a total of 7-8 mice/group, error bars are SEM.

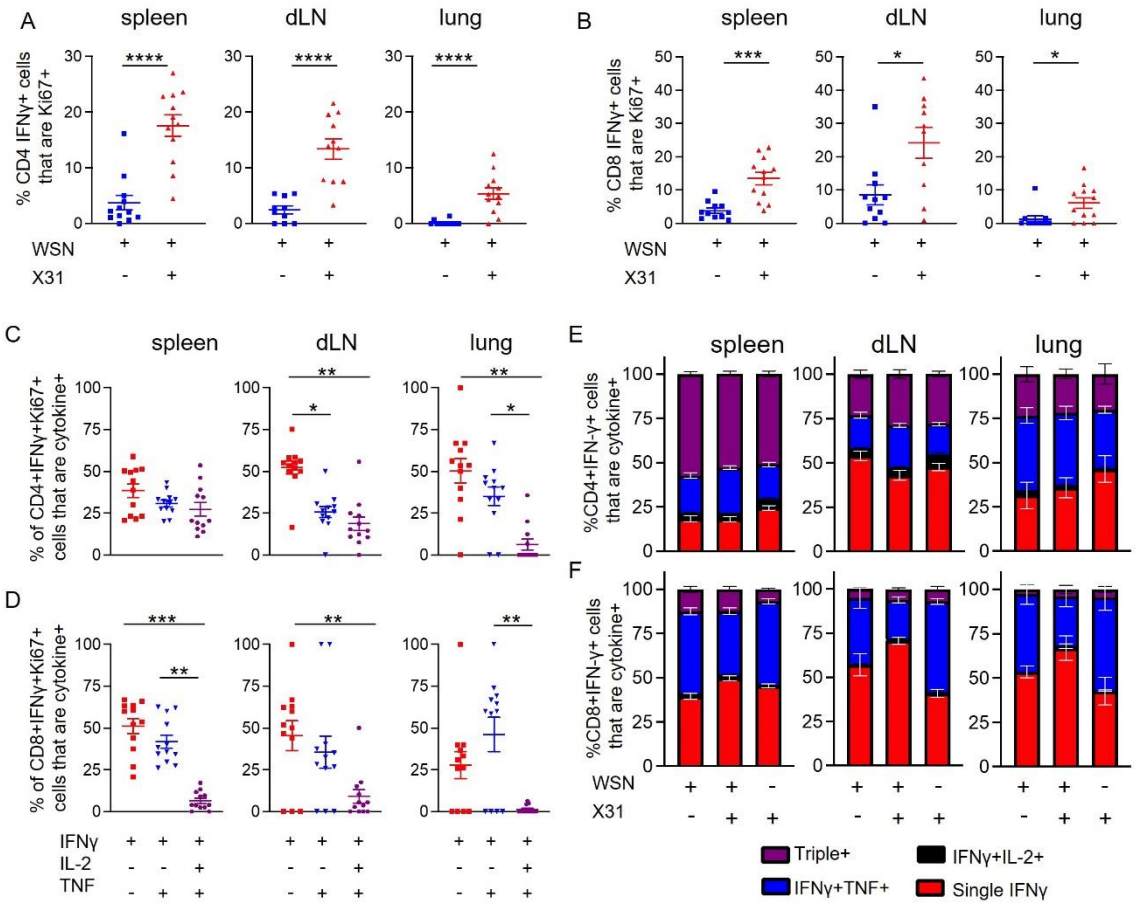

Figure 33 - Triple cytokine+ T cells are less likely to be in cell cycle than single IFNγ+ T cells following challenge infection.

C57BL/6 mice were infected i.n. with IAV on day 0. On day 30, some of these animals and age-matched naïve mice were infected with X31 IAV i.n. 5 (A-D) or 35 days (E-F) later, these mice and the remaining WSN-memory mice received anti-CD45 i.v. 3minutes prior to tissue harvest. Single cell suspensions of spleens, mediastinal draining lymph node (medLN), and lung were activated for 6 hours with IAV-Ag+ DCs. CD45iv negative IAV-specific IFNγ+ CD4 T cells or CD8 T cells were analysed by flow to detect IFNγ+ T cells that were Ki67+. In C-D, IFNγ+ that were Ki67 in the re-infected animals at day 5 post-infection were examined for production of IL-2 and TNF. Data are from two independent experiments with a total of 7-8 mice. Symbols represent each mouse and the horizontal line shows the mean of the group (A-D), in E-F error bars are SEM. In A-D significance tested by Mann-Whitney. In E-F, significance tested via ANOVA and Dunn's; *: $p<0.05$, **:$p<0.01$, ***:$p<0.001$, ****:$p<0.0001$.

4.4 Discussion

Our data demonstrate that CD4 T cells with the capacity to produce multiple different types of cytokines are found at stable numbers in secondary lymphoid organs across primary and memory timepoints. Moreover, at gene and protein level, these cells express molecules associated with cell survival. Cytokines are often required for, or associated with, memory T cell mediated immune protection[22-24, 29, 48, 58, 59, 84, 105]. Therefore, the identification of factors and cell types that promote cytokine+ cells could define how we could increase the size and protective ability of the memory T cell pool following vaccination.

Our data are consistent with the hypothesis that memory T cells with the capacity to produce cytokines are more likely to survive into and within the memory pool than those that cannot produce cytokines. This challenges findings that showed poor survival of cytokine+ cells, and supports other studies that have demonstrated stability of cytokine+ memory T cells[65, 108-110].

The numbers of multifunctional cytokine+ CD4 T cell that produced IFNγ, IL-2 and TNFα were particularly stable between day 9 and 30 post-infection. We ruled out a role for proliferation in supporting the persistence of this population. However, it is possible that the memory T cells are a dynamic and plastic population, shifting between the cytokine+ and negative populations between time points. Adoptive transfer of the different cytokine+ and negative populations would be required to address whether cytokine producing capacity is stable and test the hypothesis that cytokine+ cells do indeed display enhanced survival compared to non-cytokine+ T cells.

A further caveat of our model is that detection of the cytokine producing cells involves a short *ex vivo* reactivation stage. We therefore cannot know whether the expression of these molecules is altered during the reactivation. Our previous data did, however, demonstrate that the three cytokine+ populations could be identified as early as two hours after re-activation, suggesting that these three populations are reflective of *in vivo* CD4 T cells with distinct phenotypes and functions[25].

We were surprised that the double and triple cytokine+ CD4 memory T cells did not dominate the secondary response to IAV. These cells expressed high level of transcripts for *Myc*, *Slc7a5* and the transferrin receptor, suggesting that they are poised to proliferate following TCR activation[125]. We cannot exclude that memory triple or double cytokine+ CD4 T cells differentiate into single IFNγ+ during the re-infection. We think this is unlikely, however, given the stability of proportions of triple/double/single cytokine+ cells at days 5 and 30 following IAV re-infection.

We identified IAV-specific CD4 T cells using methods that restrict the population to a single immunodominant epitope or to T cells responding to numerous IAV epitopes. Our results are consistent between these methods suggesting that TCR

specificity does not influence T cell survival. This conclusion is reinforced by finding the same TCR clones in several of the memory clusters within the single-cell RNAseq dataset. We suggest that environment is more likely, therefore, to dictate cell fate, than signals through the TCR.

We have analysed IAV-specific CD4 and CD8 T cells in the same animals highlighting some key differences. Most notably, cytokine+ CD8 T cells display a very limited decline in lymphoid organs reflecting similar findings in LCMV infected mice[43]. We did find consistent patterns of Ki67 expression in IAV-specific CD4 and CD8 T cells. Single IFNγ+ CD4 and CD8 T cells were more likely to be Ki67+ at primary, memory and recall timepoints compared to triple or double cytokine+ T cells. These data suggest that the link between proliferation capacity and multi-functionality is common to both CD4 and CD8 T cells. Understanding the molecular mechanisms that underlie this link could, therefore, reveal pathways that can be manipulated to enhance both the CD4 and CD8 T cell responses in the context of infectious disease and cancer, or limit such responses in autoimmune pathologies.

4.5 Materials and Methods

4.5.1 Animals and Study design

10 week old female C57BL/6 mice were purchased from Envigo (UK). TRACE male and female and female C57BL/6 mice were maintained at the University of Glasgow under specific pathogen free conditions in accordance with UK home office regulations (Project Licenses P2F28B003 and PP1902420) and as approved by the local ethics committee. TRACE mice have been described previously[60].

4.5.2 Infections

IAV was prepared and titered in MDCK cells. 10-14 week old mice were briefly anesthetised using inhaled isoflurane and infected with 150-200 plaque forming units of Influenza A/WSN/33 (H1N1) in 20μl of PBS intranasally (i.n.). These mice are between 18-25g at the start of the experiment. Infected mice were rechallenged with 200PFU of Influenza A/X31 (H3N2). Infected mice were weighed daily for 14 days post-infection. Any animals that lost more than 20% of

their starting weight were humanely euthanised. TRACE mice were given Dox+ chow (Envigo) for a total of 12 days starting two days prior to infection.

4.5.3 Tissue preparation

Mice were injected intravenously (i.v.) with 1μg anti-CD45 (30F11, either labelled with Alexa 488 or PE, ThermoFisher) 3 minutes before being euthanized by cervical dislocation. Spleen and mediastinal lymph nodes were processed by mechanical disruption. Single cell suspensions of lungs were prepared by digestion with 1mg/ml collagenase D (Sigma) and 30μg/ml DNAse (Sigma) for 40 minutes at 37°C in a shaking incubator followed by mechanical disruption. Red blood cells were lysed from spleen and lungs using lysis buffer (ThermoFisher).

4.5.4 Ex vivo reactivation for intracellular cytokine staining

Bone marrow DCs were prepared as described from C567BL/6 mice[25]. After 7 days, DCs were harvested, incubated overnight with IAV antigen (MOI of 0.3) prepared as described [25]. Alternatively, DCs were incubated with 10μg/ml NP peptides (QVYSLIRPNENPAHK and ASNENMETM from JPT) for 2 hours prior to co-cultures and with indicated doses in Figure 18E-F. Single cell suspensions of *ex vivo* organs were co-cultured with DCs in complete RMPI at a ratio of approximately 10 T cells to 1 DC in the presence of Golgi Plug (BD Bioscience). Co-cultures were incubated at 37°C, 5% CO_2 for 6 hours.

4.5.5 Flow cytometry staining

Single cell suspension were stained with PE or APC-labelled $IA^b/NP_{311-325}$ or APC labelled D^b/ $NP_{368-374}$ tetramers (NIH tetramer core) at 37°C, 5% CO_2 for 2 hours in complete RPMI (RPMI with 10% foetal calf serum, 100μg/ml penicillin-streptomycin and 2mM L-glutamine) containing Fc block (24G2). Anti-CX3CR1 BV711 (SA011F11, BioLegend) was added with the MHC tetramers. Surface antibodies were added and the cells incubated for a further 20minutes at 4°C. Antibodies used were: anti-CD4 APC-Alexa647 (RM4-5, ThermoFisher), anti-CD8 BUV805 (53-6.7, BD Bioscience), anti-CD44 BUV395 (IM7, BD Bioscience), anti-PD-1 PeCy7 (29F.1A12, BioLegend), anti-PD1 BV605 (29F.1A12, BioLegend), anti-ICOS PerCP-Cy5.5 (7E.17G9, BioLegend), anti-CD127 APC (A7R34, ThermoFisher),

CD103 PeCy7 (2E7, BioLegend), anti-CD69 PerCP-Cy5.5 (H1.2F3, ThermoFisher) and 'dump' antibodies: B220 (RA3-6B2), F4/80 (BM8) and MHC II (M5114) all on eFluor-450, ThermoFisher. Cells were stained with a fixable viability dye eFluor 506 (ThermoFisher). For normalisation of CD127 and Bcl2 expression, the MFI of the EYFP+ cells was divided by the MFI of naïve (CD44lo) CD4 T cells in the same animal in the same organ.

For intracellular staining, cells were fixed with cytofix/cytoperm (BD Bioscience) for 20 minutes at 4°C and stained in permwash buffer with anti-cytokine antibodies for one hour at room temperature anti-IFNγ PE (XMG1.2, ThermoFisher) or Brilliant violet 785 (XMG1.2, BioLegend), anti-TNF Alexa-Fluor-488 (MP6-XT22, ThermoFisher) or Brilliant Violet 605 (MP6-XT22, BioLegend), anti-IL-2 APC (JES6-5H4, ThermoFisher) or Brilliant violet 711 (JES6-5H4, BioLegend), Bcl2 PeCy7 (Blc/10C4, BioLegend), anti-Ki67 PeCy7 (16A8, BioLegend) and cells washed with permwash buffer. To detect Myc, cells were first stained with unlabelled anti-Myc (D84C12, Cell Signalling Technologies), cells washed with permwash and then stained with PE-anti-rabbit (Cell signalling Technologies). Stained cells were acquired on a BD LSR or Fortessa and analysed using FlowJo.

4.5.6 BD Rhapsody single cell RNA-seq

CD4 T cells from spleens and lungs of IAV infected TRACE mice were isolated by CD4 negative selection following the manufacturer's instructions (StemCell, CD4 Isolation Kit). The cells were activated with IAV-Ag-DCs for 4 hours and then stained with anti-CD4 APC-Alexa647, anti-CD44-PerCP-Cy5.5 (IM7, ThermoFisher), anti-MHCII-e450, anti-B220-e450, CD8-e450 (53-6.7, ThermoFisher), F4/80-e450, and CD45 Sample Tags to enable multiplexing (BD Bioscience,) and AbSeq antibodies to ICOS (AMM2072) and PD1 (AMM2138). $CD44^{hi}$/EYFP+ and $CD44^{lo}$/EYFP negative cells from combined spleen or lung samples were FACS sorted on an ARIA IIU and cells transferred into BD Rhapsody Sample Buffer and loaded onto a scRNA-seq Rhapsody Cartridge (5000 EYFPnegative $CD44^{lo}$ spleen cells; 5000 EYFP+$CD44^{hi}$ spleen cells; and 1000 EYFP+$CD44^{hi}$ lung cells. Manufacturer's instructions (Mouse VDJ CDR3 library preparation) were followed to prepare libraries for sequencing with the BD Rhapsody Immune response mouse targeted panel, additional custom made

primers (Table 5), sample Tags and VDJ CDR3. Pair-end sequencing was performed by Novogene on an Illumina MiSeq PE250.

Table 5 - List of primers

Mouse ID	Organ	BD Rhapsody sample Tag number	Tag sequence
1	Spleen	1	AAGAGTCGACTGCCATGTCCCCTCCGCGGGTCCGTGCCCCCCAAG
2	Spleen	2	ACCGATTAGGTGCGAGGCGCTATAGTCGTACGTCGTTGCCGTGCC
3	Spleen	3	AGGAGGCCCCGCGTGAGAGTGATCAATCCAGGATACATTCCCGTC
4	Spleen	4	TTAACCGAGGCGTGAGTTTGGAGCGTACCGGCTTTGCGCAGGGCT
1	Lung	5	GGCAAGGTGTCACATTGGGCTACCGCGGGAGGTCGACCAGATCCT
2	Lung	6	GCGGGCACAGCGGCTAGGGTGTTCCGGGTGGACCATGGTTCAGGC
3	Lung	7	ACCGGAGGCGTGTGTACGTGCGTTTCGAATTCCTGTAAGCCCACC
4	Lung	8	TCGCTGCCGTGCTTCATTGTCGCCGTTCTAACCTCCGATGTCTCG

4.5.7 Single cell RNA-seq analysis

Data were initially processed on SevenBridges and then analysed predominantly using Seurat (V4.2.0)[126] and scRepertoire(V1.7.2) [127]. Briefly, to perform dimensionality reduction: count data was normalised using scTransform prior to principal component analysis, Uniform Manifold Approximation and Projection (UMAP) dimensional reduction, Nearest-Neighbour graph construction and cluster determination within the Seurat package, and dimensionality reduction performed. Log normalising and scaling of the count data was conducted prior to differential gene expression analysis. To test for differential gene expression, the FindAllMarkers function was used (min.pct = 0.4 & minLogFC = 0.25, model.use = MAST). Only genes with a Bonferroni corrected p value <0.05 were considered statistically different. For TCR analysis, clonal expansion was calculated based on the same TCR being detected once (Single Clone) or multiple times within the same animal. All TCR analysis utilised stock or customised code from the scRepertoire package. Further packages used for data

analysis, organisation and visualisation included: workflowR[128], dplyr, ggplot2, cowplot, ggVenn, circlize[129], plot1cell[130] and ComplexHeatmap[131]. All code used can be found at https://github.com/JonathanNoonan/Westerhof.

4.5.8 Statistical analysis

All data other than scRNAseq were analysed using Prism version 9 software (GraphPad). Differences between groups were analysed by unpaired ANOVAs, T-tests or Mann-Whitney test as indicated in figure legends. In all figures * represents a p value of <0.05; **: p<0.01, ***: p<0.001, ****: p<0.0001.

4.6 Data availability statement

scRNA-seq data have been deposited at GEO and are publicly available as of the date of publication; GSE220588.

4.7 Conflict of interest

The authors have no competing interests to declare.

4.8 CRediT authorship contribution statement

LMW: conception, investigation, formal analysis, visualization, writing - original draft and reviewing/editing. JN: formal analysis, data curation, software, visualization, writing - reviewing and editing. KEH: investigation, formal analysis, writing - reviewing and editing. ETC: investigation, formal analysis, writing - reviewing and editing, ZC: investigation, formal analysis, writing - reviewing and editing, TP: investigation, writing - reviewing and editing. MRJ: formal analysis, writing – reviewing and editing. NB: software, writing – reviewing and editing. MKLM: Supervision, project management, funding acquisition, conception, investigation, formal analysis, visualization, writing - original draft and reviewing.

4.9 Acknowledgments

We thank the staff within the School of Infection and Immunity Flow Cytometry Facility and Biological Services at the University of Glasgow for technical

assistance. Thank you to members of the Kurowska-Stolarska for technical assistance with the BD Rhapsody experiment. Thank you to Prof James Brewer and Dr Edward Roberts for critical review of the manuscript and the MacLeod lab for discussions. We thank the NIH tetramer core facility for the provision of IA^b-$NP_{311-325}$ and D^b/NP NP_{368-74} tetramers. The work was funded by a GLAZgo Discovery Centre PhD fellowship to LMW, a Marie Curie Fellowship (334430) and a Wellcome Trust Investigator Award (210703/Z/18/Z) to MKLM.

Chapter 5 Summary

My PhD project has examined the CD4 and CD8 T cell response to IAV using a mouse model. I have characterised the T cells and their cytokine responses at different stages following infection in lymphoid organs and the lung. Here I will discuss the key findings, some limitations of the research and potential future areas of research based on my findings.

My main finding is that the proportion of multifunctional T cells increases in the memory as compared to the primary pool. I was able to make this advance because I combined a number of techniques to examine IAV-specific CD4 and CD8 T cells across primary, memory and re-infection time points.

5.1 Advanced detection methods to identify IAV-specific CD4 and CD8 T cells

Different methods of detection were used to identify IAV-specific T cells. The first method used was MHC I and MHC II tetramers (tet) containing immunodominant IAV nucleoprotein (NP) peptides (NP 368–374 and NP 311–325). With this method we investigated a group of cells with less heterogenous TCRs that are known to contain immunodominant T cells[132-134]. The advantage is that we are not reliant on cytokine production to detect IAV-specific T cells. By coupling MHC tetramer analysis with reactivation of T cells from the same mice with these peptides, we can investigate the differences between IFNγ, TNFα and IL-2 producing T cells, and the T cells that do not produce these cytokines. We also used this method to compare phenotypes of IAV-specific T cells in active infection and memory without having to stain for cytokines.

The tetramer detection method combined with cytokine staining provided sub optimal results, thus these were not combined. To compare, we split up a sample and used the tetramer method on half of the cells. The other half were restimulated using the same immunodominant NP peptides to stimulate cytokine production.

A third method we used was restimulation of the T cells, again from the same mice with bmDCs which have been treated with sonicated IAV-WSN. This meant

that the bmDCs could present epitopes from all IAV proteins. The pros and cons of these different methods are summarised in Table 6.

Table 6 - Pros and cons of the different methods used

Method	Pro	Con
NP-peptide tetramer	Detect IAV NP-specific T cells Detect cells regardless of ability to make cytokine	Detected T cells have a limited TCR repertoire Limited information on T cell function
NP-peptide restimulation + i.c. staining	Compare cytokine production of IAV NP-specific cells to more heterogenous IAV-specific T cells. Investigate differences between cytokine and non-cytokine producing cells by comparing to cells labelled with the MHC tetramer.	Detected T cells have a limited TCR repertoire. Only cells that produce cytokine are investigated using i.c. staining. Unable to combine directly with MHC tetramer staining.
WSN IAV restimulation + i.c. staining	Provides a broader, possibly more complete picture about the T cells because of the higher TCR diversity.	Only cells that produce cytokine are investigated using i.c. staining. Unable to combine with tetramer staining.

5.2 Commonalities and differences in IAV-specific T cells across lymphoid organs and the lung

Many researchers have studied T cell response to IAV leading to a number of theories about how memory T cells form[20, 135, 136]. Tmem in peripheral tissues are thought to be more differentiated and more likely to undergo apoptosis than T cells in secondary lymphoid organs, and the bone marrow has been described as a site of Tmem maintenance.

5.2.1 Cytokine production in lymphoid organs compared to the site of infection

To investigate these hypotheses in the context of IAV, we looked at the ex vivo cytokine response of CD4 and CD8 T cells from mice post IAV infection. In all organs that were investigated (spleen, medLN, lung and bone marrow), we examined the populations of IFNγ, TNFα, and IL-2 producing IAV-specific T cells.

T cells in all organs were able to produce effector cytokines, which indicates that effector T cells could be found in lymphoid and non-lymphoid organs. In the primary response, lung T cells do appear to have more of an effector phenotype; more single IFNγ producing cells can be found in the lung, this evened out at the memory timepoints.

When looking at each cytokine separately, the expected decrease in the number of cytokine+ IAV-specific T cells after the contraction phase can be observed. In this data two things stand out, the first being a difference between CD4 and CD8 T cells; the number of cytokine producing CD8 T cells seems more consistent, or possibly even had an increasing trend in the secondary lymphoid organs between day 30 and day 75 post-infection.

This is in line with research on virus-specific CD4 and CD8 T cells in mice, where the number of virus-specific CD4 T cells continues to decline but the CD8 T cells go into ultraglide and the numbers remain stable[43].

When comparing the data from different sites of interest, we can see a stronger decline in the number of cytokine producing T cells in the lung than in the lymphoid organs, this is true for both CD4 and CD8 T cells.

One could argue that the steeper decline in IAV-specific lung cells is possibly caused by a larger number of IAV-specific T cells in the blood during active infection, causing a higher number of cells present in the lung after harvesting by also identifying cells that are present in the lung vasculature. We however ruled out this variable, by injecting the mice with fluorescently labelled anti-CD45 three minutes prior to euthanasia. This proved that this is not the cause of the decline. Meaning that there must be a different cause for the differences in cell survival between the lung and secondary lymphoid organs. This could be because of the hypothesis that Tmem in peripheral tissues are more differentiated than those in secondary lymphoid organs, increasing their chance of apoptosis.

For example, Slütter *et al*. have found that IAV-specific CD8 T cells in the lung are at greater risk of apoptosis than those in other organs, including the skin [137]. However, this result could be complicated by findings that show Trm cells can be

prone to apoptosis following isolation from tissues[138, 139]. It would be useful to examine the cytokine producing T cells in animals treated with the molecule that blocks the enzyme that can cause apoptosis of Trm during isolation to determine whether our results are affected by this phenomenon.

5.2.2 Phenotypical comparison of memory T cells

I performed detailed analysis of MHCI and II tetramer+ cells across time points and organs. Performing this analysis in the same mice enables an important comparison of CD4 and CD8 T cells responding to the same pathogen.

One of our key findings is that IAV-specific CD8 T cells were more likely to be found in the blood than IAV-specific CD4 T cells [26]. This suggests that IAV-specific CD8 T cells patrol the circulation more. Which fits with the higher expression of CX3CR1 on the CD8 T cells[112].

Another important difference is that Trm markers, such as CD69 and CD103, appear to be present more often on lung CD8 than CD4 IAV-specific T cells. Across the time course, IAV-specific CD8 T cells gained expression of CD103 and CD69. This may relate to differences between these cell types in their migration patterns, as found in the skin[140]. Or, as discussed by Kunzli and Masopust, CD69 and CD103 may not be useful markers for CD4 Trm cells[135].

In contrast, the pattern of expression of PD1 was similar between CD4 and CD8 T cells: a decline in expression in all organs across the time course. However, IAV-specific CD4 and CD8 T cells in the lung always expressed the highest levels.

PD1 is a cell surface molecule that increases following T cell activation and acts to inhibit TCR signals[141]. A possible explanation for the higher expression in the lung is that it might be important to regulate the T cell responses more in a delicate tissue such as the lungs, to prevent immune-mediated damage as much as possible[142, 143].

The higher levels of PD1 that can be found in lung T cells, combined with higher percentages of IFNγ single cytokine producing T cells during active infection,

show a more effector-like phenotype for lung T cells than those in lymphoid organs.

5.2.3 Tmem in the bone marrow

Radbruch and colleagues have argued that the bone marrow contains superior Tmem[85, 144]. These bone marrow T cells supposedly have increased survival compared to other T cells. We did not observe this as the cytokine producing IAV-specific bone marrow CD4 and CD8 T cells followed the same trends as the cells in the other organs that were investigated. We decided to not continue studying the bone marrow, due to the low numbers of T cells present it was too challenging to gather a statistically acceptable number of cells in further experiments.

5.3 Multifunctional memory T cells

Cytokine producing Tmem provide protection against symptomatic influenza [34-37]. Multifunctional T cells are thought to be very efficient cells due to their broad cytokine response. We hypothesise that multifunctional Tmem are a distinct population, with distinct cellular processes and fate. We think the IAV-specific Tmems have a distinct cytokine producing capacity compared to the IAV-specific T cells present at primary infection.

5.3.1 Cytokine production and T cell survival

It is thought that highly differentiated cytokine producing T cells are more likely to undergo cell death than less differentiated cells, particularly those that can produce IL-2. IL-2 has been shown to play an important role in Tmem development[27, 74]. Thus, it was expected to see a significant increase in the proportion of IL-2 producing T cells at memory timepoint. This could not be identified in our data where comparable numbers of IFNγ, TNFα and IL-2 producing CD4 T cells were found. In other words, IL-2+ T cells did not become a dominant population in the memory pool. A possible explanation for this is that the three cytokines are all produced by the same cells. To further investigate this, we studied the combined cytokine producing ability of individual cells over time, to see if the cytokines are produced by separate cells or that T cells that produce all three cytokines (multifunctional T cell) are present. This led me to

examine the difference between cytokine producing cells that were either single IFNγ+, double (IFNγ+ with TNFα or IL-2) or triple (IFNγ+, IL-2+ and TNF+).

5.3.2 The timing of cytokine production by multifunctional T cells

By examining T cells at primary and memory timepoints, my research revealed some important differences in IAV-specific T cell cytokine production. These differences include the range of cytokines the T cells produced and the timing of this cytokine production.

Not much research has been conducted to see if multifunctional T cells produce their cytokines simultaneously or consecutively. We set up an experiment to investigate the kinetics of cytokine production between 0 to 2, 2 to 4 and 4 to 6 hours of restimulation. The data shows that all cytokines were produced simultaneously.

A study from 2011 by Han and colleagues[145] investigated the timing of cytokine production in human T cells, stimulated with PMA + ionomycin. They concluded that human CD3+ T cells were more likely to secrete IFNγ, IL-2 and TNFα sequentially rather than simultaneously, and found that simultaneous secretion likely occurred at transitions between states. No association was found between timing of initiation and the T cell subset. However, T cells that initiated secretion within 4 hours post stimulation showed higher chances of producing multiple cytokines, either simultaneously or sequentially.

However, in line with our data, Han *et al.* found simultaneous cytokine production at 4 and 6 hours post re-activation[145]. They did analyse the T cells for a longer amount of time, enabling them to generate more nuanced data.

Assenmacher *et al.* also reported sequential cytokine production[146], but their timepoints are at a scale based on days which is very from different our experiment. They have no data on the cytokine production within the first 20 hours post activation.

We could have also investigated the cells with a longer time course, this would have given us the ability to investigate the durability of the response of the

different cytokines. We however chose to focus on the first 6 hours post reactivation, as we want our data to stay as relevant as possible to the *in vivo* setting. Keeping the cells ex vivo for prolonged amounts of time might cause them to incorporate signals from the *in vitro* setting. Also, we are interested in what the T cells can do rapidly following reactivation.

We found that CD8 T cells showed a sustained or even increasing response at 4 to 6 hours in cells taken from primary and memory time points. Primary responding CD4 T cells from secondary lymphoid organs do not have a sustained cytokine profile but rather show a decrease in production at the latest analysis timepoint.

This might be because of a functional difference; CD4 T cells' main function is to attract other immune cells, whereas a key role for CD8 T cells is to drive apoptosis of infected cells. This could mean it is more important for CD8 T cells to have a sustained response to fulfil their function.

In the lung, CD4 T cells from the primary infection already showed this sustained response, which suggests these lung T cells are differently regulated. It is possible that functionally superior T cells are more likely to enter the lung tissues as these cells are needed to control the virus. Another hypothesis is that the T cells receive signal that can cause alterations when they enter the lung tissue. One could study this by examining differential expression of genes that are involved in efficient protein production in lung versus spleen CD4 T cells.

Interestingly, CD4 Tmem from the lymphoid organs do show a more sustained response across the three in vitro time points. These results might indicate that functionally superior CD4 T cells have preferential survival or access into the memory pool, that CD4 T cells functionally mature when becoming memory cells or that functionally superior T cells undergo more proliferation creating an increasing percentage of these cells within the memory pool.

5.3.3 Multifunctional T cell increase proportionally in the memory pool compared to the primary T cell pool

Cytokine producing IAV-specific Tmems have distinct characteristics compared to T cells during active IAV infection. We found that for both CD4 and CD8 T cells, over time in all organs there was an increase of the percentage of cells that produced all three of the examined cytokines; IFNγ, TNFα and IL-2. These are the multifunctional T cells. In memory, a higher percentage of multifunctional CD4 T cells was found in the spleen, medLN and the lung compared to the CD4 T cells present during the primary response. This shift was connected to a decrease in singular IFNγ producing cells.

CD8 T cells had much smaller proportions of multifunctional and singularly IL-2 producing cells than CD4 T cells. However, CD8 Tmem still contained more IL-2 producing cells than primary responding CD8 T cells.

The increased percentage of multifunctional IAV-specific CD4 and CD8 T cells at a memory timepoint could be caused by preferential survival, increased proliferation or non-multifunctional T cells gaining cytokine producing abilities and thus becoming multifunctional over time. Unfortunately, there are experimental limitations when trying to differentiate between these hypotheses. Currently there are no known surface markers for cytokine producing cells that could be used to isolate the different populations for an adoptive transfer experiment. With reporter mice one is unable to differentiate between singular and multifunctional cytokine producing populations. This means permeabilisation is usually necessary to distinguish multifunctional T cells, making transfer of live cells extremely challenging.

Some studies have used cytokine capture system that enables the identification of cytokine+ T cells and their isolation by FACS. Human triple cytokine+ peripheral blood CD4 T cells reactive to *Plasmodium falciparum* or influenza virus expressed higher levels of a number of chemokines and molecules involved in cytokine or chemokine signalling[147]. This study suggested that IL-27 may enhance the development and/or survival of triple cytokine+ T cells.

The cytokine capture assay has also been used to examine the survival of activated CD4 T cells into memory cells using adoptive transfer mouse models. Using *in vitro* activated mouse CD4 T cells or *in vivo* activated LCMV-specific CD4 T cells, Löhning *et al* found that cytokine positive cells could become memory cells, supporting the survival phenotype we have observed [108]. In contrast, using similar methods, Wu *et al* found that IFNγ + CD4 T cells failed to become memory CD4 T cells [110]. These different results suggest additional research is required to more fully understand the generation of cytokine positive and negative memory CD4.

Other techniques have been used to examine multifunctional T cells. Healy *et al*. developed a technique to examine gene expression in fixed and permeabilised cells [148]. They examined human CMV-specific CD8 T cells and identified that multifunctional cells expressed high levels of genes associated with cell survival and proliferation and suggested a role for STAT5, which is required for IL-2 receptor signalling in promoting multifunctional T cell survival. I attempted to perform similar experiments on FACS sorted single IFNγ+ and triple cytokine+ IAV-specific mouse T cells. Unfortunately, the depth of sequencing of the memory CD4 T cells was too low to generate results of publishable quality but analysis for an undergraduate honour project suggested a pro-survival signal in triple cytokine+ CD4 T cells corresponds with our later findings [26].

An alternative method, as used in my publication [26] is to examine CD4 T cells using single cell RNA sequencing. Here single and multifunctional cytokine+ cells can be identified by transcript expression. Using this method, Meckiff *et al*. found that human IAV-specific CD4 T cells were enriched for multifunctional cells [149].

5.3.4 Multifunctional T cells are less likely to proliferate than singular IFNγ producers.

Thus far we have discussed differences in the timing of cytokine production, and in the percentage of T cells that have the ability produce multiple cytokines. We have three potential hypothesis that could explain these differences:

- Functionally superior CD4 T cells might have preferential survival or access into the memory pool

- T cells functionally mature when becoming memory cells and gain cytokine producing abilities.

- Functionally superior T cells undergo more proliferation creating an increasing percentage of these cells within the memory pool.

The next step is to determine whether there is evidence to support one or more of these hypotheses. First, we investigated proliferation of multifunctional and single cytokine producing T cells by looking at Ki67 expression at d9 and d30 post IAV infection.

The Ki67+ IFNγ+ T cells contained a higher proportion of single IFNγ-producing cells than multifunctional cells. This means I found that the increase in multifunctional T cells and sustained cytokine production in memory was not due to a high level of proliferation. Rather, work that led on from this thesis project found that multifunctional CD4 T cell expressed higher levels of pro-survival molecules[26]. This might indicate increased quiescence or survival for multifunctional memory T cells.

A transfer study would be needed to discriminate between these hypotheses. It is challenging to transfer live T cells based on cytokine expression, this however could be accomplished by performing a cytokine capture assay to isolate cytokine positive and negative T cells. Transferred cells could be tested for their duration of survival and ability to protect the host.

5.4 IAV-specific T cells after infection and re-infection.

No matter the location, the importance of memory T cells is their functionality. So they can prevent against or inhibit a re-infection. When it comes to IAV, the cross-strain protection that IAV-specific T cells could potentially provide is particularly interesting.

A number of studies have examined whether CD4 or CD8 IAV-specific memory T cells can protect against a re-infection. These studies have shown that these T cells can successfully protect hosts by killing infected cells, and by recruiting innate immune cells. They also found that protection requires IFNγ production[45, 48, 58, 84].

However, not many studies have performed a detailed examination of the memory CD4 or CD8 T cells themselves. Van Braeckel-Budimir found that the proportion of lung IAV-specific CD8 T cells with a Trm phenotype increased following subsequent rounds of re-activation and that these cells increased their expression of pro-survival molecule Bcl2[150].

Soerens *et al.* examined repeated reactivation of CD8 T cells, and demonstrated that memory T cells retained their ability to proliferate in response to antigen. While they found that memory CD8 T cells could still express cytokine, they did not compare the proliferative responses of different cytokine producing populations[151].

Summarised, the two papers above show that re-activated memory CD8 T cells can return to the memory pool and that these cells remain functional. For CD4 T cells, a number of studies have shown that different populations of memory CD4 T cells can respond to a secondary stimulation[60, 76, 152-155]. We chose to focus on cytokine producing T cells because of the link between cytokine production and protection from IAV in both animal models and humans[35-37, 58, 156].

In our data, we found that the proportion of T cells that are multifunctional remained very consistent after re-infection with a different IAV strain. When comparing the T cells 5 days after a second IAV infection, to those 35 days post re-infection, and those only receiving the initial IAV infection we see very similar proportions of single cytokine producing, double cytokine producing and multifunctional T cells. This is true for both CD4 and CD8 T cells.

We do not know yet what the mechanism is causing the proportion of multifunctional T cells to remain so stable. We expected to see a further increase but this what not the case. IFNγ single producing T cells underwent

more proliferation during the re-infection than multifunctional cells but the percentage of single IFNγ producers stayed stable too.

Detailed time course studies of the T cells following reinfection would be needed to track the survival and proliferation of the different populations across the expansion and contraction phases of the response. Including BrdU, which is incorporated into the DNA of dividing cells in the flow panel alongside pro-survival molecules such as Bcl2 and apoptotic indicators would strengthen our ability to determine the fate of the different cytokine positive cells.

5.5 Reflection on hypothesis

Formation of Tmem

My initial hypothesis was that multifunctional Tmem are a distinct population, with distinct cellular processes and fate that leads to a proportional increase in multifunctional cells from the primary to the memory pool (Figure 34). This increased percentage of multifunctional IAV-specific T cells at memory could be due to increased survival of multifunctional Tmem, or, non-multifunctional T cells could gain an increased cytokine producing ability and become multifunctional over time. My data supports this hypothesis.

Response of Tmem to second IAV infection

My second hypothesis was that, after a second IAV infection, the proportion of multifunctional cells will not alter as the multifunctional Tmem will proliferate and respond at a similar pace to secondary infection as non-multifunctional T cells. I did find sustained diversity in the secondary memory pool, with similar proportions as the initial memory pool. However, this was not due to proliferation, as multifunctional CD4 and CD8 T cells expressed lower levels of Ki67 (Figure 34).

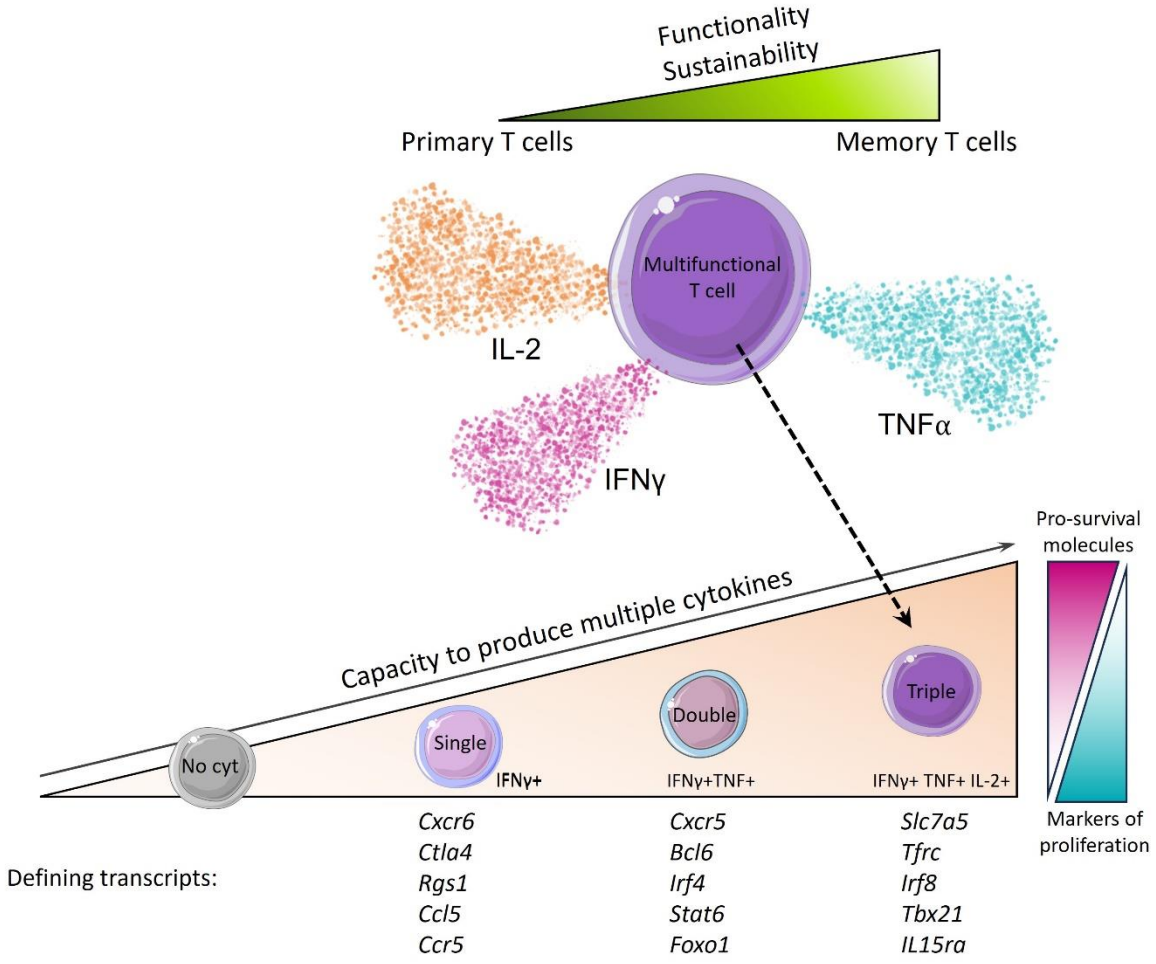

Figure 34 – Memory T cells are functionally superior to primary T cells. Multifunctional CD4 T cells express more transcripts for pro-survival molecules and less markers of proliferation than cytokine negative CD4 T cells.

List of References

1. Kurd N, Robey EA. T-cell selection in the thymus: a spatial and temporal perspective. Immunol Rev. 2016;271(1):114-26.

2. Ebert A, Hill L, Busslinger M. Spatial Regulation of V-(D)J Recombination at Antigen Receptor Loci. Adv Immunol. 2015;128:93-121.

3. James KD, Jenkinson WE, Anderson G. T-cell egress from the thymus: Should I stay or should I go? J Leukoc Biol. 2018;104(2):275-84.

4. Taniuchi I. CD4 Helper and CD8 Cytotoxic T Cell Differentiation. Annu Rev Immunol. 2018;36:579-601.

5. Ruterbusch M, Pruner KB, Shehata L, Pepper M. In Vivo CD4(+) T Cell Differentiation and Function: Revisiting the Th1/Th2 Paradigm. Annu Rev Immunol. 2020;38:705-25.

6. Verdon DJ, Mulazzani M, Jenkins MR. Cellular and Molecular Mechanisms of CD8(+) T Cell Differentiation, Dysfunction and Exhaustion. Int J Mol Sci. 2020;21(19).

7. Duttagupta PA, Boesteanu AC, Katsikis PD. Costimulation signals for memory CD8+ T cells during viral infections. Crit Rev Immunol. 2009;29(6):469-86.

8. Pepper M, Pagan AJ, Igyarto BZ, Taylor JJ, Jenkins MK. Opposing signals from the Bcl6 transcription factor and the interleukin-2 receptor generate T helper 1 central and effector memory cells. Immunity. 2011;35(4):583-95.

9. Peng C, Huggins MA, Wanhainen KM, Knutson TP, Lu H, Georgiev H, et al. Engagement of the costimulatory molecule ICOS in tissues promotes establishment of CD8(+) tissue-resident memory T cells. Immunity. 2022;55(1):98-114 e5.

10. Park SL, Christo SN, Wells AC, Gandolfo LC, Zaid A, Alexandre YO, et al. Divergent molecular networks program functionally distinct CD8(+) skin-resident memory T cells. Science. 2023;382(6674):1073-9.

11. Gaspal FM, Kim MY, McConnell FM, Raykundalia C, Bekiaris V, Lane PJ. Mice deficient in OX40 and CD30 signals lack memory antibody responses because of deficient CD4 T cell memory. J Immunol. 2005;174(7):3891-6.

12. Gaspal F, Bekiaris V, Kim MY, Withers DR, Bobat S, MacLennan IC, et al. Critical synergy of CD30 and OX40 signals in CD4 T cell homeostasis and Th1 immunity to Salmonella. J Immunol. 2008;180(5):2824-9.

13. Rogers PR, Song J, Gramaglia I, Killeen N, Croft M. OX40 promotes Bcl-xL and Bcl-2 expression and is essential for long-term survival of CD4 T cells. Immunity. 2001;15(3):445-55.

14. Hendriks J, Xiao Y, Rossen JW, van der Sluijs KF, Sugamura K, Ishii N, et al. During viral infection of the respiratory tract, CD27, 4-1BB, and OX40 collectively determine formation of CD8+ memory T cells and their capacity for secondary expansion. J Immunol. 2005;175(3):1665-76.

15. Lee HW, Park SJ, Choi BK, Kim HH, Nam KO, Kwon BS. 4-1BB promotes the survival of CD8+ T lymphocytes by increasing expression of Bcl-xL and Bfl-1. J Immunol. 2002;169(9):4882-8.

16. Hendriks J, Xiao Y, Borst J. CD27 promotes survival of activated T cells and complements CD28 in generation and establishment of the effector T cell pool. J Exp Med. 2003;198(9):1369-80.

17. Desai P, Tahiliani V, Hutchinson TE, Dastmalchi F, Stanfield J, Abboud G, et al. The TNF Superfamily Molecule LIGHT Promotes the Generation of Circulating and Lung-Resident Memory CD8 T Cells following an Acute Respiratory Virus Infection. J Immunol. 2018;200(8):2894-904.

18. Yang CY, Best JA, Knell J, Yang E, Sheridan AD, Jesionek AK, et al. The transcriptional regulators Id2 and Id3 control the formation of distinct memory CD8+ T cell subsets. Nat Immunol. 2011;12(12):1221-9.

19. Alberts B. Essential cell biology. 3rd ed. New York: Garland Science; 2009.

20. Strutt TM, McKinstry KK, Marshall NB, Vong AM, Dutton RW, Swain SL. Multipronged CD4(+) T-cell effector and memory responses cooperate to provide potent immunity against respiratory virus. Immunol Rev. 2013;255(1):149-64.

21. Harty JT, Tvinnereim AR, White DW. CD8+ T cell effector mechanisms in resistance to infection. Annu Rev Immunol. 2000;18:275-308.

22. Almeida JR, Price DA, Papagno L, Arkoub ZA, Sauce D, Bornstein E, et al. Superior control of HIV-1 replication by CD8+ T cells is reflected by their avidity, polyfunctionality, and clonal turnover. J Exp Med. 2007;204(10):2473-85.

23. Darrah PA, Patel DT, De Luca PM, Lindsay RW, Davey DF, Flynn BJ, et al. Multifunctional TH1 cells define a correlate of vaccine-mediated protection against Leishmania major. Nat Med. 2007;13(7):843-50.

24. Lindenstrom T, Agger EM, Korsholm KS, Darrah PA, Aagaard C, Seder RA, et al. Tuberculosis subunit vaccination provides long-term protective immunity characterized by multifunctional CD4 memory T cells. J Immunol. 2009;182(12):8047-55.

25. Westerhof LM, McGuire K, MacLellan L, Flynn A, Gray JI, Thomas M, et al. Multifunctional cytokine production reveals functional superiority of memory CD4 T cells. Eur J Immunol. 2019;49(11):2019-29.

26. Westerhof LM, Noonan J, Hargrave KE, Chimbayo ET, Cheng Z, Purnell T, et al. Multifunctional cytokine production marks influenza A virus-specific CD4 T cells with high expression of survival molecules. Eur J Immunol. 2023:e2350559.

27. Alam F, Singh A, Flores-Malavet V, Sell S, Cooper AM, Swain SL, et al. CD25-Targeted IL-2 Signals Promote Improved Outcomes of Influenza Infection and Boost Memory CD4 T Cell Formation. J Immunol. 2020;204(12):3307-14.

28. DeBerge MP, Ely KH, Enelow RI. Soluble, but not transmembrane, TNF-alpha is required during influenza infection to limit the magnitude of immune responses and the extent of immunopathology. J Immunol. 2014;192(12):5839-51.

29. Liang S, Mozdzanowska K, Palladino G, Gerhard W. Heterosubtypic immunity to influenza type A virus in mice. Effector mechanisms and their longevity. J Immunol. 1994;152(4):1653-61.

30. Mehta AK, Gracias DT, Croft M. TNF activity and T cells. Cytokine. 2018;101:14-8.

31. Ross SH, Cantrell DA. Signaling and Function of Interleukin-2 in T Lymphocytes. Annu Rev Immunol. 2018;36:411-33.

32. Genesca M, Rourke T, Li J, Bost K, Chohan B, McChesney MB, et al. Live attenuated lentivirus infection elicits polyfunctional simian immunodeficiency virus Gag-specific CD8+ T cells with reduced apoptotic susceptibility in rhesus macaques that control virus replication after challenge with pathogenic SIVmac239. J Immunol. 2007;179(7):4732-40.

33. Kwissa M, Amara RR, Robinson HL, Moss B, Alkan S, Jabbar A, et al. Adjuvanting a DNA vaccine with a TLR9 ligand plus Flt3 ligand results in enhanced cellular immunity against the simian immunodeficiency virus. J Exp Med. 2007;204(11):2733-46.

34. Hayward AC, Wang L, Goonetilleke N, Fragaszy EB, Bermingham A, Copas A, et al. Natural T Cell-mediated Protection against Seasonal and Pandemic Influenza. Results of the Flu Watch Cohort Study. Am J Respir Crit Care Med. 2015;191(12):1422-31.

35. Sridhar S, Begom S, Bermingham A, Hoschler K, Adamson W, Carman W, et al. Cellular immune correlates of protection against symptomatic pandemic influenza. Nat Med. 2013;19(10):1305-12.

36. Tsang TK, Lam KT, Liu Y, Fang VJ, Mu X, Leung NHL, et al. Investigation of CD4 and CD8 T cell-mediated protection against influenza A virus in a cohort study. BMC Med. 2022;20(1):230.

37. Wilkinson TM, Li CK, Chui CS, Huang AK, Perkins M, Liebner JC, et al. Preexisting influenza-specific CD4+ T cells correlate with disease protection against influenza challenge in humans. Nat Med. 2012;18(2):274-80.

38. Chen SMY, Wong YC, Yim LY, Zhang H, Wang H, Lui GCY, et al. Enhanced Cross-Reactive and Polyfunctional Effector-Memory T Cell Responses by ICVAX-a Human PD1-Based Bivalent HIV-1 Gag-p41 Mosaic DNA Vaccine. J Virol. 2022;96(7):e0216121.

39. Duckworth BC, Qin RZ, Groom JR. Spatial determinates of effector and memory CD8(+) T cell fates. Immunol Rev. 2022;306(1):76-92.

40. Gray JI, Westerhof LM, MacLeod MKL. The roles of resident, central and effector memory CD4 T-cells in protective immunity following infection or vaccination. Immunology. 2018;154(4):574-81.

41. Heeg M, Goldrath AW. Insights into phenotypic and functional CD8(+) T(RM) heterogeneity. Immunol Rev. 2023.

42. Nguyen QP, Deng TZ, Witherden DA, Goldrath AW. Origins of CD4(+) circulating and tissue-resident memory T-cells. Immunology. 2019;157(1):3-12.

43. Homann D, Teyton L, Oldstone MB. Differential regulation of antiviral T-cell immunity results in stable CD8+ but declining CD4+ T-cell memory. Nat Med. 2001;7(8):913-9.

44. Hammarlund E, Lewis MW, Hansen SG, Strelow LI, Nelson JA, Sexton GJ, et al. Duration of antiviral immunity after smallpox vaccination. Nat Med. 2003;9(9):1131-7.

45. Strutt TM, McKinstry KK, Dibble JP, Winchell C, Kuang Y, Curtis JD, et al. Memory CD4+ T cells induce innate responses independently of pathogen. Nat Med. 2010;16(5):558-64, 1p following 64.

46. Anthony RM, Urban JF, Jr., Alem F, Hamed HA, Rozo CT, Boucher JL, et al. Memory T(H)2 cells induce alternatively activated macrophages to mediate protection against nematode parasites. Nat Med. 2006;12(8):955-60.

47. Cenerenti M, Saillard M, Romero P, Jandus C. The Era of Cytotoxic CD4 T Cells. Front Immunol. 2022;13:867189.

48. McKinstry KK, Strutt TM, Kuang Y, Brown DM, Sell S, Dutton RW, et al. Memory CD4+ T cells protect against influenza through multiple synergizing mechanisms. J Clin Invest. 2012;122(8):2847-56.

49. Alexander J, Bilsel P, del Guercio MF, Stewart S, Marinkovic-Petrovic A, Southwood S, et al. Universal influenza DNA vaccine encoding conserved CD4+ T cell epitopes protects against lethal viral challenge in HLA-DR transgenic mice. Vaccine. 2010;28(3):664-72.

50. Topham DJ, Tripp RA, Doherty PC. CD8+ T cells clear influenza virus by perforin or Fas-dependent processes. J Immunol. 1997;159(11):5197-200.

51. Mueller SN, Gebhardt T, Carbone FR, Heath WR. Memory T cell subsets, migration patterns, and tissue residence. Annu Rev Immunol. 2013;31:137-61.

52. Lugli E, Galletti G, Boi SK, Youngblood BA. Stem, Effector, and Hybrid States of Memory CD8(+) T Cells. Trends Immunol. 2020;41(1):17-28.

53. Metais JY, Winkler T, Geyer JT, Calado RT, Aplan PD, Eckhaus MA, et al. BCL2A1a over-expression in murine hematopoietic stem and progenitor cells

decreases apoptosis and results in hematopoietic transformation. PLoS One. 2012;7(10):e48267.

54. Somes MP, Turner RM, Dwyer LJ, Newall AT. Estimating the annual attack rate of seasonal influenza among unvaccinated individuals: A systematic review and meta-analysis. Vaccine. 2018;36(23):3199-207.

55. Webster RG, Govorkova EA. Continuing challenges in influenza. Ann N Y Acad Sci. 2014;1323:115-39.

56. Kim H, Webster RG, Webby RJ. Influenza Virus: Dealing with a Drifting and Shifting Pathogen. Viral Immunol. 2018;31(2):174-83.

57. Khalil N, Bernstein DI. Influenza vaccines: where we are, where we are going. Curr Opin Pediatr. 2022;34(2):119-25.

58. Bot A, Bot S, Bona CA. Protective role of gamma interferon during the recall response to influenza virus. J Virol. 1998;72(8):6637-45.

59. Soudja SM, Chandrabos C, Yakob E, Veenstra M, Palliser D, Lauvau G. Memory-T-cell-derived interferon-gamma instructs potent innate cell activation for protective immunity. Immunity. 2014;40(6):974-88.

60. Gray JI, Al-Khabouri S, Morton F, Clambey ET, Gapin L, Matsuda JL, et al. Tolerance induction in memory CD4 T cells is partial and reversible. Immunology. 2021;162(1):68-83.

61. Inaba K, Inaba M, Romani N, Aya H, Deguchi M, Ikehara S, et al. Generation of large numbers of dendritic cells from mouse bone marrow cultures supplemented with granulocyte/macrophage colony-stimulating factor. J Exp Med. 1992;176(6):1693-702.

62. Jaigirdar SA, MacLeod MK. Development and Function of Protective and Pathologic Memory CD4 T Cells. Front Immunol. 2015;6:456.

63. Yamane H, Paul WE. Early signaling events that underlie fate decisions of naive CD4(+) T cells toward distinct T-helper cell subsets. Immunol Rev. 2013;252(1):12-23.

64. Iijima N, Iwasaki A. Tissue instruction for migration and retention of TRM cells. Trends Immunol. 2015;36(9):556-64.

65. Harrington LE, Janowski KM, Oliver JR, Zajac AJ, Weaver CT. Memory CD4 T cells emerge from effector T-cell progenitors. Nature. 2008;452(7185):356-60.

66. Jacob J, Baltimore D. Modelling T-cell memory by genetic marking of memory T cells in vivo. Nature. 1999;399(6736):593-7.

67. Opferman JT, Ober BT, Ashton-Rickardt PG. Linear differentiation of cytotoxic effectors into memory T lymphocytes. Science. 1999;283(5408):1745-8.

68. Swain SL, Agrewala JN, Brown DM, Jelley-Gibbs DM, Golech S, Huston G, et al. CD4+ T-cell memory: generation and multi-faceted roles for CD4+ T cells in protective immunity to influenza. Immunol Rev. 2006;211:8-22.

69. Catron DM, Rusch LK, Hataye J, Itano AA, Jenkins MK. CD4+ T cells that enter the draining lymph nodes after antigen injection participate in the primary response and become central-memory cells. J Exp Med. 2006;203(4):1045-54.

70. Jelley-Gibbs DM, Brown DM, Dibble JP, Haynes L, Eaton SM, Swain SL. Unexpected prolonged presentation of influenza antigens promotes CD4 T cell memory generation. J Exp Med. 2005;202(5):697-706.

71. Sarkar S, Kalia V, Haining WN, Konieczny BT, Subramaniam S, Ahmed R. Functional and genomic profiling of effector CD8 T cell subsets with distinct memory fates. J Exp Med. 2008;205(3):625-40.

72. MacLeod MK, Clambey ET, Kappler JW, Marrack P. CD4 memory T cells: what are they and what can they do? Semin Immunol. 2009;21(2):53-61.

73. Macleod MK, David A, Jin N, Noges L, Wang J, Kappler JW, et al. Influenza nucleoprotein delivered with aluminium salts protects mice from an influenza A

virus that expresses an altered nucleoprotein sequence. PLoS One. 2013;8(4):e61775.

74. McKinstry KK, Strutt TM, Bautista B, Zhang W, Kuang Y, Cooper AM, et al. Effector CD4 T-cell transition to memory requires late cognate interactions that induce autocrine IL-2. Nat Commun. 2014;5:5377.

75. Strutt TM, McKinstry KK, Kuang Y, Bradley LM, Swain SL. Memory CD4+ T-cell-mediated protection depends on secondary effectors that are distinct from and superior to primary effectors. Proc Natl Acad Sci U S A. 2012;109(38):E2551-60.

76. Teijaro JR, Turner D, Pham Q, Wherry EJ, Lefrancois L, Farber DL. Cutting edge: Tissue-retentive lung memory CD4 T cells mediate optimal protection to respiratory virus infection. J Immunol. 2011;187(11):5510-4.

77. Nayak JL, Richards KA, Chaves FA, Sant AJ. Analyses of the specificity of CD4 T cells during the primary immune response to influenza virus reveals dramatic MHC-linked asymmetries in reactivity to individual viral proteins. Viral Immunol. 2010;23(2):169-80.

78. Richards KA, Chaves FA, Sant AJ. The memory phase of the CD4 T-cell response to influenza virus infection maintains its diverse antigen specificity. Immunology. 2011;133(2):246-56.

79. Taylor JJ, Jenkins MK. CD4+ memory T cell survival. Curr Opin Immunol. 2011;23(3):319-23.

80. Mazo IB, Honczarenko M, Leung H, Cavanagh LL, Bonasio R, Weninger W, et al. Bone marrow is a major reservoir and site of recruitment for central memory CD8+ T cells. Immunity. 2005;22(2):259-70.

81. Okhrimenko A, Grun JR, Westendorf K, Fang Z, Reinke S, von Roth P, et al. Human memory T cells from the bone marrow are resting and maintain long-lasting systemic memory. Proc Natl Acad Sci U S A. 2014;111(25):9229-34.

82. Reinhardt RL, Khoruts A, Merica R, Zell T, Jenkins MK. Visualizing the generation of memory CD4 T cells in the whole body. Nature. 2001;410(6824):101-5.

83. Sercan Alp O, Durlanik S, Schulz D, McGrath M, Grun JR, Bardua M, et al. Memory CD8(+) T cells colocalize with IL-7(+) stromal cells in bone marrow and rest in terms of proliferation and transcription. Eur J Immunol. 2015;45(4):975-87.

84. Teijaro JR, Verhoeven D, Page CA, Turner D, Farber DL. Memory CD4 T cells direct protective responses to influenza virus in the lungs through helper-independent mechanisms. J Virol. 2010;84(18):9217-26.

85. Tokoyoda K, Zehentmeier S, Hegazy AN, Albrecht I, Grun JR, Lohning M, et al. Professional memory CD4+ T lymphocytes preferentially reside and rest in the bone marrow. Immunity. 2009;30(5):721-30.

86. Anderson KG, Mayer-Barber K, Sung H, Beura L, James BR, Taylor JJ, et al. Intravascular staining for discrimination of vascular and tissue leukocytes. Nat Protoc. 2014;9(1):209-22.

87. Mueller SN, Langley WA, Li G, Garcia-Sastre A, Webby RJ, Ahmed R. Qualitatively different memory CD8+ T cells are generated after lymphocytic choriomeningitis virus and influenza virus infections. J Immunol. 2010;185(4):2182-90.

88. Finlay D, Cantrell D. The coordination of T-cell function by serine/threonine kinases. Cold Spring Harb Perspect Biol. 2011;3(1):a002261.

89. Han JM, Patterson SJ, Levings MK. The Role of the PI3K Signaling Pathway in CD4(+) T Cell Differentiation and Function. Front Immunol. 2012;3:245.

90. Khanolkar A, Williams MA, Harty JT. Antigen experience shapes phenotype and function of memory Th1 cells. PLoS One. 2013;8(6):e65234.

91. Nelson RW, McLachlan JB, Kurtz JR, Jenkins MK. CD4+ T cell persistence and function after infection are maintained by low-level peptide:MHC class II presentation. J Immunol. 2013;190(6):2828-34.

92. Miller MA, Ganesan AP, Luckashenak N, Mendonca M, Eisenlohr LC. Endogenous antigen processing drives the primary CD4+ T cell response to influenza. Nat Med. 2015;21(10):1216-22.

93. Chandok MR, Okoye FI, Ndejembi MP, Farber DL. A biochemical signature for rapid recall of memory CD4 T cells. J Immunol. 2007;179(6):3689-98.

94. Watson AR, Lee WT. Differences in signaling molecule organization between naive and memory CD4+ T lymphocytes. J Immunol. 2004;173(1):33-41.

95. Berod L, Heinemann C, Heink S, Escher A, Stadelmann C, Drube S, et al. PI3Kgamma deficiency delays the onset of experimental autoimmune encephalomyelitis and ameliorates its clinical outcome. Eur J Immunol. 2011;41(3):833-44.

96. Ladygina N, Gottipati S, Ngo K, Castro G, Ma JY, Banie H, et al. PI3Kgamma kinase activity is required for optimal T-cell activation and differentiation. Eur J Immunol. 2013;43(12):3183-96.

97. Liu D, Uzonna JE. The p110 delta isoform of phosphatidylinositol 3-kinase controls the quality of secondary anti-Leishmania immunity by regulating expansion and effector function of memory T cell subsets. J Immunol. 2010;184(6):3098-105.

98. Okkenhaug K, Patton DT, Bilancio A, Garcon F, Rowan WC, Vanhaesebroeck B. The p110delta isoform of phosphoinositide 3-kinase controls clonal expansion and differentiation of Th cells. J Immunol. 2006;177(8):5122-8.

99. Soond DR, Bjorgo E, Moltu K, Dale VQ, Patton DT, Torgersen KM, et al. PI3K p110delta regulates T-cell cytokine production during primary and secondary immune responses in mice and humans. Blood. 2010;115(11):2203-13.

100. Stark AK, Sriskantharajah S, Hessel EM, Okkenhaug K. PI3K inhibitors in inflammation, autoimmunity and cancer. Curr Opin Pharmacol. 2015;23:82-91.

101. Britto CJ, Brady V, Lee S, Dela Cruz CS. Respiratory Viral Infections in Chronic Lung Diseases. Clin Chest Med. 2017;38(1):87-96.

102. McMaster SR, Wilson JJ, Wang H, Kohlmeier JE. Airway-Resident Memory CD8 T Cells Provide Antigen-Specific Protection against Respiratory Virus Challenge through Rapid IFN-gamma Production. J Immunol. 2015;195(1):203-9.

103. Stuller KA, Cush SS, Flano E. Persistent gamma-herpesvirus infection induces a CD4 T cell response containing functionally distinct effector populations. J Immunol. 2010;184(7):3850-6.

104. Stoiber D, Stockinger S, Steinlein P, Kovarik J, Decker T. Listeria monocytogenes modulates macrophage cytokine responses through STAT serine phosphorylation and the induction of suppressor of cytokine signaling 3. J Immunol. 2001;166(1):466-72.

105. Turtle L, Bali T, Buxton G, Chib S, Chan S, Soni M, et al. Human T cell responses to Japanese encephalitis virus in health and disease. J Exp Med. 2016;213(7):1331-52.

106. Heiny AT, Miotto O, Srinivasan KN, Khan AM, Zhang GL, Brusic V, et al. Evolutionarily conserved protein sequences of influenza a viruses, avian and human, as vaccine targets. PLoS One. 2007;2(11):e1190.

107. Wang M, Lamberth K, Harndahl M, Roder G, Stryhn A, Larsen MV, et al. CTL epitopes for influenza A including the H5N1 bird flu; genome-, pathogen-, and HLA-wide screening. Vaccine. 2007;25(15):2823-31.

108. Lohning M, Hegazy AN, Pinschewer DD, Busse D, Lang KS, Hofer T, et al. Long-lived virus-reactive memory T cells generated from purified cytokine-secreting T helper type 1 and type 2 effectors. J Exp Med. 2008;205(1):53-61.

109. Wherry EJ, Teichgraber V, Becker TC, Masopust D, Kaech SM, Antia R, et al. Lineage relationship and protective immunity of memory CD8 T cell subsets. Nat Immunol. 2003;4(3):225-34.

110. Wu CY, Kirman JR, Rotte MJ, Davey DF, Perfetto SP, Rhee EG, et al. Distinct lineages of T(H)1 cells have differential capacities for memory cell generation in vivo. Nat Immunol. 2002;3(9):852-8.

111. Masopust D, Soerens AG. Tissue-Resident T Cells and Other Resident Leukocytes. Annu Rev Immunol. 2019;37:521-46.

112. Gerlach C, Moseman EA, Loughhead SM, Alvarez D, Zwijnenburg AJ, Waanders L, et al. The Chemokine Receptor CX3CR1 Defines Three Antigen-Experienced CD8 T Cell Subsets with Distinct Roles in Immune Surveillance and Homeostasis. Immunity. 2016;45(6):1270-84.

113. Yui MA, Hernandez-Hoyos G, Rothenberg EV. A new regulatory region of the IL-2 locus that confers position-independent transgene expression. J Immunol. 2001;166(3):1730-9.

114. Krueger PD, Goldberg MF, Hong SW, Osum KC, Langlois RA, Kotov DI, et al. Two sequential activation modules control the differentiation of protective T helper-1 (Th1) cells. Immunity. 2021;54(4):687-701 e4.

115. Kondrack RM, Harbertson J, Tan JT, McBreen ME, Surh CD, Bradley LM. Interleukin 7 regulates the survival and generation of memory CD4 cells. J Exp Med. 2003;198(12):1797-806.

116. Crotty S. T Follicular Helper Cell Biology: A Decade of Discovery and Diseases. Immunity. 2019;50(5):1132-48.

117. Krishnamoorthy V, Kannanganat S, Maienschein-Cline M, Cook SL, Chen J, Bahroos N, et al. The IRF4 Gene Regulatory Module Functions as a Read-Write Integrator to Dynamically Coordinate T Helper Cell Fate. Immunity. 2017;47(3):481-97 e7.

118. Stone EL, Pepper M, Katayama CD, Kerdiles YM, Lai CY, Emslie E, et al. ICOS coreceptor signaling inactivates the transcription factor FOXO1 to promote Tfh cell differentiation. Immunity. 2015;42(2):239-51.

119. Croft M, So T, Duan W, Soroosh P. The significance of OX40 and OX40L to T-cell biology and immune disease. Immunol Rev. 2009;229(1):173-91.

120. Flores-Fernandez R, Aponte-Lopez A, Suarez-Arriaga MC, Gorocica-Rosete P, Pizana-Venegas A, Chavez-Sanchez L, et al. Prolactin Rescues Immature B Cells from Apoptosis-Induced BCR-Aggregation through STAT3, Bcl2a1a, Bcl2l2, and Birc5 in Lupus-Prone MRL/lpr Mice. Cells. 2021;10(2).

121. Leonard WJ, Lin JX, O'Shea JJ. The gammac Family of Cytokines: Basic Biology to Therapeutic Ramifications. Immunity. 2019;50(4):832-50.

122. Nishimura H, Yajima T, Muta H, Podack ER, Tani K, Yoshikai Y. A novel role of CD30/CD30 ligand signaling in the generation of long-lived memory CD8+ T cells. J Immunol. 2005;175(7):4627-34.

123. Tang C, Yamada H, Shibata K, Muta H, Wajjwalku W, Podack ER, et al. A novel role of CD30L/CD30 signaling by T-T cell interaction in Th1 response against mycobacterial infection. J Immunol. 2008;181(9):6316-27.

124. Wang R, Xie H, Huang Z, Shang W, Sun Z. Developing and activated T cell survival depends on differential signaling pathways to regulate anti-apoptotic Bcl-x(L). Clin Dev Immunol. 2012;2012:632837.

125. Marchingo JM, Sinclair LV, Howden AJ, Cantrell DA. Quantitative analysis of how Myc controls T cell proteomes and metabolic pathways during T cell activation. Elife. 2020;9.

126. Hao Y, Hao S, Andersen-Nissen E, Mauck WM, 3rd, Zheng S, Butler A, et al. Integrated analysis of multimodal single-cell data. Cell. 2021;184(13):3573-87 e29.

127. Borcherding N, Bormann NL, Kraus G. scRepertoire: An R-based toolkit for single-cell immune receptor analysis. F1000Res. 2020;9:47.

128. Blischak JD, Carbonetto P, Stephens M. Creating and sharing reproducible research code the workflowr way. F1000Res. 2019;8:1749.

129. Gu Z, Gu L, Eils R, Schlesner M, Brors B. circlize Implements and enhances circular visualization in R. Bioinformatics. 2014;30(19):2811-2.

130. Wu H, Gonzalez Villalobos R, Yao X, Reilly D, Chen T, Rankin M, et al. Mapping the single-cell transcriptomic response of murine diabetic kidney disease to therapies. Cell Metab. 2022;34(7):1064-78 e6.

131. Gu Z. Complex heatmap visualization. iMeta. 2022;1(3):e43.

132. Crowe SR, Miller SC, Brown DM, Adams PS, Dutton RW, Harmsen AG, et al. Uneven distribution of MHC class II epitopes within the influenza virus. Vaccine. 2006;24(4):457-67.

133. Falk K, Rotzschke O, Stevanovic S, Jung G, Rammensee HG. Allele-specific motifs revealed by sequencing of self-peptides eluted from MHC molecules. Nature. 1991;351(6324):290-6.

134. Townsend AR, Rothbard J, Gotch FM, Bahadur G, Wraith D, McMichael AJ. The epitopes of influenza nucleoprotein recognized by cytotoxic T lymphocytes can be defined with short synthetic peptides. Cell. 1986;44(6):959-68.

135. Kunzli M, Masopust D. CD4(+) T cell memory. Nat Immunol. 2023;24(6):903-14.

136. Zens KD, Farber DL. Memory CD4 T cells in influenza. Curr Top Microbiol Immunol. 2015;386:399-421.

137. Slutter B, Van Braeckel-Budimir N, Abboud G, Varga SM, Salek-Ardakani S, Harty JT. Dynamics of influenza-induced lung-resident memory T cells underlie waning heterosubtypic immunity. Sci Immunol. 2017;2(7).

138. Fernandez-Ruiz D, Ng WY, Holz LE, Ma JZ, Zaid A, Wong YC, et al. Liver-Resident Memory CD8(+) T Cells Form a Front-Line Defense against Malaria Liver-Stage Infection. Immunity. 2016;45(4):889-902.

139. Rissiek B, Danquah W, Haag F, Koch-Nolte F. Technical Advance: a new cell preparation strategy that greatly improves the yield of vital and functional Tregs and NKT cells. J Leukoc Biol. 2014;95(3):543-9.

140. Gebhardt T, Whitney PG, Zaid A, Mackay LK, Brooks AG, Heath WR, et al. Different patterns of peripheral migration by memory CD4+ and CD8+ T cells. Nature. 2011;477(7363):216-9.

141. Sharpe AH, Pauken KE. The diverse functions of the PD1 inhibitory pathway. Nat Rev Immunol. 2018;18(3):153-67.

142. McCormick S, Shaler CR, Small CL, Horvath C, Damjanovic D, Brown EG, et al. Control of pathogenic CD4 T cells and lethal immunopathology by signaling immunoadaptor DAP12 during influenza infection. J Immunol. 2011;187(8):4280-92.

143. Schmit T, Guo K, Tripathi JK, Wang Z, McGregor B, Klomp M, et al. Interferon-gamma promotes monocyte-mediated lung injury during influenza infection. Cell Rep. 2022;38(9):110456.

144. Cendon C, Du W, Durek P, Liu YC, Alexander T, Serene L, et al. Resident memory CD4(+) T lymphocytes mobilize from bone marrow to contribute to a systemic secondary immune reaction. Eur J Immunol. 2022;52(5):737-52.

145. Han Q, Bagheri N, Bradshaw EM, Hafler DA, Lauffenburger DA, Love JC. Polyfunctional responses by human T cells result from sequential release of cytokines. Proc Natl Acad Sci U S A. 2012;109(5):1607-12.

146. Assenmacher M, Lohning M, Scheffold A, Manz RA, Schmitz J, Radbruch A. Sequential production of IL-2, IFN-gamma and IL-10 by individual staphylococcal enterotoxin B-activated T helper lymphocytes. Eur J Immunol. 1998;28(5):1534-43.

147. Burel JG, Apte SH, Groves PL, McCarthy JS, Doolan DL. Polyfunctional and IFN-gamma monofunctional human CD4(+) T cell populations are molecularly distinct. JCI Insight. 2017;2(3):e87499.

148. Healy ZR, Weinhold KJ, Murdoch DM. Transcriptional Profiling of CD8+ CMV-Specific T Cell Functional Subsets Obtained Using a Modified Method for Isolating High-Quality RNA From Fixed and Permeabilized Cells. Front Immunol. 2020;11:1859.

149. Meckiff BJ, Ramirez-Suastegui C, Fajardo V, Chee SJ, Kusnadi A, Simon H, et al. Imbalance of Regulatory and Cytotoxic SARS-CoV-2-Reactive CD4(+) T Cells in COVID-19. Cell. 2020;183(5):1340-53 e16.

150. Van Braeckel-Budimir N, Varga SM, Badovinac VP, Harty JT. Repeated Antigen Exposure Extends the Durability of Influenza-Specific Lung-Resident Memory CD8(+) T Cells and Heterosubtypic Immunity. Cell Rep. 2018;24(13):3374-82 e3.

151. Soerens AG, Kunzli M, Quarnstrom CF, Scott MC, Swanson L, Locquiao JJ, et al. Functional T cells are capable of supernumerary cell division and longevity. Nature. 2023;614(7949):762-6.

152. Kunzli M, Schreiner D, Pereboom TC, Swarnalekha N, Litzler LC, Lotscher J, et al. Long-lived T follicular helper cells retain plasticity and help sustain humoral immunity. Sci Immunol. 2020;5(45).

153. Luthje K, Kallies A, Shimohakamada Y, Belz GT, Light A, Tarlinton DM, et al. The development and fate of follicular helper T cells defined by an IL-21 reporter mouse. Nat Immunol. 2012;13(5):491-8.

154. MacLeod MK, David A, McKee AS, Crawford F, Kappler JW, Marrack P. Memory CD4 T cells that express CXCR5 provide accelerated help to B cells. J Immunol. 2011;186(5):2889-96.

155. Marshall HD, Chandele A, Jung YW, Meng H, Poholek AC, Parish IA, et al. Differential expression of Ly6C and T-bet distinguish effector and memory Th1 CD4(+) cell properties during viral infection. Immunity. 2011;35(4):633-46.

156. Epstein SL, Lo CY, Misplon JA, Lawson CM, Hendrickson BA, Max EE, et al. Mechanisms of heterosubtypic immunity to lethal influenza A virus infection in fully immunocompetent, T cell-depleted, beta2-microglobulin-deficient, and J chain-deficient mice. J Immunol. 1997;158(3):1222-30.